

1

Ozone and Climate: A Review of Interconnections

Coordinating Lead Authors

John Pyle (UK), Theodore Shepherd (Canada)

Lead Authors

Gregory Bodeker (New Zealand), Pablo Canziani (Argentina), Martin Dameris (Germany), Piers Forster (UK), Aleksandr Gruzdev (Russia), Rolf Müller (Germany), Nzioka John Muthama (Kenya), Giovanni Pitari (Italy), William Randel (USA)

Contributing Authors

Vitali Fioletov (Canada), Jens-Uwe Grooß (Germany), Stephen Montzka (USA), Paul Newman (USA), Larry Thomason (USA), Guus Velders (The Netherlands)

Review Editors

Mack McFarland (USA)

Contents

EXECUTIVE SUMMARY	85	1.4 Past and future stratospheric ozone changes (attribution and prediction)	110
1.1 Introduction	87	1.4.1 Current understanding of past ozone changes	110
1.1.1 Purpose and scope of this chapter	87	1.4.2 The Montreal Protocol, future ozone changes and their links to climate	117
1.1.2 Ozone in the atmosphere and its role in climate	87		
1.1.3 Chapter outline	93	1.5 Climate change from ODSs, their substitutes and ozone depletion	120
1.2 Observed changes in the stratosphere	93	1.5.1 Radiative forcing and climate sensitivity	120
1.2.1 Observed changes in stratospheric ozone	93	1.5.2 Direct radiative forcing of ODSs and their substitutes	121
1.2.2 Observed changes in ODSs	96	1.5.3 Indirect radiative forcing of ODSs	123
1.2.3 Observed changes in stratospheric aerosols, water vapour, methane and nitrous oxide	96	1.5.4 Net radiative forcing	124
1.2.4 Observed temperature changes in the stratosphere	98	References	126
1.3 Stratospheric ozone and climate feedback processes	99		
1.3.1 Impact of ODSs on stratospheric ozone	101		
1.3.2 Impact of temperature changes on ozone chemistry	102		
1.3.3 Impact of methane and water vapour changes on ozone chemistry	104		
1.3.4 The role of transport for ozone changes	105		
1.3.5 Stratosphere-troposphere dynamical coupling	107		
1.3.6 Possible dynamical feedbacks of ozone changes	108		

EXECUTIVE SUMMARY

Stratospheric ozone has been depleted over the last 25 years following anthropogenic emissions of a number of chlorine- and bromine-containing compounds (ozone-depleting substances, ODSs), which are now regulated under the Montreal Protocol. The Protocol has been effective in controlling the net growth of these compounds in the atmosphere. As chlorine and bromine slowly decrease in the future, ozone levels are expected to increase in the coming decades, although the evolution will also depend on the changing climate system.

- *Emissions of chlorofluorocarbons (CFCs) and hydrochlorofluorocarbons (HCFCs) have depleted stratospheric ozone.* Globally, ozone has decreased by roughly 3% since 1980. The largest decreases since 1980 have been observed over the Antarctic in spring (the ‘ozone hole’), where the monthly column-ozone amounts in September and October have been about 40–50% below pre-ozone-hole values. Arctic ozone shows high year-to-year variability during winter-spring due to variability in dynamical transport and chemical loss (which act in concert). Chemical losses of up to 30% are observed during cold winters, whereas they are small for dynamically active warm years.
 - *Due to the control of ODSs under the Montreal Protocol and its Amendments and Adjustments, the abundance of anthropogenic chlorine in the troposphere has peaked and is now declining.* The tropospheric abundance of anthropogenic bromine began decreasing in the late 1990s. Stratospheric concentrations of ODSs lag those in the troposphere by several years. Stratospheric chlorine levels have approximately stabilized and may have already started to decline.
 - *Changing ODS concentrations will be a dominant factor controlling changes in stratospheric ozone for the next few decades.* Stratospheric ozone depletion is likely to be near its maximum, but ozone abundance is subject to considerable interannual variability. Assuming full compliance with measures adopted under the Montreal Protocol, ozone should slowly recover. Currently, there is no unequivocal evidence from measurements in the atmosphere that the onset of ozone recovery has begun.
 - *Models suggest that in Antarctica the peak in springtime ozone depletion may already have occurred or should occur within the next few years.* Because of greater variability, predicting the timing of the peak in springtime Arctic ozone depletion is more uncertain but models suggest it should occur within the first two decades of the 21st century. Based on these model calculations, we do not expect an Arctic ‘ozone hole’ similar to that observed over the Antarctic.
 - *The ozone layer will not necessarily return to its pre-depleted state, even when the abundance of stratospheric chlorine and bromine returns to previous levels.* ‘Recovery’ of the ozone layer is a complex issue: it depends not just on the extent to which the ODSs are replaced by non-ODSs, but also on emissions of gases (including ODS substitutes) that affect the climate system directly.
- There are many complex two-way interactions between stratospheric ozone and climate. Changes in stratospheric temperature and transport affect the concentration and distribution of stratospheric ozone; changes in tropospheric climate affect stratospheric circulation; changes in stratospheric ozone influence the radiative forcing of the atmosphere, and hence surface climate, as well as the chemistry of the troposphere. While our understanding is still far from complete, new evidence about some of these interactions has emerged in recent years.
- *Stratospheric ozone depletion has led to a cooling of the stratosphere.* A significant annual-mean cooling of the lower stratosphere over the past two decades (of approximately 0.6 K per decade) has been found over the mid-latitudes of both hemispheres. Modelling studies indicate that changes in stratospheric ozone, well-mixed greenhouse gases and stratospheric water vapour could all have contributed to these observed temperature changes. In the upper stratosphere the annual mean temperature trends are larger, with an approximately uniform cooling over 1979–1998 of roughly 2 K per decade at an altitude of around 50 km. Model studies indicate that stratospheric ozone changes and carbon dioxide changes are each responsible for about 50% of the upper stratospheric temperature trend.
 - *The southern polar vortex, which creates the dynamical setting for the Antarctic ozone hole, tends to persist longer now than in the decades before the appearance of the ozone hole.* During the period 1990–2000, the vortex break-up in the late spring to early summer has been delayed by two to three weeks relative to the 1970–1980 period.
 - *Future temperature changes in the stratosphere could either enhance or reduce stratospheric ozone depletion, depending on the region.* Increases in the concentrations of well-mixed greenhouse gases, which are expected to cool the stratosphere, could reduce the rate of gas-phase ozone destruction in much of the stratosphere and hence reduce stratospheric ozone depletion. However ozone depletion in the polar lower stratosphere depends on the low temperatures there. Until stratospheric ODS abundances return to pre-ozone-hole levels, temperature reductions in polar latitudes could enhance polar ozone depletion; this effect is expected to be most important in the Arctic late winter to spring where a small decrease in temperature could have a large effect on ozone.
 - *Ozone abundance in Northern Hemisphere mid-latitudes and the Arctic is particularly sensitive to dynamical effects*

(transport and temperature). The dynamical feedbacks from greenhouse-gas increases could either enhance or reduce ozone abundance in these regions; currently, not even the sign of the feedback is known. Furthermore, dynamical variability can affect ozone in these regions on decadal time scales.

- *Statistical and modelling studies suggest that changes in stratospheric circulation regimes (e.g., between strong and weak polar vortices) can have an impact on surface climate patterns.* Because future changes in ozone will have an impact on the circulation of the stratosphere, these changes could also influence the troposphere. In particular there are indications that the Antarctic ozone hole has led to a change in surface temperature and circulation – including the cooling that has been observed over the Antarctic continent, except over the Antarctic Peninsula where a significant warming has been observed.

Halocarbons are particularly strong greenhouse gases (gases that absorb and emit thermal infrared radiation); a halocarbon molecule can be many thousands of times more efficient at absorbing radiant energy emitted from the Earth than a molecule of carbon dioxide. Ozone is a greenhouse gas that also strongly absorbs ultraviolet and visible radiation. Changes in these gases have affected the Earth's radiative balance in the past and will continue to affect it in the future.

- *Over the period 1750–2000 halocarbon gases have contributed a positive direct radiative forcing of about 0.33 W m^{-2} , which represents about 13% of the total well-mixed greenhouse gas radiative forcing over this period.* Over the period 1970–2000 halocarbon gases represent about 23% of the total well-mixed greenhouse gas radiative forcing. Over the same period, only about 5% of the total halocarbon radiative forcing is from the ODS substitutes; ODSs themselves account for 95%.
- *Stratospheric ozone depletion has led to a negative radiative forcing of about 0.15 W m^{-2} with a range of $\pm 0.1 \text{ W m}^{-2}$ from different model estimates.* Therefore the positive radiative forcing due to the combined effect of all ODSs (0.32 W m^{-2}) over the period 1750–2000 is larger than the negative forcing due to stratospheric ozone depletion.

- *Assuming that the observed changes in ozone are caused entirely by ODSs, the ozone radiative forcing can be considered an indirect forcing from the ODSs.* However, there is evidence that some fraction of the observed global ozone changes cannot be attributed to ODSs, in which case the indirect forcing by ODSs would be weaker.
- *The relative contributions of various halocarbons to positive direct and negative indirect forcing differ from gas to gas.* Gases containing bromine (such as halons) are particularly effective ozone depleters, so their relative contribution to negative forcing is greater than that of other ozone-depleting gases, such as the CFCs.
- *The same magnitudes of positive direct radiative forcing from halocarbons and of negative indirect forcing from ozone depletion are highly likely to have a different magnitude of impact on global mean surface temperature.* The climate responses will also have different spatial patterns. As a consequence, the two forcings do not simply offset one another.
- *Both the direct and indirect radiative forcings of ODSs will be reduced as a result of the Montreal Protocol.* Nevertheless, these forcings are expected to remain significant during the next several decades. The precise change of each of the forcings will be affected by several factors, including (1) the way climate change may affect stratospheric ozone chemistry and hence the ozone indirect radiative forcing; (2) future emissions of ODSs and their substitutes (see Chapter 2); and (3) continuing emissions from 'ODS banks' (ODSs that have already been manufactured but have not yet been released into the atmosphere).

1.1 Introduction

1.1.1 Purpose and scope of this chapter

Ozone absorbs solar ultraviolet (UV) radiation (thereby warming the stratosphere) and is a greenhouse gas (thereby warming the troposphere). It thus plays an important role in the climate system. Furthermore, absorption of potentially damaging UV radiation by the stratospheric ozone layer protects life at the Earth's surface. Stratospheric ozone amounts have been depleted in recent decades, following emission into the atmosphere of various ozone-depleting substances (ODSs), most of which are also greenhouse gases. The CFCs (chlorofluorocarbons) and halons, the major anthropogenic depleters of stratospheric ozone, are now controlled under the Montreal Protocol and its Amendments and Adjustments. They are being replaced by a variety of substances with lower ozone depletion potentials (ODPs) but that are generally still greenhouse gases, often with large global warming potentials (GWPs). The scientific connection between the different environmental problems of climate change and ozone depletion, and between the provisions of the Montreal Protocol and the Kyoto Protocol (and the United Nations Framework Convention on Climate Change, UNFCCC), is the subject of this chapter.

The scientific issues are complex and the connections between the two problems more intricate than suggested above. For example, not only is ozone a greenhouse gas, so that any change in ozone abundance could have an impact on climate, but changes in climate could affect ozone in a number of different ways. So, the ozone distribution in the future will depend, among other things, on the emission and impact of other greenhouse gases and not just on those that deplete ozone. For this reason, ozone recovery following the reduction in atmospheric abundances of the ODSs will not be a simple return to the pre-ozone-hole atmosphere (WMO, 1999, Chapter 12).

Climate change and ozone depletion have both been the subject of recent assessments (IPCC, 2001; WMO, 2003) describing the advances in understanding made in recent years. It is now well established, for example, that observed polar and mid-latitude ozone depletion is a consequence of the increase in stratospheric chlorine and bromine concentrations. The chemical processes involving these compounds and leading to polar ozone depletion are well understood. Similarly, the important role of ozone and the ODSs in the climate system has been documented. Stratospheric ozone depletion during recent decades has represented a negative radiative forcing of the climate system; in contrast, the increase in ODSs has been a positive radiative forcing. These earlier reports form an important basis for this special report, which aims to address specifically the coupling between the chemistry and climate problems. In particular, this report will explore the scientific issues arising from the phase-out and replacement of ODSs as they affect stratospheric composition and climate change. The earlier reports did not have this particular emphasis (although the issues were addressed by a European Commission report (EC, 2003)).

1.1.2 Ozone in the atmosphere and its role in climate

Figure 1.1 illustrates a number of important concepts concerning the ozone layer (Figure 1.1a) and its role in the stratosphere (the region between approximately 15 and 50 km altitude in which temperature rises with altitude, Figure 1.1b). Ozone, like water vapour and carbon dioxide, is an important and naturally occurring greenhouse gas; that is, it absorbs and emits radiation in the thermal infrared (Figure 1.1c), trapping heat to warm the Earth's surface (Figure 1.1d). In contrast to the so-called well-mixed greenhouse gases (WMGHGs), stratospheric ozone has two distinguishing properties. First, its relatively short chemical lifetime means that it is not uniformly mixed throughout the atmosphere and therefore its distribution is controlled by both dynamical and chemical processes (Section 1.3). In fact, unlike the WMGHGs, ozone is produced entirely within the atmosphere rather than being emitted into it. Second (Figure 1.1c), it is a very strong absorber of short wavelength UV radiation (it is also a weak absorber of visible radiation). The ozone layer's absorption of this UV radiation leads to the characteristic increase of temperature with altitude in the stratosphere and, in consequence, to a strong resistance to vertical motion. As well as ozone's role in climate it also has more direct links to humans: its absorption of UV radiation protects much of Earth's biota from this potentially damaging short wavelength radiation. In contrast to the benefits of stratospheric ozone, high surface ozone values are detrimental to human health.

The distribution of ozone in the atmosphere is maintained by a balance between photochemical production and loss, and by transport between regions of net production and net loss. A number of different chemical regimes can be identified for ozone. In the upper stratosphere, the ozone distribution arises from a balance between production following photolysis of molecular oxygen and destruction via a number of catalytic cycles involving hydrogen, nitrogen and halogen radical species (see Box 1.1). The halogens arise mainly from anthropogenic ODSs (the CFCs, HCFCs and halons). In the upper stratosphere, the rates of ozone destruction depend on temperature (a reduction in temperature slows the destruction of ozone, see Section 1.3.2) and on the concentrations of the radical species. In the lower stratosphere, reactions on aerosols become important. The distribution of the radicals (and the partitioning of the nitrogen, hydrogen and halogen species between radicals and 'reservoirs' that do not destroy ozone) can be affected by heterogeneous and multiphase chemistry acting on condensed matter (liquid and solid particles). At the low temperature of the wintertime polar lower stratosphere, this is the chemistry that leads to the ozone hole (see Box 1.1).

The large-scale circulation of the stratosphere, known as the Brewer-Dobson circulation (see Box 1.2), systematically transports ozone poleward and downward (figure in Box 1.2). Because ozone photochemical reactions proceed quickly in the sunlit upper stratosphere, this transport has little effect on the ozone distribution there as ozone removal by transport is quickly replenished by photochemical production. However, this trans-

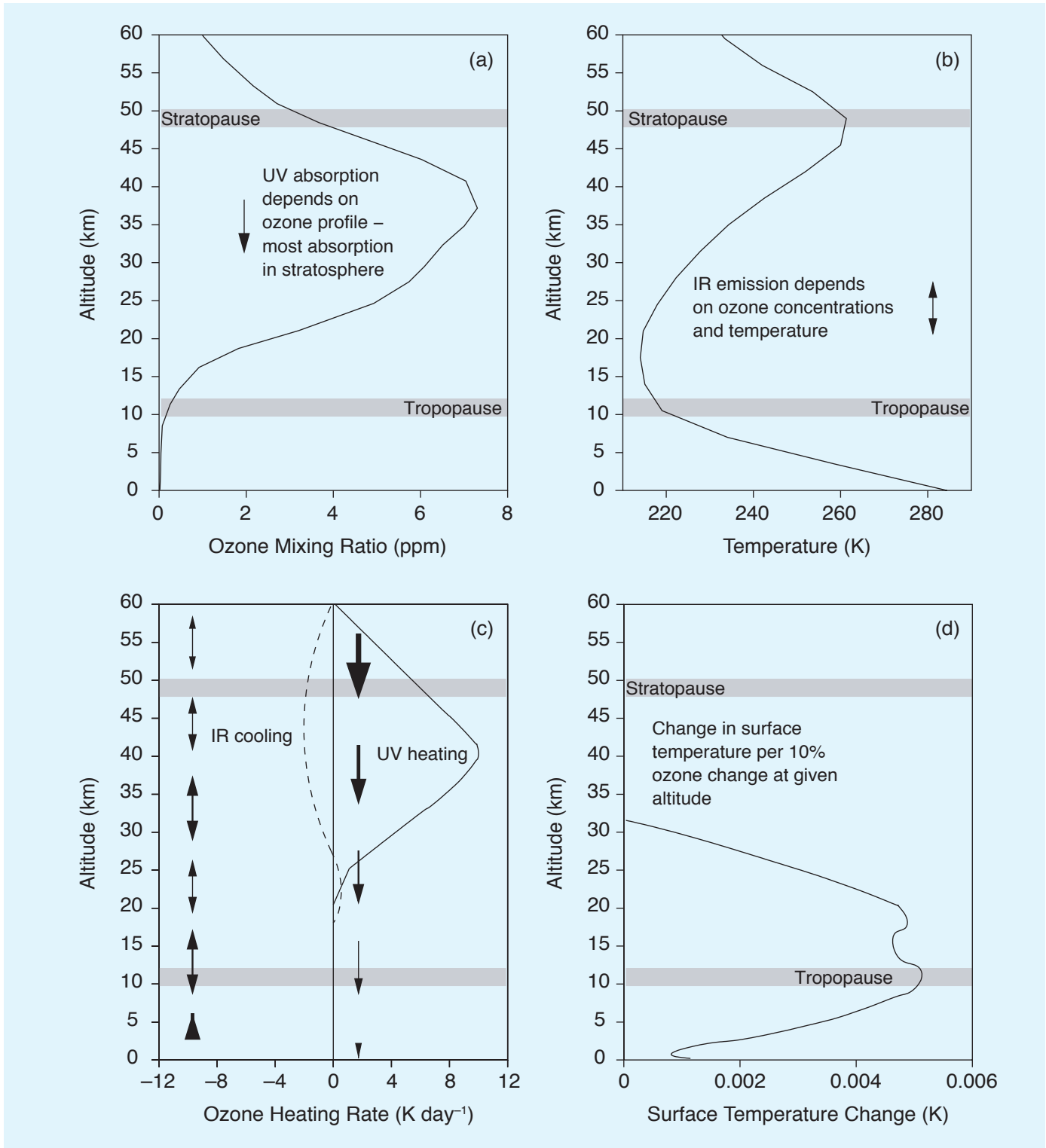


Figure 1.1. Vertical profiles of ozone-related quantities. (a) Typical mid-latitude ozone mixing ratio profile, based on an update of Fortuin and Langematz (1994); (b) atmospheric temperature profile, based on Fleming *et al.* (1990), showing the stratosphere bounded by the tropopause below and the stratopause above; (c) schematic showing the ultraviolet (UV) radiative flux through the atmosphere (single-headed arrows) and infrared (IR) emission at around 9.6 μm (the ozone absorption band, double-headed arrows), and the heating in the ultraviolet (solid curve) and infrared (dashed curve) associated with these fluxes; (d) schematic of the change in surface temperature due to a 10% change in ozone concentration at different altitudes (based on Figure 6.1 of IPCC, 2001). Figure provided by Peter Braesicke, University of Cambridge.

Box 1.1. Ozone chemistry

Stratospheric ozone is produced naturally by photolysis of molecular oxygen (O_2) at ultraviolet wavelengths below 242 nm,



The atomic oxygen produced in this reaction reacts rapidly with O_2 to form ozone (O_3),



where M denotes a collision partner, not affected by the reaction. O_3 itself is photolyzed rapidly,



O_3 and O establish a rapid photochemical equilibrium through Reactions [2] and [3], and together are called 'odd oxygen'. Finally, in this sequence of reactions (known as the Chapman reactions), ozone is removed by



Destruction by Reaction [4] alone cannot explain observed ozone abundances in the stratosphere and it is now known that, away from polar latitudes, the ozone production through Reaction [1] is largely balanced by destruction in catalytic cycles of the form



The net reaction is equivalent to Reaction [4]. Note that, because O and O_3 are in rapid photochemical equilibrium, the loss of one oxygen atom also effectively implies the loss of an ozone molecule, so that the cycle destroys two molecules of 'odd oxygen'. Notice also that the catalyst, X, is not used up in the reaction cycle. The most important cycles of this type in the stratosphere involve reactive nitrogen ($X = NO$), halogen ($X = Cl$) and hydrogen ($X = H, OH$) radicals. In the lower stratosphere, cycles catalyzed by Br also contribute to the ozone loss. Owing to the large increase of O with altitude, the rates of these cycles increase substantially between 25 and 40 km, as does the rate of ozone production.

In polar regions, the abundance of ClO is greatly enhanced during winter as a result of reactions on the surfaces of polar stratospheric cloud particles that form at the low temperatures found there. However, atomic oxygen, O, has very low concentrations there, which limits the efficiency of Cycle 1. In that case, two other catalytic cycles become the dominant reaction mechanisms for polar ozone loss. The first, the so-called ClO dimer cycle, is initiated by the reaction of ClO with another ClO,



and the second, the ClO-BrO cycle, is initiated by the reaction of ClO with BrO:

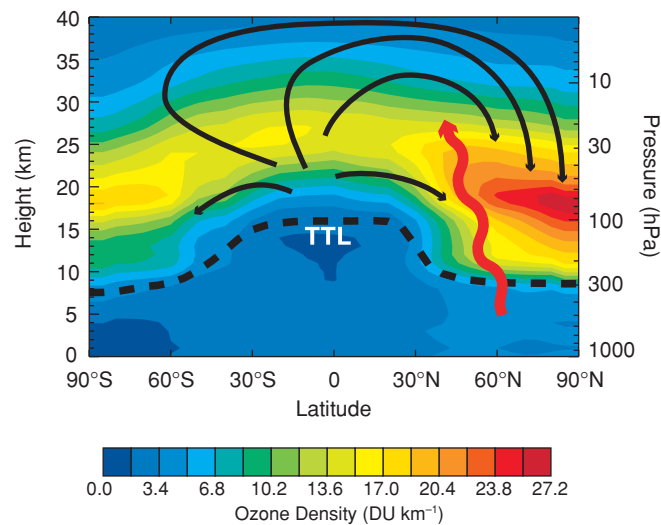


The net result of both Cycle 2 and Cycle 3 is to destroy two ozone molecules and to produce three oxygen molecules. Both cycles are catalytic, as chlorine (Cl) and bromine (Br) are not lost in the cycles. Sunlight is required to complete the cycles and to help maintain the large ClO abundance. Cycles 2 and 3 account for most of the ozone loss observed in the late winter-spring season in the Arctic and Antarctic stratosphere. At high ClO abundances, the rate of ozone destruction can reach 2 to 3% per day in late winter-spring. Outside the polar regions the ClO-BrO cycle is of minor importance because of much lower ClO concentrations, and the effect of the ClO dimer cycle is negligible as the cycle is only effective at the low polar temperatures.

Box 1.2. Stratospheric transport, planetary waves and the Brewer-Dobson circulation

The stratospheric Brewer-Dobson circulation consists of rising motion in the tropics and sinking motion in the extratropics, together with an associated poleward mass flux. Its effect on chemical species is complemented by mixing (mainly quasi-horizontal) that acts to transport air parcels both poleward and equatorward. Both processes are primarily driven by mechanical forcing (wave drag) arising from the dissipation of planetary-scale waves in the stratosphere. These planetary waves are generated in the troposphere by topographic and thermal forcing, and by synoptic meteorological activity, and propagate vertically into the stratosphere. Because of filtering by the large-scale stratospheric winds, vertical propagation of planetary waves into the stratosphere occurs primarily during winter, and this seasonality in wave forcing accounts for the winter maximum in the Brewer-Dobson circulation. In the case of ozone, the Brewer-Dobson circulation (together with the associated horizontal mixing) transports ozone poleward and downward and leads to a springtime maximum in extra-tropical ozone abundance (see figure).

Because air enters the stratosphere primarily in the tropics, the physical and chemical characteristics of air near the tropical tropopause behave as boundary conditions for the global stratosphere. For example, dehydration of air near the cold tropical tropopause accounts for the extreme dryness of the global stratosphere (Brewer, 1949). Overall, the region of the tropical atmosphere between about 12 km and the altitude of the tropopause (about 17 km) has characteristics intermediate to those of the troposphere and stratosphere, and is referred to as the *tropical tropopause layer* (TTL).



Box 1.2, Figure. Meridional cross-section of the atmosphere showing ozone density (colour contours; in Dobson units (DU) per km) during Northern Hemisphere (NH) winter (January to March), from the climatology of Fortuin and Kelder (1998). The dashed line denotes the tropopause, and TTL stands for tropical tropopause layer (see text). The black arrows indicate the Brewer-Dobson circulation during NH winter, and the wiggly red arrow represents planetary waves that propagate from the troposphere into the winter stratosphere.

port leads to significant variations of ozone in the extra-tropical lower stratosphere, where the photochemical relaxation time is very long (several months or longer) and ozone can accumulate on seasonal time scales. Due to the seasonality of the Brewer-Dobson circulation (maximum during winter and spring), ozone builds up in the extra-tropical lower stratosphere during winter and spring through transport, and then decays photochemically during the summer when transport is weaker. The column-ozone distribution (measured in Dobson units, DU) is dominated by its distribution in the lower stratosphere and reflects this seasonality (Figure 1.2). Furthermore, planetary waves are stronger (and more variable) in the Northern Hemisphere

(NH) than in the Southern Hemisphere (SH), because of the asymmetric distribution of the surface features (topography and land-sea thermal contrasts) that, in combination with surface winds, force the waves. Accordingly, the stratospheric Brewer-Dobson circulation is stronger during the NH winter, and the resulting extra-tropical build-up of ozone during the winter and spring is greater in the NH than in the SH (Andrews *et al.*, 1987; Figure 1.2).

Variations in the Brewer-Dobson circulation also influence polar temperatures in the lower stratosphere (via the vertical motions); stronger wave forcing coincides with enhanced circulation and higher polar temperatures (and more ozone trans-

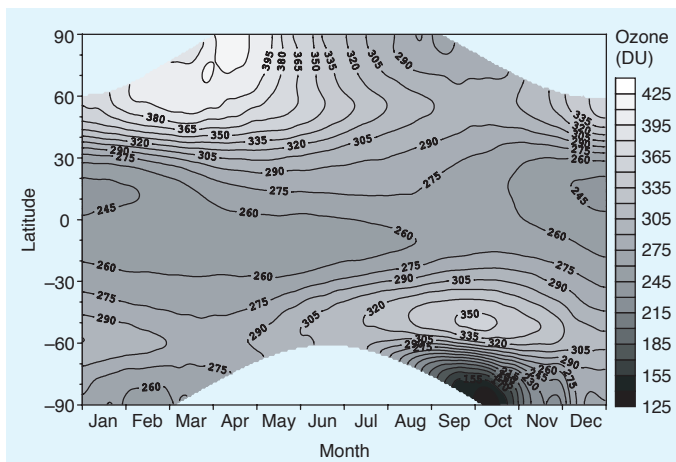


Figure 1.2. A climatology of total column ozone plotted as a function of latitude and month. Version 8 Total Ozone Mapping Spectrometer (TOMS) data were used together with version 3.1 Global Ozone Monitoring Experiment (GOME) data over the period 1994 to 2003. Updated from Bodeker *et al.* (2001).

port). Since temperature affects ozone chemistry, dynamical and chemical effects on column ozone thus tend to act in concert and are coupled.

Human activities have led to changes in the atmospheric concentrations of several greenhouse gases, including tropospheric and stratospheric ozone and ODSs and their substitutes. Changes to the concentrations of these gases alter the radiative balance of the Earth's atmosphere by changing the balance between incoming solar radiation and outgoing infrared radiation. Such an alteration in the Earth's radiative balance is called a *radiative forcing*. This report, past IPCC reports and climate change protocols have universally adopted the concept of radiative forcing as a tool to gauge and contrast *surface* climate change caused by different mechanisms (see Box 1.3). Positive radiative forcings are expected to warm the Earth's surface and negative radiative forcings are expected to cool it. The radiative forcings from the principal greenhouse gases are summarized in Figure 1.3 and Table 1.1 (in Section 1.5.2). Other significant contributors to radiative forcing that are not shown in Figure 1.3 include tropospheric aerosol changes and changes in the Sun's output. Changes in carbon dioxide (CO_2) provide the largest radiative forcing term and are expected to be the largest overall contributor to climate change. In contrast with the positive radiative forcings due to increases in other greenhouse gases, the radiative forcing due to stratospheric ozone depletion is negative.

Halocarbons are particularly effective greenhouse gases in part because they absorb the Earth's outgoing infrared radiation in a spectral range where energy is not removed by carbon dioxide or water vapour (sometimes referred to as the *atmospheric window*). Halocarbon molecules can be many thousands of times more efficient at absorbing the radiant energy emitted from the Earth than a molecule of carbon dioxide, which ex-

plains why relatively small amounts of these gases can contribute significantly to radiative forcing of the climate system. Because halocarbons have low concentrations and absorb in the atmospheric window, the magnitude of the direct radiative forcing from a halocarbon is given by the product of its tropospheric mixing ratio and its radiative efficiency. In contrast, for the more abundant greenhouse gases (carbon dioxide, methane and nitrous oxide) there is a nonlinear relationship between the mixing ratio and the radiative forcing.

Since 1970 the growth in halocarbon concentrations and the changes in ozone concentrations (depletion in the stratosphere and increases in the troposphere) have been very significant contributors to the total radiative forcing of the Earth's atmosphere. Because halocarbons have likely caused most of the stratospheric ozone loss (see Section 1.4.1), there is the possibility of a partial offset between the positive forcing of halocarbon that are ODSs and the negative forcing from stratospheric ozone loss. This is discussed further in Section 1.5.

The climate impacts of ozone changes are not confined to the surface: stratospheric ozone changes are probably responsible for a significant fraction of the observed cooling in the lower stratosphere over the last two decades (Section 1.2.4) and may alter atmospheric dynamics and chemistry (Section 1.3.6). Further, it was predicted that depletion of stratospheric ozone would lead to a global increase in erythemal UV radiation (the radiation that causes sunburn) at the surface of about 3%, with much larger increases at high latitudes; these predicted high lat-

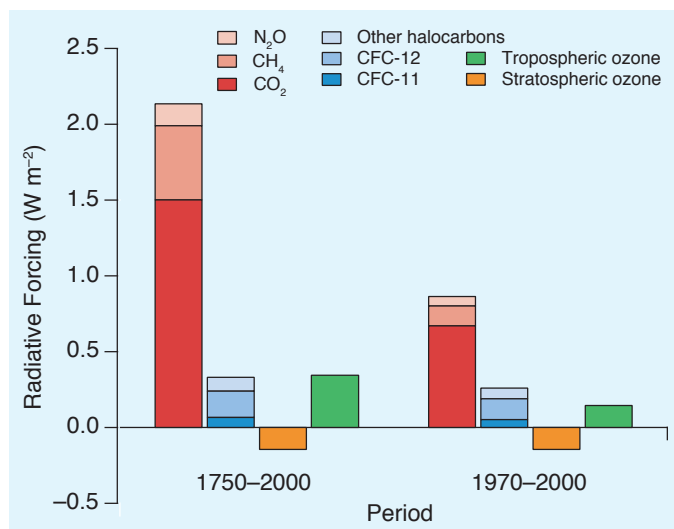


Figure 1.3. Changes in radiative forcing (in W m^{-2}) from WMGHGs and ozone over two periods: 1750–2000 and 1970–2000. Numbers are taken from estimates in Tables 6.11 and 6.13 of IPCC (2001). The halocarbon direct radiative forcing is shown separately from the other WMGHG forcing. The negative forcing from stratospheric ozone is largely a result of the stratospheric ozone depletion, which resulted from halocarbon emissions between 1970 and 2000; it can therefore be considered an indirect radiative forcing from halocarbons, which offsets their positive direct forcing. In contrast, the tropospheric ozone radiative forcing is largely independent of the halocarbon forcing.

Box 1.3. Radiative forcing and climate sensitivity

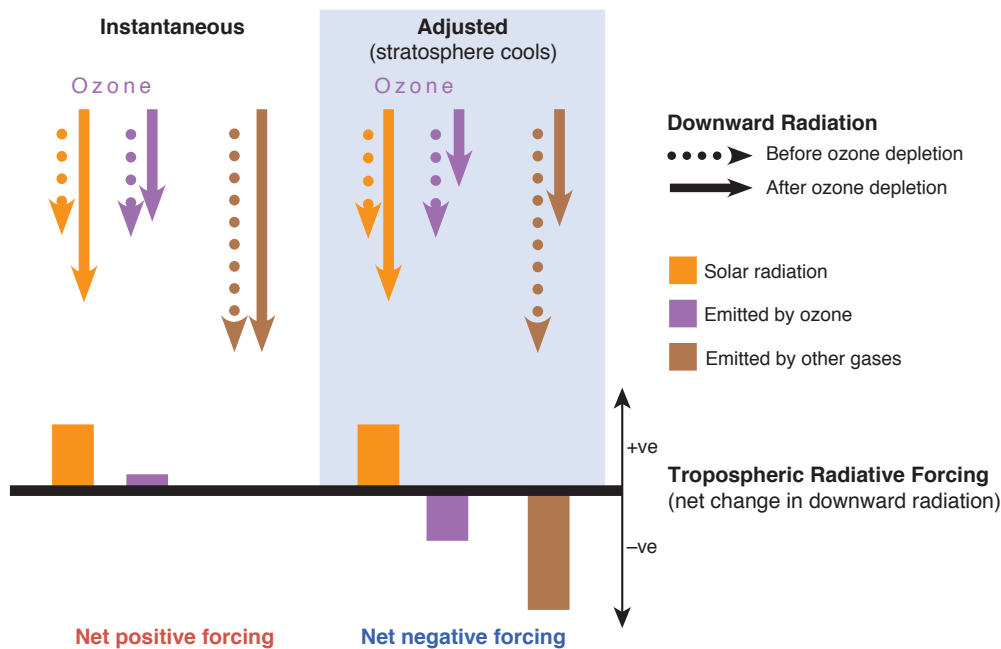
Radiative forcing is a useful tool for estimating the relative climate impacts, in the global mean, of different climate change mechanisms. Radiative forcing uses the notion that the globally averaged radiative forcing (ΔF) is related to the globally averaged equilibrium surface temperature change (ΔT_s) through the climate sensitivity (λ):

$$\Delta T_s = \lambda \Delta F$$

The reason surface temperature changes in different models are not usually compared directly is that the climate sensitivity is poorly known and varies by a factor of three between different climate models (IPCC, 2001, Chapter 9). Further, climate model studies have shown that, for many forcing mechanisms, λ in an individual climate model is more or less independent of the mechanism. These two factors enable the climate change potential of different mechanisms to be quantitatively contrasted through their radiative forcings, while they remain difficult to compare through their predicted surface temperature changes. Unfortunately, certain radiative forcings, including ozone changes, have been shown to have different climate sensitivities compared with carbon dioxide changes (IPCC, 2001, Chapter 6; WMO, 2003, Chapter 4). One of the reasons for this difference is that some aspects of the radiative forcing definition, such as tropopause height, have a large impact on the ozone radiative forcing (see below). These factors are the main reasons for the large uncertainty in the ozone radiative forcing and the global mean climate response.

Why is the radiative forcing of stratospheric ozone negative?

The radiative forcing is defined as the change in net radiative flux at the tropopause after allowing for stratospheric temperatures to readjust to radiative equilibrium (IPCC, 2001, Chapter 6). The details of this definition are crucial for stratospheric ozone, and are explained in the figure.



Box 1.3, Figure. The instantaneous effect of stratospheric ozone depletion (left-hand side of schematic) is to increase the shortwave radiation from the Sun reaching the tropopause (because there is less ozone to absorb it), and to slightly reduce the downward longwave radiation from the stratosphere, as there is less ozone in the stratosphere to emit radiation. This gives an instantaneous net positive radiative forcing. However, in response to less absorption of both shortwave and longwave radiation in the stratosphere, the region cools, which leads to an overall reduction of thermal radiation emitted downward from the stratosphere (right-hand side of schematic). The size of this adjustment term depends on the vertical profile of ozone change and is largest for changes near the tropopause. For the observed stratospheric ozone changes the adjustment term is larger than the positive instantaneous term, thus the stratospheric ozone radiative forcing is negative.

itude increases in surface UV dose have indeed been observed (WMO, 2003, Chapter 5).

1.1.3 Chapter outline

Our aim in this chapter is to review the scientific understanding of the interactions between ozone and climate. We interpret the term ‘climate’ broadly, to include stratospheric temperature and circulation, and refer to tropospheric effects as ‘tropospheric climate’. This is a broad topic; our review will take a more restricted view concentrating on the interactions as they relate to stratospheric ozone and the role of the ODSs and their substitutes. For this reason the role of tropospheric ozone in the climate system is mentioned only briefly. Similarly, some broader issues, including possible changes in stratospheric water vapour (where the role of the ODSs and their substitutes should be minor) and climate-dependent changes in biogenic emissions (whose first order effect is likely to be in the troposphere), will not be discussed in any detail. The relationship between ozone and the solar cycle is well established, and the solar cycle has been used as an explanatory variable in ozone trend analysis. The connection between ozone and the solar cycle was assessed most recently in Chapter 12 of WMO (1999) and will not be discussed further here.

Section 1.2 presents an update on stratospheric observations of ozone, ozone-related species and temperature. Section 1.3 considers, at a process level, the various feedbacks connecting stratospheric ozone and the climate system. The understanding of these processes leads, in Section 1.4, to a discussion of the attribution of past changes in ozone, the prediction of future changes, and the connection of both with climate. Finally, Section 1.5 reviews the trade-offs between ozone depletion and radiative forcing, focusing on ODSs and their substitutes.

1.2 Observed changes in the stratosphere

1.2.1 Observed changes in stratospheric ozone

Global and hemispheric-scale variations in stratospheric ozone can be quantified from extensive observational records covering the past 20 to 30 years. There are numerous ways to measure ozone in the atmosphere, but they fall broadly into two categories: measurements of column ozone (the vertically integrated amount of ozone above the surface), and measurements of the vertical profile of ozone. Approximately 90% of the vertically integrated ozone column resides in the stratosphere. There are more independent measurements, longer time-series, and better global coverage for column ozone. Regular measurements of column ozone are available from a network of surface stations, mostly in the mid-latitude NH, with reasonable coverage extending back to the 1960s. Near-global, continuous column ozone data are available from satellite measurements beginning in 1979. The different observational data sets can be used to estimate past ozone changes, and the differences between data sets provide a lower bound of overall uncertainty. The differ-

ences indicate good overall agreement between different data sources for changes in column ozone, and thus we have reasonable confidence in describing the spatial and temporal characteristics of past changes (WMO, 2003, Chapter 4).

Five data sets of zonal and monthly mean column ozone values developed by different scientific teams were used to quantify past ozone changes in Chapter 4 of WMO (2003); they include ground-based measurements covering 1964–2001, and several different satellite data sets extending in time over 1979–2001. Figure 1.4a shows globally averaged column ozone changes derived from each of these data sets, updated through 2004. The analyses first remove the seasonal cycle from each

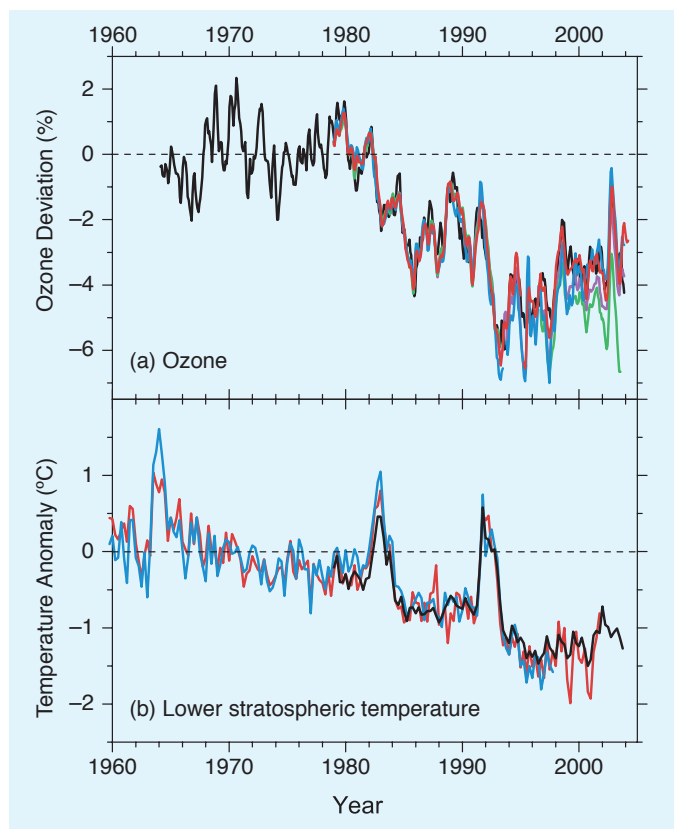


Figure 1.4. (a) Time-series of de-seasonalized global mean column ozone anomalies estimated from five different data sets, including ground-based (black line) and satellite measurements (colour lines). Anomalies are expressed as percentage differences from the 1964–1980 average, and the seasonal component of the linear trend has been removed. Updated from Fioletov *et al.* (2002). (b) Time-series of de-seasonalized global mean lower-stratospheric temperature anomalies estimated from radiosondes (colour lines) and satellite data (black line). Anomalies (in °C) are calculated with respect to the 1960–1980 average. The radiosonde data represent mean temperature in the 100–50 hPa layer (about 16–22 km), and are derived from the HadRT and LKS data sets described in Seidel *et al.* (2004). Satellite temperatures (available for 1979–2003) are from the Microwave Sounding Unit Channel 4, and represent mean temperature in a layer over about 13–22 km. For direct comparison, the satellite data have been normalized to equal the radiosonde time means over 1979–1997. Panel (b) is discussed in Section 1.2.4.

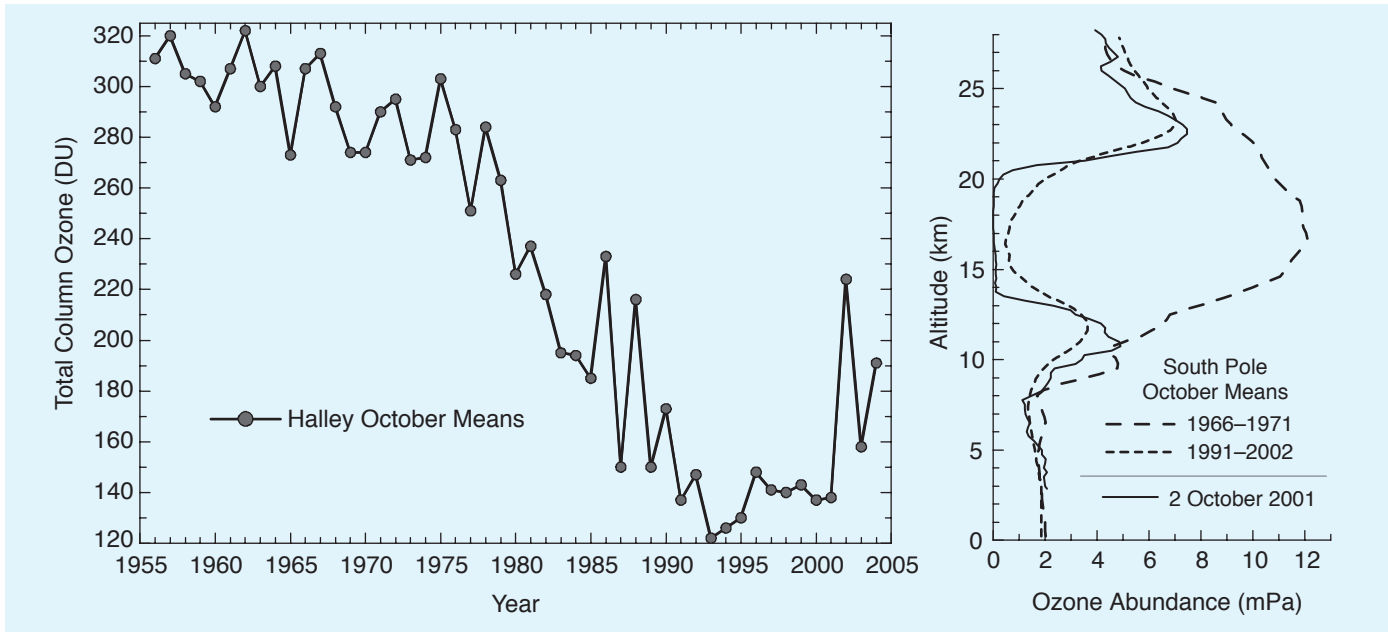


Figure 1.5. Left panel: October mean total column ozone measurements from the Dobson spectrophotometer at Halley, Antarctica (73.5°S, 26.7°W). Right panel: Vertical ozone profiles measured by ozonesondes at South Pole station, Antarctica (90°S). These data are from the WOUDC (World Ozone and UV Data Centre) and NDSC (Network for Detection of Stratospheric Change) databases. The 1966–1971 October mean profile is shown using a long-dashed line, the 1991–2002 October mean profile as a short-dashed line, and the single ozonesonde flight on 2 October 2001 as a solid line.

data set (mean and linear trend), and the deviations are area weighted and expressed as anomalies with respect to the period 1964–1980. The global ozone amount shows decreasing values between the late 1970s and the early 1990s, a relative minimum during 1992–1994, and slightly increasing values during the late 1990s. Global ozone for the period 1997–2004 was approximately 3% below the 1964–1980 average values. Since systematic global observations began in the mid-1960s, the lowest annually averaged global ozone occurred during 1992–1993 (5% below the 1964–1980 average). These changes are evident in each of the available global data sets.

The global ozone changes shown in Figure 1.4a occur mainly in the extratropics of both hemispheres (poleward of 25°–35°). No significant long-term changes in column ozone have been observed in the tropics (25°N to 25°S). Column ozone changes averaged over mid-latitudes (from 35° to 60° latitude) are significantly larger in the SH than in the NH; averaged for the period 1997–2001, SH values are 6% below pre-1980 values, whereas NH values are 3% lower. Also, there is significant seasonality to the NH mid-latitude losses (4% losses in the winter-spring period and 2% in summer), whereas long-term SH losses are about 6% year round (WMO, 2003, Chapter 4).

The most dramatic changes in ozone have occurred during the spring season over Antarctica, with the development during the 1980s of a phenomenon known as the *ozone hole* (Figure 1.5). The ozone hole now recurs every spring, with some inter-annual variability and occasional extreme behaviour (see Box 1.6 in Section 1.4.1). In most years the ozone concentration

is reduced to nearly zero over a layer several kilometres deep within the lower stratosphere in the Antarctic polar vortex. Since the early 1990s, the average October column ozone poleward of

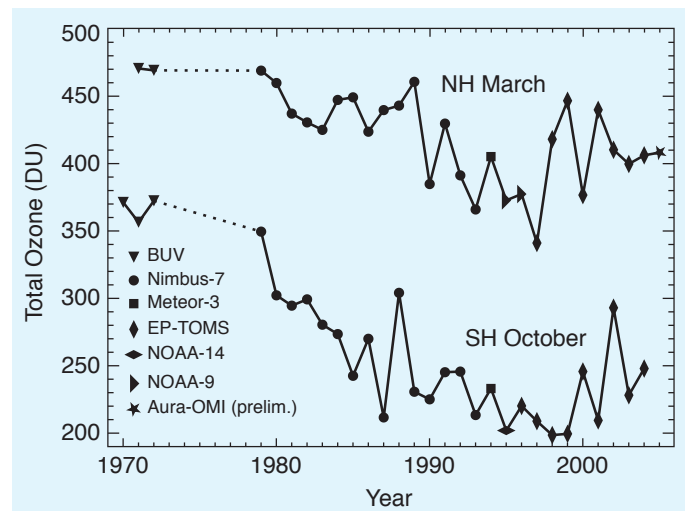


Figure 1.6. Average column ozone poleward of 63° latitude in the springtime of each hemisphere (March for the NH and October for the SH), in Dobson units, based on data from various satellite instruments as indicated. The data point from the Ozone Monitoring Instrument (OMI) is preliminary. Updated from Newman *et al.* (1997), courtesy of NIVR (Netherlands), KNMI (Netherlands), FMI (Finland), and NASA (USA).

63°S has been more than 100 DU below pre-ozone-hole values (a 40 to 50% decrease), with up to a 70% local decrease for periods of a week or so (WMO, 2003, Chapter 3; Figure 1.6).

Compared with the Antarctic, Arctic ozone abundance in the winter and spring is highly variable (Figure 1.6), because of interannual variability in chemical loss and in dynamical transport. Dynamical variability within the winter stratosphere leads to changes in ozone transport to high latitudes, and these transport changes are correlated with polar temperature variability – with less ozone transport being associated with lower temperatures. Low temperatures favour halogen-induced chemical ozone loss. Thus, in recent decades, halogen-induced polar ozone chemistry has acted in concert with the dynamically induced ozone variability, and has led to Arctic column ozone losses of up to 30% in particularly cold winters (WMO, 2003, Chapter 3). In particularly dynamically active, warm winters,

however, the estimated chemical ozone loss has been very small.

Changes in the vertical profile of ozone are derived primarily from satellites, ground-based measurements and balloon-borne ozonesondes. Long records from ground-based and balloon data are available mainly for stations over NH mid-latitudes. Ozone profile changes over NH mid-latitudes exhibit two maxima, with decreasing trends in the upper stratosphere (about 7% per decade at 35–45 km) and in the lower stratosphere (about 5% per decade at 15–25 km) during the period 1979–2000. Ozone profile trends show a minimum (about 2% per decade decrease) near 30 km. The vertically integrated profile trends are in agreement with the measured changes in column ozone (WMO, 2003, Chapter 4).

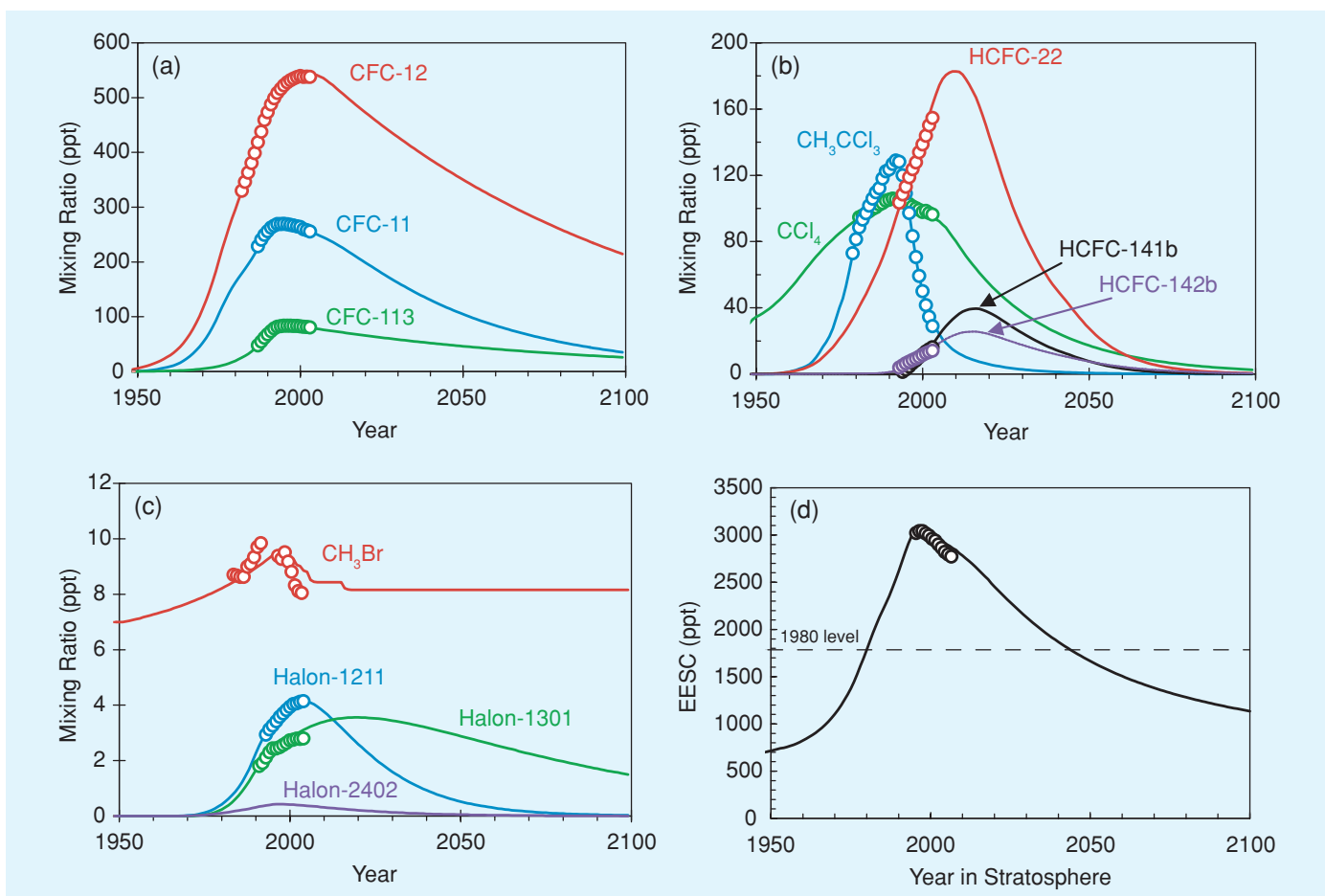


Figure 1.7. Global atmospheric mixing ratios (in ppt) in the WMO (2003) baseline scenario Ab (lines) of the most abundant CFCs, HCFCs, chlorinated solvents and brominated gases at the Earth's surface. Also shown are measured annual means (circles) that are based on results from two independent, global sampling networks (an update of Figure 1-22 of WMO, 2003) for all gases except CH₃Br. Global surface means for CH₃Br are taken from Khalil *et al.* (1993) for the years before 1992, and from Montzka *et al.* (2003) for 1996–2003. Panel (d) shows past and potential future changes in the total ozone-depleting halogen burden of the stratosphere, estimated as equivalent effective stratospheric chlorine (EESC). The EESC values are derived from the baseline scenario Ab (line) or surface measurements (circles). EESC is derived from measured surface mixing ratios of the most abundant CFCs, HCFCs, chlorinated solvents, halons and methyl bromide; it is based on the assumption of a 3-year time lag between the troposphere and mid-stratosphere and a factor of 45 to account for the enhanced reactivity of Br relative to Cl in depleting stratospheric ozone (Daniel *et al.*, 1999).

1.2.2 Observed changes in ODSs

As a result of reduced emissions because of the Montreal Protocol and its Amendments and Adjustments, mixing ratios for most ODSs have stopped increasing near the Earth's surface (Montzka *et al.*, 1999; Prinn *et al.*, 2000). The response to the Protocol, however, is reflected in quite different observed behaviour for different substances. By 2003, the mixing ratios for CFC-12 were close to their peak, CFC-11 had clearly decreased, while methyl chloroform (CH_3CCl_3) had dropped by 80% from its maximum (Figure 1.7; see also Chapter 1 of WMO, 2003).

Halons and HCFCs are among the few ODSs whose mixing ratios were still increasing in 2000 (Montzka *et al.*, 2003; O'Doherty *et al.*, 2004). Halons contain bromine, which is on average 40 to 50 times more efficient on a per-atom basis at destroying stratospheric ozone than chlorine. However, growth rates for most halons have steadily decreased during recent years (Fraser *et al.*, 1999; Montzka *et al.*, 2003). Furthermore, increases in tropospheric bromine from halons have been offset by the decline observed for methyl bromide (CH_3Br) since 1998

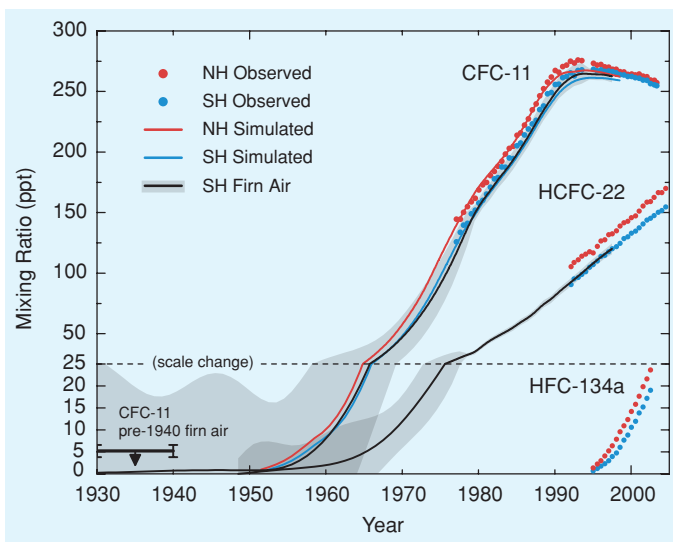


Figure 1.8. Estimated global atmospheric mixing ratios (in ppt) of CFC-11, HCFC-22 and HFC-134a, shown separately for the NH (red) and SH (blue). Circles show measurements from the AGAGE (Advanced Global Atmospheric Gases Experiment) and CMDL (Climate Monitoring and Diagnostics Laboratory) networks, while colour lines show simulated CFC-11 concentrations based on estimates of emissions and atmospheric lifetimes (updated from Walker *et al.*, 2000). The black lines and the shaded areas show estimates and uncertainty bands, respectively, for CFC-11 and HCFC-22 that were derived by synthesis inversion of Antarctic firn air measurements and *in situ* Cape Grim atmospheric measurements (Sturrock *et al.*, 2002). The thick black horizontal line with an arrow and an error bar shows a separate upper-bound estimate of pre-1940 CFC-11 concentrations based on South Pole firn air measurements (see Battle and Butler, 'Determining the atmospheric mixing ratio of CFC-11 from firn air samples', which is available at <ftp://ftp.cmdl.noaa.gov/hats/firnair/> and is based on the analysis of Butler *et al.*, 1999).

(Yokouchi *et al.*, 2002; Montzka *et al.*, 2003; Simmonds *et al.*, 2004).

Atmospheric amounts of HCFCs continue to increase because of their use as CFC substitutes (Figure 1.7b). Chlorine from HCFCs has increased at a fairly constant rate of 10 ppt Cl yr^{-1} since 1996, although HCFCs accounted for only 5% of all chlorine from long-lived gases in the atmosphere by 2000 (WMO, 2003, Chapter 1). The ODPs of the most abundant HCFCs are only about 5–10% of those of the CFCs (Table 1.2 in Section 1.5.3).

Figure 1.8 contrasts the observed atmospheric abundances of CFC-11 with those of HCFC-22 and HFC-134a. The behaviour of CFC-11 is representative of the behaviour of CFCs in general, and the behaviour of HCFC-22 and HFC-134a is representative of HCFCs (as well as HFCs) in general (see Figure 2.3 in Chapter 2). The most rapid growth rates of CFC-11 occurred in the 1970s and 1980s. The largest emissions were in the NH, and concentrations in the SH lagged behind those in the NH, consistent with an inter-hemispheric mixing time scale of about 1 to 2 years. In recent years, following the implementation of the Montreal Protocol, the observed growth rate has declined, concentrations appear to be at their peak and, as emissions have declined, the inter-hemispheric gradient has almost disappeared. In contrast, HCFC-22 and HFC-134a concentrations are still growing rapidly and there is a marked inter-hemispheric gradient.

Ground-based observations suggest that by 2003 the cumulative totals of both chlorine- and bromine-containing gases regulated by the Montreal Protocol were decreasing in the lower atmosphere (Montzka *et al.*, 2003). Although tropospheric chlorine levels peaked in the early 1990s and have since declined, atmospheric bromine began decreasing in 1998 (Montzka *et al.*, 2003).

The net effect of changes in the abundance of both chlorine and bromine on the total ozone-depleting halogens in the stratosphere is estimated roughly by calculating the equivalent effective stratospheric chlorine (EESC; Daniel *et al.*, 1995) (Figure 1.7d). The calculation of EESC (see Box 1.8 in Section 1.5.3) includes consideration of the total amount of chlorine and bromine accounted for by long-lived halocarbons, how rapidly these halocarbons degrade and release their halogen in the stratosphere and a nominal lag time of three years to allow for transport from the troposphere into the stratosphere. The tropospheric observational data suggest that EESC peaked in the mid-1990s and has been decreasing at a mean rate of 22 ppt yr^{-1} (0.7% yr^{-1}) over the past eight years (Chapter 1 of WMO, 2003). Direct stratospheric measurements show that stratospheric chlorine reached a broad plateau after 1996, characterized by variability (Rinsland *et al.*, 2003).

1.2.3 Observed changes in stratospheric aerosols, water vapour, methane and nitrous oxide

In addition to ODSs, stratospheric ozone is influenced by the abundance of stratospheric aerosols, water vapour, methane

(CH₄) and nitrous oxide (N₂O). Observed variations in these constituents are summarized in this section.

During the past three decades, aerosol loading in the stratosphere has primarily reflected the effects of a few volcanic eruptions that inject aerosol and its gaseous precursors (primarily sulphur dioxide, SO₂) into the stratosphere. The most noteworthy of these eruptions are El Chichón (1982) and Pinatubo (1991). The 1991 Pinatubo eruption likely had the largest impact of any event in the 20th century (McCormick *et al.*, 1995), producing about 30 Tg of aerosol (compared with approximately 12 Tg from El Chichón) that persisted into at least the late 1990s. Current aerosol loading, which is at the lowest observed levels, is less than 0.5 Tg, so the Pinatubo event represents nearly a factor of 100 enhancement relative to non-volcanic levels. The source of the non-volcanic stratospheric aerosol is primarily carbonyl sulfide (OCS), and there is general agreement between the aerosols estimated by modelling the transformation of observed OCS to sulphate aerosols and observed aerosols. However, there is a significant dearth of SO₂ measurements, and the role of tropospheric SO₂ in the stratospheric aerosol budget – while significant – remains a matter of some uncertainty. Because of the high variability of stratospheric aerosol loading it is difficult to detect trends in the non-volcanic aerosol component. Trends derived from the late 1970s to the current period are likely to encompass a value of zero.

The recent Stratospheric Processes And their Role in Climate (SPARC) Assessment of Upper Tropospheric and Stratospheric Water Vapour (SPARC, 2000) provided an extensive review of data sources and quality for stratospheric water vapour, together with detailed analyses of observed seasonal and interannual variability. The longest continuous reliable data set is at a single location (Boulder, Colorado, USA), is based on balloon-borne frost-point hygrometer measurements (approximately one per month), and dates back to 1980. Over the period 1980–2000, a statistically significant positive trend of approximately 1% yr⁻¹ is observed at all levels between about 15 and 26 km in altitude (SPARC, 2000; Oltmans *et al.*, 2000). However, although a linear trend can be fitted to these data, there is a high degree of variability in the infrequent sampling, and the increases are neither continuous nor steady (Figure 1.9). Long-term increases in stratospheric water vapour are also inferred from a number of other ground-based, balloon, aircraft and satellite data sets spanning approximately 1980–2000 (Rosenlof *et al.*, 2001), although the time records are short and the sampling uncertainty is high in many cases.

Global stratospheric water vapour measurements have been made by the Halogen Occultation Experiment (HALOE) satellite instrument for more than a decade (late 1991 to 2004). Interannual changes in water vapour derived from HALOE data show excellent agreement with Polar Ozone and Aerosol Measurement (POAM) satellite data, and also exhibit strong coherence with tropical tropopause temperature changes (Randel *et al.*, 2004). An updated comparison of the HALOE measurements with the Boulder balloon data for the period 1992–2004 is shown in Figure 1.9. The Boulder and HALOE data show

reasonable agreement for the early part of the record (1992–1996), but there is an offset after 1997, with the Boulder data showing higher values than HALOE measurements. As a result, linear trends derived from these two data sets for the (short) period 1992–2004 show very different results (increases for the Boulder data, but not for HALOE). The reason for the differences between the balloon and satellite data (for the same time period and location) is unclear at present, but the discrepancy calls into question interpretation of water vapour trends derived from short or infrequently sampled data records. It will be important to reconcile these differences because these data sets are the two longest and most continuous data records available for stratospheric water vapour.

It is a challenge to explain the magnitude of the water vapour increases seen in the Boulder frost-point data. Somewhat less than half the observed increase of about 10% per decade (through 2001) can be explained as a result of increasing tropospheric methane (transported to the stratosphere and oxidized to form water vapour). The remaining increase could be reconciled with a warming of the tropical tropopause of approximately 1 K per decade, assuming that air entered the stratosphere with water vapour in equilibrium with ice. However, observations suggest that the tropical tropopause has cooled slightly for this time period, by approximately 0.5 K per decade, and risen slightly in altitude by about 20 m per decade (e.g., Seidel *et al.*, 2001; Zhou *et al.*, 2001). Although regional-scale processes may also influence stratospheric water vapour (such as summer monsoon circulations, e.g., Potter and Holton, 1995), there is no evidence

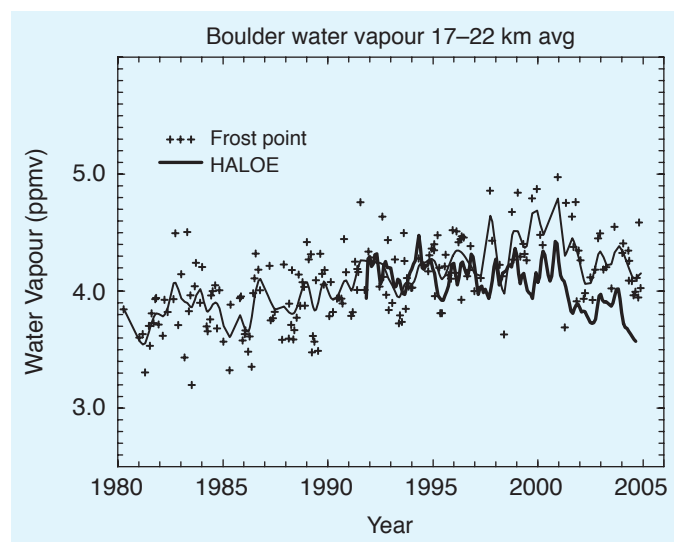


Figure 1.9. Time-series of stratospheric water vapour. Symbols show frost-point hygrometer measurements (averaged over 17–22 km) from Boulder, Colorado covering 1980–2004. The thin line shows a smooth fit through the measurements, using a running Gaussian window with a half-width of three months. The heavy line shows HALOE satellite water vapour data during 1992–2004 for the same altitude region, and using measurements near Boulder (over latitudes 35°N–45°N and longitudes 80°W–130°W). Note the difference between the two data sets after about 1997. Updated from Randel *et al.* (2004).

for increases in tropopause temperature in these regions either (Seidel *et al.*, 2001). From this perspective, the extent of the decadal water vapour increases inferred from the Boulder measurements is inconsistent with the observed tropical tropopause cooling, and this inconsistency limits confidence in predicting the future evolution of stratospheric water vapour.

The atmospheric abundance of methane has increased by a factor of about 2.5 since the pre-industrial era (IPCC, 2001, Chapter 4). Measurements of methane from a global monitoring network showed increasing values through the 1990s, but approximately constant values during 1999–2002 (Dlugokenky *et al.*, 2003). Changes in stratospheric methane have been monitored on a global scale using HALOE satellite measurements since 1991. The HALOE data show increases in lower stratospheric methane during 1992–1997 that are in reasonable agreement with tropospheric increases during this time (Randel *et al.*, 1999). In the upper stratosphere the HALOE data show an overall decrease in methane since 1991, which is likely attributable to a combination of chemical and dynamical influences (Nedoluha *et al.*, 1998; Considine *et al.*, 2001; Röckmann *et al.*, 2004).

Measurements of tropospheric N₂O show a consistent increase of about 3% per decade (IPCC, 2001, Chapter 4). Because tropospheric air is transported into the stratosphere, these positive N₂O trends produce increases in stratospheric reactive nitrogen (NO_y), which plays a key role in ozone photochemistry. Measurements of stratospheric column NO₂ (a main component of NO_y) from the SH (1980–2000) and the NH (1985–2000) mid-latitudes (about 45°) show long-term increases of approximately 6% per decade (Liley *et al.*, 2000; WMO, 2003, Chapter 4), and these are reconciled with the N₂O changes by considering effects of changing levels of stratospheric ozone, water vapour and halogens (Fish *et al.*, 2000; McLinden *et al.*, 2001).

1.2.4 Observed temperature changes in the stratosphere

There is strong evidence of a large and significant cooling in most of the stratosphere since 1980. Recent updates to the observed changes in stratospheric temperature and to the understanding of those changes have been presented in Chapters 3 and 4 of WMO (2003). Current long-term monitoring of stratospheric temperature relies on satellite instruments and radiosonde analyses. The Microwave Sounding Unit (MSU) and Stratospheric Sounding Unit (SSU) instruments record temperatures in several 10–15 km thick layers between 17 and 50 km in altitude. Radiosonde trend analyses are available up to altitudes of roughly 25 km. Determining accurate trends with these data sets is difficult. In particular the radiosonde coverage is not global and suffers from data quality concerns, whereas the satellite trend data is a result of merging data sets from several different instruments. Figure 1.4b shows global temperature time-series in the lower and middle stratosphere derived from satellites and radiosondes. It reveals a strong imprint of 1 to 2 years of warming following the volcanic eruptions of Agung (1963), El Chichón (1982) and Mt. Pinatubo (1991).

When these years are excluded from long-term trend analyses, a significant global cooling is seen in both the radiosonde and the satellite records over the last few decades. This cooling is significant (at the 97% level or greater) at all levels of the stratosphere except the 30 km (10 hPa) level in the SSU record (Figure 1.10). The largest global cooling is found in the upper stratosphere, where it is fairly uniform in time at a rate of about 2 K per decade (for 1979–1997). In the lower stratosphere (below 25 km) this long-term global cooling manifests itself as more of a step-like change following the volcanic warming events (Figure 1.4b). The cooling also varies with latitude. The lower stratosphere extratropics (from 20° to 60° latitude) show a cooling of 0.4–0.8 K per decade in both hemispheres, which remains roughly constant throughout the year. At high latitudes most of the cooling, up to 2 K per decade for both hemispheres, occurs during spring.

Much recent progress has been made in modelling these temperature trends (see Shine *et al.*, 2003; WMO, 2003, Chapters 3 and 4). Models range from one-dimensional (1-D) fixed dynamical heating rate (FDH) calculations to three-dimensional (3-D) coupled chemistry-climate models; many of their findings are presented later in this chapter. FDH is a simple way of determining the radiative response to an imposed change whilst ‘fixing’ the background dynamical heating to its climatological value; this makes the calculation of temperature change simpler, as only a radiation model needs to be used. Changes in dynamical circulations simulated by models can lead to effects over latitudinal bands, which vary between models. However, dynamics cannot easily produce a global mean temperature change. Because of this, global mean temperature is radiatively controlled and provides an important focus for attribution (Figure 1.10). For the global mean in the upper stratosphere the models suggest roughly equal contributions to the cooling from ozone decreases and carbon dioxide increases. In the global mean mid-stratosphere there appears to be some discrepancy between the SSU and modelled trends near 30 km: models predict a definite radiative cooling from carbon dioxide at these altitudes, which is not evident in the SSU record. In the lower stratosphere the cooling from carbon dioxide is much smaller than higher in the stratosphere. Although ozone depletion probably accounts for up to half of the observed cooling trend, it appears that a significant cooling from another mechanism may be needed to account for the rest of the observed cooling. One possible cause of this extra cooling could be stratospheric water vapour increases. However, stratospheric water vapour changes are currently too uncertain (see Section 1.2.3) to pinpoint their precise role. Tropospheric ozone increases have probably contributed slightly to lower stratospheric cooling by reducing upwelling thermal radiation; one estimate suggests a cooling of 0.05 K per decade at 50 hPa and a total cooling of up to 0.5 K over the last century (Sexton *et al.*, 2003). The springtime cooling in the Antarctic lower stratosphere is almost certainly nearly all caused by stratospheric ozone depletion. However, the similar magnitude of cooling in the Arctic spring does not seem to be solely caused by ozone changes, which are much smaller

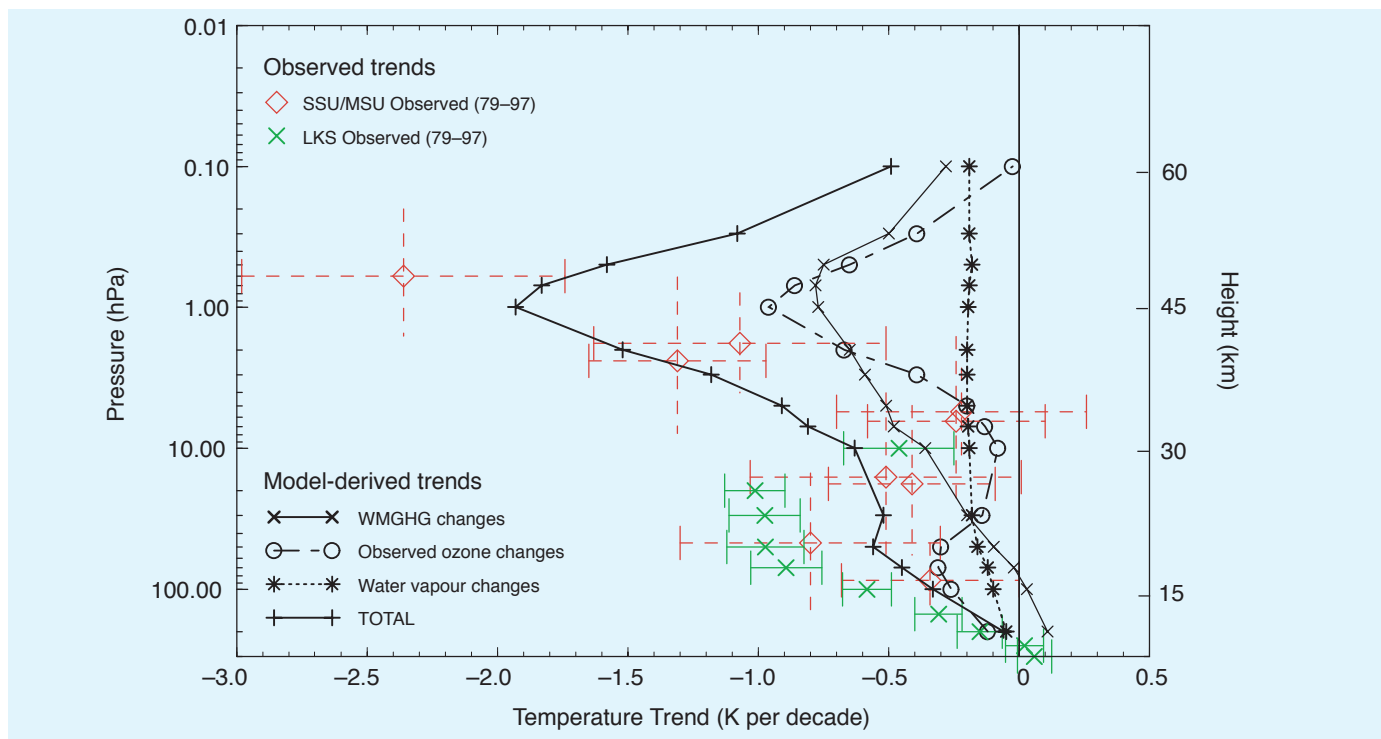


Figure 1.10. Observed and model-derived global and annual mean temperature trends in the stratosphere. The model-derived trends show the contributions of observed changes in WMGHGs, ozone and water vapour to the total temperature trend, based on an average of several model results for ozone and WMGHGs and a single model result for stratospheric water vapour, which is based on satellite-derived trends. The satellite temperature trends are from MSU and SSU (WMO, 2003, Chapter 4) and the radiosonde trends are from the LKS data set. The horizontal bars show the 2σ errors in the observations; the vertical bars give the approximate altitude range sensed by the particular satellite channel. After Shine *et al.* (2003).

than in the Antarctic; interannual variability may contribute substantially to the cooling observed in the Arctic wintertime (see Section 1.4.1).

One mechanism for altering temperatures in the upper troposphere and lower stratosphere comes from the direct radiative effects of halocarbons (WMO, 1986; Ramaswamy *et al.*, 1996; Hansen *et al.*, 1997). In contrast with the role of carbon dioxide, halocarbons can actually warm the upper tropospheric and lower stratospheric region (see Box 1.4).

In summary, stratospheric temperature changes over the past few decades are significant (they are, in fact, substantially larger than those seen in the surface temperature record over the same period), and there are clear quantifiable features of the contributions from ozone, carbon dioxide and volcanism in the past stratospheric temperature record. More definite attribution of the causes of these trends is limited by the short time-series. Future increases of carbon dioxide can be expected to substantially cool the upper stratosphere. However, this cooling could be partially offset by any future ozone increase (Section 1.4.2). In the lower stratosphere, both ozone recovery and halocarbon increases would warm this region compared with the present. Any changes in stratospheric water vapour or changes in tropospheric conditions, such as high-cloud properties and tropospheric ozone, would also affect future temperatures in

the lower stratosphere. Furthermore, circulation changes can affect temperatures over sub-global scales, especially at mid- and polar latitudes. Several studies have modelled parts of these expected temperature changes, and are discussed in the rest of this chapter (see especially Section 1.4.2).

1.3 Stratospheric ozone and climate feedback processes

The distribution of ozone depends on a balance between chemical processes, which can be affected by changes in the concentration of the ODSs, and transport processes, which can be affected by climate change. Climate change, in its broadest sense, can also affect ozone chemistry directly by modifying the rates of temperature-dependent reactions. These interactions are discussed in Sections 1.3.1 to 1.3.4. In these sections we also discuss the possible impact on ozone of changing stratospheric water vapour abundances, which may be regulated by climate.

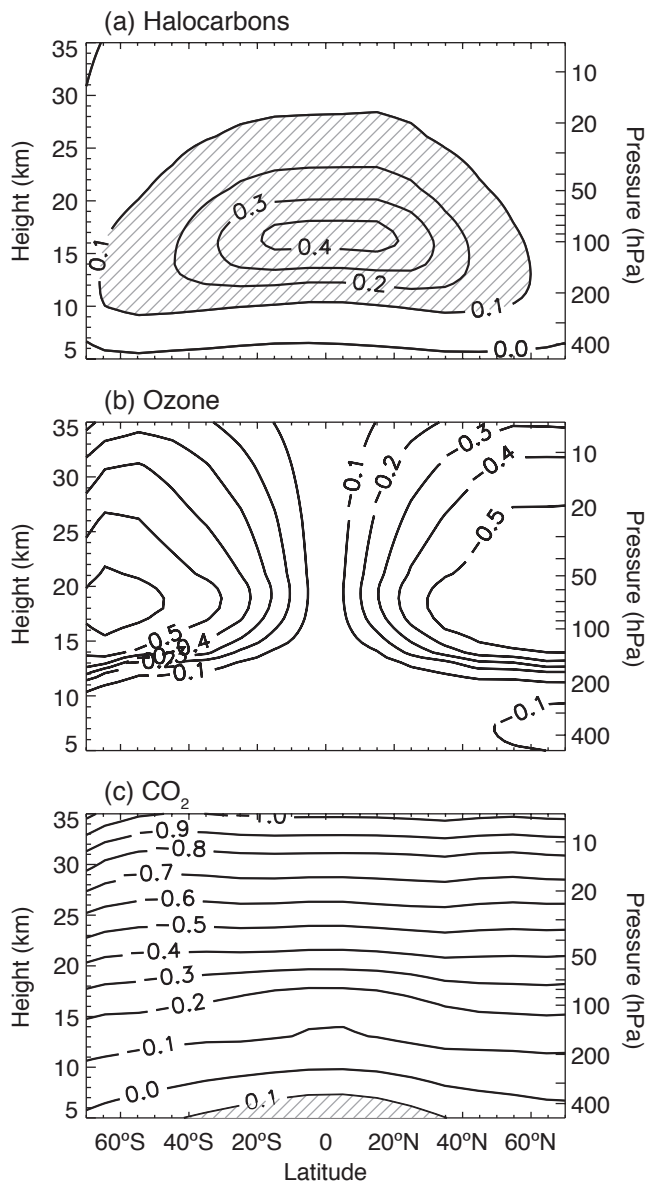
Changes in stratospheric ozone can also affect climate. The impact of ozone changes on stratospheric temperatures has already been discussed in Section 1.2.4. As well as the direct impact of ozone as an absorber of UV radiation and as a greenhouse gas, there are other effects that could be important. For example, changes in ozone could affect the lifetime of reactive

Box 1.4. Halocarbons and the tropical tropopause

Halocarbons and carbon dioxide are greenhouse gases: they trap longwave radiation to warm the Earth's surface. However, compared with carbon dioxide halocarbons have quite different spectral absorption characteristics and they interact very differently with the Earth's radiation field. The very strong 15 μm band dominates the role of carbon dioxide, whereas the halocarbons tend to absorb weakly in the 8–13 μm atmospheric window, a region of the spectrum where other gases have only a small effect on outgoing longwave radiation. These absorption properties, combined with a typical vertical temperature profile, means that halocarbons usually warm the atmosphere locally, whereas carbon dioxide generally cools it (the atmosphere only warms as a response to the induced surface warming). Further, this effect is largest at the tropical tropopause (about 17 km altitude), where temperatures are most different from those of the underlying surface (e.g., Dickinson, 1978; Wang *et al.*, 1991). The tropical tropopause can be defined as the height at which the coldest temperatures are found in a vertical temperature profile (see Figure 1.1b). The effects of halocarbon, carbon dioxide and ozone changes are contrasted in the figure in this box.

Panel (a) shows that halocarbons may have warmed the tropical upper troposphere and lower stratosphere by as much as 0.3 K, which is locally larger than the cooling effects of carbon dioxide. For the calculation of a globally averaged temperature change this warming can be thought of as partially cancelling out the cooling effect of ozone depletion in the extra-tropical lower stratosphere. However, the patterns are quite distinct (compare panels (a) and (b)), and as a result the equator-to-pole temperature gradient in the lower stratosphere, where temperature increases towards higher latitudes, would be reduced.

Although halocarbons are potentially important, because of their coupling to water vapour, it is unlikely that halocarbons dominate the response of the tropical tropopause to changing greenhouse gases, as there is some observational evidence for a general cooling of the tropical tropopause over the last few decades (Seidel *et al.*, 2001; Zhou *et al.*, 2001).



Box 1.4, Figure. The expected contribution (in kelvin) to the upper-tropospheric and lower-stratospheric temperature changes over 1970–2000 from changes in (a) halocarbons, (b) ozone and (c) carbon dioxide. Results are based on FDH model calculations. The hatched area denotes positive changes greater than 0.1 K. After Forster and Joshi (2005).

greenhouse gases, by changing the penetration of UV radiation. Changes in the structure of the stratosphere, caused by ozone changes, could alter the interaction between the troposphere and stratosphere and lead to further changes in stratospheric ozone. These latter interactions are discussed in Sections 1.3.5 and 1.3.6.

Improved knowledge of these various feedback processes is essential for informing the numerical models used to predict future chemistry-climate interactions; these models are discussed in Section 1.4.

Note that other factors, which are not discussed in detail here, can also affect the interaction between ozone and climate. Perhaps the most obvious is the impact of major volcanic eruptions. These can lead to an increase in volcanic aerosol in the stratosphere, which can influence both climate and the chemical processes controlling the ozone layer.

1.3.1 Impact of ODSs on stratospheric ozone

The abundance of ozone in the stratosphere at a particular location is governed by three processes: photochemical production, destruction by catalytic cycles, and transport processes. Photochemical production in the stratosphere occurs mostly through the photolysis of O_2 , with loss via catalytic cycles involving hydrogen (HO_x), nitrogen (NO_x), and halogen (ClO_x , BrO_x) radicals (see Box 1.1). The relative importance of the various loss cycles in the stratosphere varies substantially with altitude (Figure 1.11). Above about 45 km, loss through HO_x dominates, while below this altitude NO_x -catalyzed ozone loss is most important. The importance of the ClO_x -catalyzed ozone loss cycle, which varies with chlorine loading, peaks at about 40 km. Below about 25 km HO_x -driven ozone loss cycles dominate again.

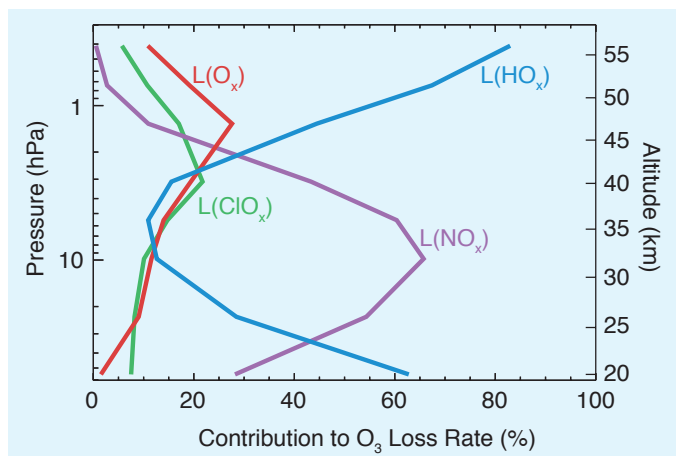


Figure 1.11. The vertical distribution of the relative importance of the individual contributions to ozone loss by the HO_x , ClO_x and NO_x cycles as well as the Chapman loss cycle (O_x). The calculations are based on HALOE (V19) satellite measurements and are for overhead sun ($23^\circ S$, January) and for total inorganic chlorine (Cl_y) in the stratosphere corresponding to 1994 conditions. Reaction rate constants were taken from DeMore *et al.* (1997). Updated and extended in altitude range from Grooß *et al.* (1999) and Chapter 6 of WMO (1999).

1.3.1.1 Upper stratosphere

In the upper stratosphere the ozone budget is largely understood, although uncertainties remain regarding the rate constants of key radical reactions. In particular, strong evidence has been accumulated that the observed ozone depletion in the upper stratosphere is caused by increased levels of stratospheric chlorine (WMO, 1999, Chapter 6; WMO, 2003, Chapter 4), as originally proposed by Molina and Rowland (1974) and Crutzen (1974). Because of the direct correspondence between the stratospheric chlorine abundance and ozone depletion in the upper stratosphere, it has been suggested (e.g., WMO, 1999, Chapter 12) that the response of stratospheric ozone to the declining stratospheric chlorine levels might be first detectable in the upper stratosphere (see also Box 1.7 in Section 1.4.2).

1.3.1.2 Polar regions

In recent decades stratospheric ozone losses have been most pronounced in polar regions during winter and spring (WMO 2003, Chapter 3; see also Figures 1.5 and 1.6). These losses are determined largely by three chemical factors: (1) the conversion of chlorine reservoirs into active, ozone-destroying forms through heterogeneous reactions on the surfaces of polar stratospheric cloud particles; (2) the availability of sunlight that drives the catalytic photochemical cycles that destroy ozone; and (3) the timing of the deactivation of chlorine (i.e., the timing of the conversion of active chlorine back to the reservoir species). Temperature controls the formation and destruction of polar stratospheric clouds (PSCs) and thus the timing of activation (1) and deactivation (3) of chlorine. Furthermore, temperature controls the efficiency of the catalytic cycles (especially the ClO dimer cycle; see Box 1.1) that destroy ozone in the presence of sunlight (2).

However, polar ozone loss would not occur without a prominent dynamical feature of the stratosphere in winter and spring: the polar vortex. In both hemispheres, the polar vortex separates polar air from mid-latitude air to a large extent, and within the vortex the low-temperature conditions that develop are the key factor for polar ozone loss. These two factors are dynamically related: a strong vortex is generally also a colder vortex. The two crucial questions for future polar ozone are whether, in an increased greenhouse-gas climate, the region of low stratospheric temperatures will increase in area and whether it will persist for longer in any given year (see Section 1.3.2).

When anthropogenically emitted ODSs are eventually removed from the stratosphere, the stratospheric halogen burden will be much lower than it is today and will be controlled by the naturally occurring source gases methyl chloride (CH_3Cl) and methyl bromide (CH_3Br). Under such conditions, dramatic losses of polar ozone in winter and spring as we see today are not expected to occur. However, the rate of removal of anthropogenic halogens from the atmosphere depends on the atmospheric lifetimes of CFCs (typically 50–100 years) and is considerably slower than the rate at which halogens have been increasing in the decades prior to approximately the year 2000, when the stratospheric halogen loading peaked (Figure 1.7). A

complete removal of anthropogenic halogens from the atmosphere will take more than a century. During this period of enhanced levels of halogens caused by past anthropogenic emissions, the polar stratosphere will remain vulnerable to climate perturbations, such as increasing water vapour or a cooling of the stratosphere, that lead to enhanced ozone destruction.

1.3.1.3 Lower-stratospheric mid-latitudes

It is well established that ozone in the lower stratosphere at mid-latitudes has been decreasing for a few decades; both measurements of ozone locally in the lower stratosphere and measurements of column ozone (a quantity that is dominated by the amount of ozone in the lower stratosphere) show a clear decline (WMO, 2003, Chapter 4). However, because mid-latitude ozone loss is much less severe than polar ozone loss, it cannot be identified in measurements in any one year but is rather detected as a downward trend in statistical analyses of longer time-series. It is clear that chemical loss driven by halogens is very important, but other possible effects that may contribute to the observed mid-latitude trends have also been identified. A definitive quantitative attribution of the trends to particular mechanisms has not yet been achieved. Chapter 4 of WMO (2003) reviewed this issue most recently; we will not repeat that detailed analysis here but instead provide a brief summary.

The chemical processes that may affect trends of mid-latitude ozone are essentially related to the ODS trends that are known to be responsible for the observed ozone loss in the upper stratosphere and in the polar regions. (Transport effects are discussed in Section 1.3.4.) Halogen chemistry may lead to ozone depletion in the mid-latitude lower stratosphere through a number of possible mechanisms, including:

1. Export of air that has encountered ozone destruction during the winter from the polar vortex (e.g., Prather *et al.*, 1990).
2. Export of air with enhanced levels of active chlorine from the polar vortex (e.g., Prather and Jaffe, 1990; Norton and Chipperfield, 1995).
3. *In situ* activation of chlorine either on cold liquid sulfate aerosol particles (e.g., Keim *et al.*, 1996) or on ice particles (e.g., Borrmann *et al.*, 1997; Bregman *et al.*, 2002). Further, the reaction of N_2O_5 with water on liquid aerosol particles at higher temperatures indirectly enhances the concentrations of ClO at mid-latitudes (McElroy *et al.*, 1992).
4. Ozone depletion due to elevated levels of BrO in the lower stratosphere, possibly caused by transport of very short-lived halogen-containing compounds or BrO across the tropopause (WMO, 2003, Chapter 2).

The first mechanism results from transport combined with polar ozone loss, whereas the remaining three mechanisms all involve *in situ* chemical destruction of ozone at mid-latitudes. All four mechanisms listed above are ultimately driven by the increase of halogens in the atmosphere over the past decades. Thus, while Millard *et al.* (2002) emphasized the strong interannual variability in the relative contributions of the different mechanisms to the seasonal mid-latitude ozone loss during the

winter-spring period, they nonetheless showed that ozone loss driven by catalytic cycles involving halogens was always an important contributor (40–70%) to the simulated mid-latitude ozone loss in the five winters in the 1990s that they studied. Similarly, Chipperfield (2003) found that the observed mid-latitude column ozone decrease from 1980 to the early 1990s could be reproduced in long-term simulations in a 3-D chemistry-transport model (CTM). The modelled ozone is affected by dynamical interannual variability, but the overall decreases are dominated by halogen trends; and about 30–50% of the modelled halogen-induced change is a result of high latitude processing on PSCs.

Under climate change the strength of the polar vortex may change (see Section 1.3.2), but the sign of this change is uncertain. A change in the strength and temperature of the vortex will affect chlorine activation and ozone loss there and, through mechanisms (1) and (2), ozone loss in mid-latitudes.

The possibility that chlorine might be activated on cirrus clouds or on cold liquid aerosol particles in the lowermost stratosphere (mechanism (3)) was revisited recently by Bregman *et al.* (2002). Based on their model results it seems unlikely that this process is the main mechanism for the observed long-term decline of ozone in the mid-latitude lower stratosphere.

Very short-lived organic chlorine-, bromine-, and iodine-containing compounds possess a potential to deplete stratospheric ozone. However a quantitative assessment of their impact on stratospheric ozone is made difficult by their short lifetime, so there is need to consider the transport pathways from the troposphere to the stratosphere of these compounds in detail (WMO, 2003, Chapter 2). An upper limit for total stratospheric iodine, I_y , of 0.10 ± 0.02 ppt was recently reported (for below 20 km) by Bösch *et al.* (2003). The impact of this magnitude of iodine loading on stratospheric ozone is negligible.

The disturbance of the mid-latitude ozone budget caused by anthropogenic emissions of ODSs will ultimately cease when the stratospheric halogen burden has reached low enough levels (see Section 1.2.2 and Box 1.7 in Section 1.4.2). However, like polar ozone, mid-latitude ozone will for many decades remain vulnerable to an enhancement of halogen-catalyzed ozone loss caused by climate change and by natural phenomena such as volcanic eruptions.

1.3.2 Impact of temperature changes on ozone chemistry

The increasing abundance of WMGHGs in the atmosphere is expected to lead to an increase in temperature in the troposphere. Furthermore, increasing concentrations of most of these gases, notably CO_2 , N_2O and CH_4 , are expected to lead to a temperature decrease in the stratosphere. By far the strongest contribution to stratospheric cooling from the WMGHGs comes from CO_2 (Section 1.2.4). As noted in Section 1.2.4, temperatures in the stratosphere are also believed to have decreased in part because of the observed reductions in ozone concentrations; any such cooling would have a feedback on the ozone changes.

Decreasing stratospheric temperatures lead to a reduction of

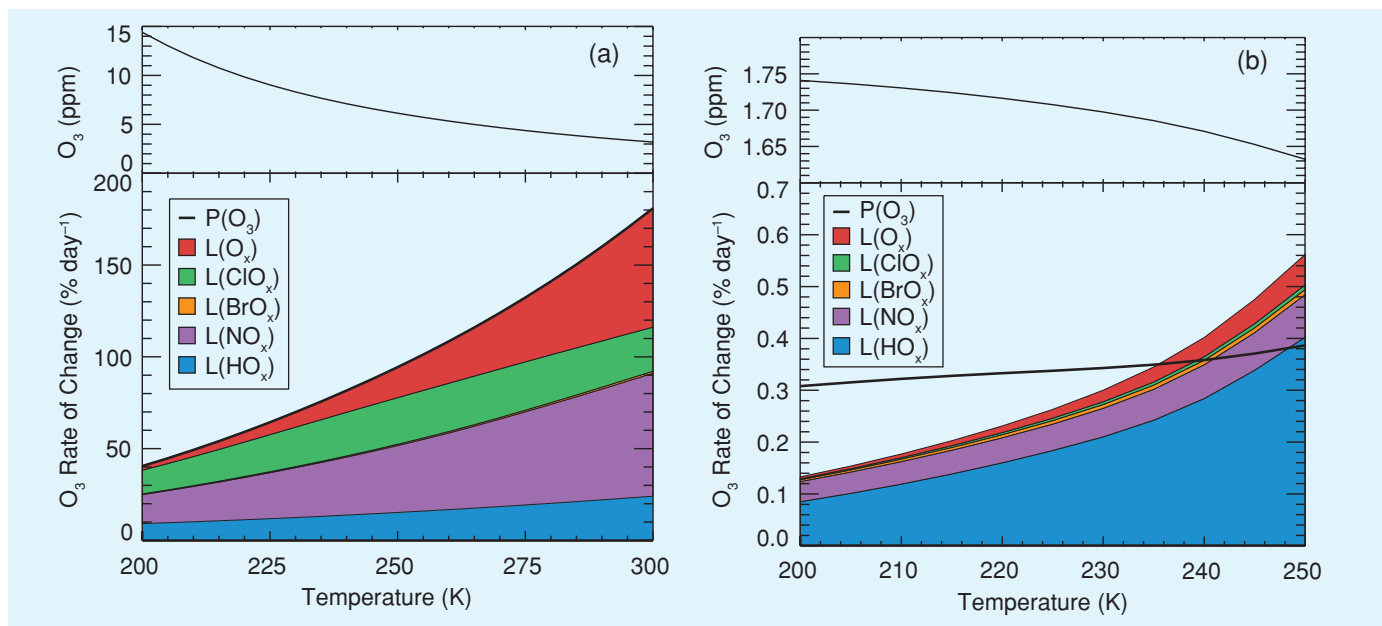


Figure 1.12. An estimate of the contribution of the various ozone loss cycles to the ozone loss rate, together with the ozone production rate $P(\text{O}_3)$, at 45°N for equinox conditions (end of March) as a function of temperature (bottom panels). The estimates were obtained from short (20-day) runs of a chemical box model, starting from climatological values of ozone; the ozone mixing ratios at the end of the run are shown in the top panels. Panels (a) show conditions for 40 km altitude (2.5 hPa), where the climatological temperature is about 250 K; panels (b) show conditions for 20 km (55 hPa), where the climatological temperature is about 215 K. Reaction rate constants were taken from Sander *et al.* (2003). The production and loss rates are for the simulated ozone value. Note that at 40 km ozone is in steady-state (i.e., production equals the sum of all loss terms) and thus ozone is under photochemical control. At 20 km ozone production does not equal loss, implying that transport also has a strong influence on ozone concentrations. At 20 km the simulated ozone value after 20 days remains close to its initial climatological value of 1.70 ppm.

the ozone loss rate in the upper stratosphere, thereby indirectly leading to more ozone in this region. This reduction of ozone loss is caused by the very strong positive temperature dependence of the ozone loss rate, mainly owing to the Chapman reactions and the NO_x cycle (Figure 1.12). This inverse relationship between ozone and temperature changes in the upper stratosphere has been known for many years (Barnett *et al.*, 1975). More recently, differences in temperature between the two hemispheres have been identified (Li *et al.*, 2002) as a cause of inter-hemispheric differences in both the seasonal cycle of upper-stratospheric ozone abundances and in the upper-stratospheric ozone trend deduced from satellite measurements.

In the mid-latitude lower stratosphere, one mechanism that leads to ozone loss and is directly sensitive to temperature changes involves heterogeneous reactions on the surfaces of cloud and cold aerosol particles (see mechanism (3) in Section 1.3.1.3). The rates of many of these reactions increase strongly with decreasing temperature. Similarly, the reaction rates increase with increasing water-vapour concentrations, so that future increases in water, should they occur, would also have an impact (see Sections 1.2.3 and 1.3.3). Note, however, that in the lower-stratospheric mid-latitudes the most important heterogeneous reactions are hydrolysis of N_2O_5 and bromine nitrate, which are relatively insensitive to temperature and water vapour concentrations. Therefore, the expected impact of cli-

mate change on the chemical mechanism (3) is expected to be relatively small. In addition to this impact on heterogeneous chemistry, Zeng and Pyle (2003) have argued that a reduction in temperature in the lower stratosphere can slow the rate of HO_x -driven ozone destruction.

Polar ozone loss occurs when temperatures in a large enough region sink below the threshold temperature for the existence of PSCs (approximately 195 K), because chlorine is activated by heterogeneous reactions on the surfaces of PSCs. Therefore, a cooling of the stratosphere enhances Arctic ozone loss if the volume of polar air with temperatures below the PSC threshold value increases. (The Antarctic in winter and spring is already consistently below this threshold.) Moreover, a stronger PSC activity is expected to lead to a greater denitrification of the Arctic vortex, hence a slower deactivation of chlorine and, consequently, a greater chemical ozone loss (Waibel *et al.*, 1999; Tabazadeh *et al.*, 2000). Rex *et al.* (2004) have deduced an empirical relation between observed temperatures and observed winter-spring chemical loss of Arctic ozone (Figure 1.13). Based on this relation, and for current levels of chlorine, about 15 DU additional loss of total ozone is expected for each 1 K cooling of the Arctic lower stratosphere.

Although the lower stratosphere is expected to generally cool with increasing greenhouse-gas concentrations (Section 1.2.4), the temperature changes in the lower stratosphere dur-

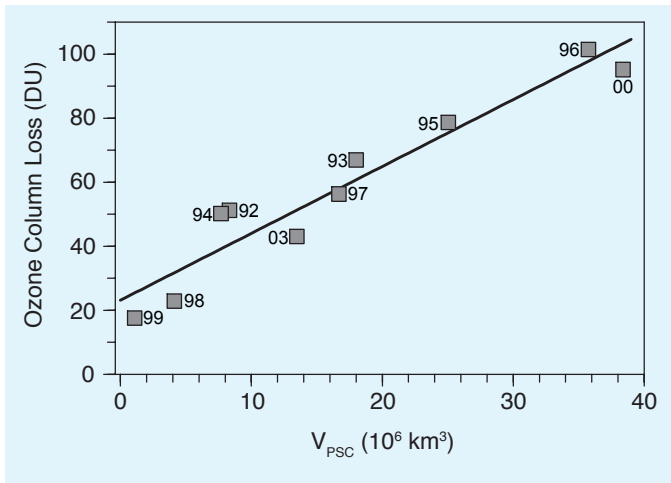


Figure 1.13. The overall chemical loss in average polar column ozone during a given Arctic winter versus the winter average of the stratospheric volume where conditions were cold enough (based on ECMWF temperature data) for the existence of PSCs (V_{PSC}). Also shown is the linear fit to the data. The calculations could not be performed for 2001 or 2002. Adapted from Rex *et al.* (2004).

ing the polar wintertime will be sensitive to any change in circulation associated with dynamical feedbacks, principally from changes in planetary wave drag (see Section 1.3.4.1). In principle, these feedbacks could be of either sign and thus could lead to enhanced cooling or even to warming. An early model study found enhanced cooling, to the extent that polar ozone loss would be expected to increase during the next 10 to 15 years even while halogen levels decreased (Shindell *et al.*, 1998). More recent studies with higher-resolution models have found a much less dramatic dynamical feedback, with some models showing an increase and some a decrease in planetary wave drag, and with all models predicting a relatively small change in Arctic ozone over the next few decades (Austin *et al.*, 2003). However, it should be noted that model results for the Arctic are difficult to assess because the processes leading to polar ozone depletion show so much natural variability that the atmosphere may evolve anywhere within (or even outside) the envelope provided by an ensemble of model simulations (see Section 3.5 of WMO, 2003).

In any event, it is the Arctic that is most sensitive to the effects caused by climate change that are discussed above. Present-day temperatures in the Arctic lie close to the threshold value for the onset of heterogeneous chlorine activation and thus close to the threshold value for the onset of rapid ozone loss chemistry; in the Antarctic temperatures are much lower and thus ozone loss is not as sensitive to temperature changes.

1.3.3 Impact of methane and water vapour changes on ozone chemistry

With the exception of the high latitudes in winter, ozone in the upper stratosphere is in a photochemical steady-state; photo-

chemical reactions are sufficiently fast that ozone concentrations are determined by a local balance between photochemical production and loss. Nonetheless, transport has a significant indirect influence on upper stratospheric ozone insofar as it determines the concentrations of trace compounds such as CH_4 , H_2O , CFCs and N_2O , all of which act as precursors of the radicals that determine the ozone chemistry. Furthermore, CH_4 is of particular importance because it is the primary mechanism for the conversion of reactive Cl to the unreactive HCl reservoir via the reaction $\text{CH}_4 + \text{Cl} \rightarrow \text{HCl} + \text{CH}_3$, and thus affects the efficiency of the chlorine-driven ozone loss.

Changes in upper stratospheric CH_4 (Section 1.2.3) have important implications for upper stratospheric ozone. Siskind *et al.* (1998) found that for the period 1992–1995, the increase in active chlorine (Cl and ClO) resulting from the CH_4 decrease was the largest contributor to the ozone changes occurring over that time. Indeed, a measured increase in upper-stratospheric ClO between 1991 and 1997, which is significantly greater than that expected from the increase in the chlorine source gases alone, may be explained by the observed concurrent decrease of CH_4 (Froidevaux *et al.*, 2000). Further, Li *et al.* (2002) find that inter-hemispheric differences in CH_4 are partly responsible (together with inter-hemispheric differences in temperature) for observed differences in upper stratospheric ozone trends between the two hemispheres (from the SAGE I and SAGE II satellite experiments for 1979–1997).

Stratospheric water vapour is the primary source of the HO_x radicals that drive the dominant ozone loss cycles in the upper stratosphere (Figure 1.11). An increase in stratospheric water vapour is therefore expected to lead to a greater chemical loss of ozone in the upper stratosphere (e.g., Siskind *et al.*, 1998). This effect has been investigated quantitatively in model simulations. In a study of conditions for the year 2010, Jucks and Salawitch (2000) find that above 45 km an increase of 1% in the water vapour mixing ratio would completely negate the increase of ozone driven by the 15% decrease of inorganic chlorine that is expected by the year 2010. At 40 km the increase of ozone would still be reduced by about 50%. Shindell (2001) conducted a general circulation model (GCM) study for the period 1979–1996. The simulations show a significant chemical effect of water vapour increases on ozone concentrations, with a reduction of more than 1% between 45 and 55 km, and a maximum impact of about 4% at 50 km. Further, Li *et al.* (2002) found that the annually averaged (downward) ozone trend at 45°S and 1.8 hPa (45 km) increases by 1% per decade for a water vapour increase of 1% yr^{-1} . These model results point to an anticorrelation between ozone and water vapour in the upper stratosphere and lower mesosphere. However, such an anticorrelation is not seen in observations and ozone in this region varies much less than predicted by models (Siskind *et al.*, 2002).

In the mid-latitude lower stratosphere, any increase in water vapour would also be expected to lead to ozone loss because of an intensified HO_x ozone loss cycle (see Box 1.1). The model results of Dvortsov and Solomon (2001) predict that an increase in stratospheric water vapour of 1% yr^{-1} translates to an ad-

ditional depletion of mid-latitude column ozone by 0.3% per decade.

In the polar lower stratosphere, the rates of the heterogeneous reactions that are responsible for the activation of chlorine (which eventually leads to chemical ozone destruction) increase with increasing water vapour concentrations. An increase in stratospheric water vapour essentially means that the temperature threshold at which PSCs form, and thus heterogeneous reactions rates begin to become significant for chlorine activation, is shifted to higher values. If stratospheric water vapour were to increase it could lead to a substantially enhanced Arctic ozone loss in the future (e.g., Kirk-Davidoff *et al.*, 1999).

In considering the above discussion concerning stratospheric water vapour, it needs to be borne in mind that there is considerable uncertainty about the sign of future water vapour changes in light of the puzzling past record (Section 1.2.3).

1.3.4 The role of transport for ozone changes

Transport is a key factor influencing the seasonal and inter-annual variability of stratospheric ozone. Seasonal variations in transport force the large winter-spring build-up of extra-tropical total ozone in both hemispheres, and inter-hemispheric differences in transport (larger in the NH) cause corresponding differences in extra-tropical total ozone (see Box 1.2). In both hemispheres, mid-latitude ozone decreases during summer and returns to approximate photochemical balance by autumn, and there is a strong persistence of the dynamically forced anomalies throughout summer (Fioletov and Shepherd, 2003; Weber *et al.*, 2003). The interannual variability in the winter-spring build-up is greater in the NH, reflecting the greater dynamical variability of the NH stratosphere.

1.3.4.1 Stratospheric planetary-wave-induced transport and mixing

Large-scale transport of ozone is a result of advection by the Brewer-Dobson circulation and of eddy transport effects; both of these mechanisms are first-order terms in the zonal mean ozone transport equation (Andrews *et al.*, 1987). The strength of the Brewer-Dobson circulation is directly tied to dissipating planetary waves forced from the troposphere, and eddy transports of ozone are also linked to planetary wave activity (although this latter linkage is difficult to quantify), so that net ozone transport is tied to the variability of forced planetary waves. The amount of dissipating wave activity (also called planetary wave drag, PWD) within the stratosphere is related to the vertical component of wave activity entering the lower stratosphere (the so-called Eliassen-Palm (EP) flux). This quantity can be derived from conventional meteorological analyses and is a convenient proxy used to quantify PWD. A significant correlation has been found between interannual changes in PWD and total ozone build-up during winter and spring (Fusco and Salby, 1999; Randel *et al.*, 2002). The fact that the effect of PWD on ozone is seasonal and has essentially no interannual memory suggests that long-term changes in PWD can be

expected to lead to long-term changes in winter-spring ozone, all else being equal. However, although the basic physics of the ozone-PWD connection is well understood, its quantification via correlations is at best crude, and this limits our ability to attribute changes in ozone to changes in PWD.

In the NH, there have been interannual variations in various meteorological parameters during the period 1980–2000 that together paint a fairly consistent, albeit incomplete, picture. During the mid-1990s the NH exhibited a number of years when the Arctic wintertime vortex was colder and stronger (Graf *et al.*, 1995; Pawson and Naujokat, 1999) and more persistent (Waugh *et al.*, 1999). Any dynamically induced component of these changes requires a weakened Brewer-Dobson circulation, which in turn requires a decrease in PWD. Such a decrease in PWD during this period has been documented (Newman and Nash, 2000), although the results were sensitive to which months and time periods were considered. Randel *et al.* (2002) show that for the period 1979–2000, PWD in the NH increased during early winter (November to December) and decreased during mid-winter (January to February). This seasonal variation is consistent with the Arctic early winter warming and late winter cooling seen over the same time period at 100 hPa (Langematz *et al.*, 2003; see also Figure 1.16 in Section 1.4.1.2). The weakened Brewer-Dobson circulation during mid-winter implies a decrease in the winter build-up of mid-latitude ozone, and Randel *et al.* (2002) estimated that the decreased wave driving may account for about 20–30% of the observed changes in ozone in the January to March period. Changes in SH dynamics are not as clear as in the NH, primarily because meteorological reanalysis data sets are less well constrained by observations.

Planetary waves, in addition to affecting the temperature and chemistry of the polar stratosphere through the processes described earlier, can also displace the centre of the polar vortex off the pole. This has important implications for ozone and NO_x chemistry because air parcel trajectories within the vortex are then no longer confined to the polar night but experience short periods of sunlight (Solomon *et al.*, 1993). Polar ozone loss processes are usually limited by the poleward retreat of the terminator (the boundary that delineates polar night). Planetary wave distortion of the vortex can expose deeper vortex air to sunlight (Lee *et al.*, 2000) and cause ozone depletion chemistry to start earlier than it would have otherwise. In this way, wave-induced displacements of the vortex can drive a mid-winter start to Antarctic ozone depletion (Roscoe *et al.*, 1997; Bodeker *et al.*, 2001).

Because wave-induced forcing in the stratosphere is believed to come primarily from planetary-scale Rossby waves that are generated in the troposphere during wintertime, future changes in the generation of tropospheric waves may influence polar ozone abundance. However there is as yet no consensus from models on the sign of this change (Austin *et al.*, 2003).

1.3.4.2 Tropopause variations and ozone mini-holes

Tropospheric circulation and tropopause height variations also

affect the mid-latitude distribution of column ozone. The relationship between local mid-latitude tropopause height and column ozone on day-to-day time scales is well documented (e.g., Dobson, 1963; Bojkov *et al.*, 1993). Day-to-day changes in tropopause height are associated with the passage of synoptic-scale disturbances in the upper troposphere and lower stratosphere, which affect ozone in the lower stratosphere through transport (Salby and Callaghan, 1993) and can result in large local changes in column ozone, particularly in the vicinity of storm tracks (James, 1998). In extreme situations, they can lead to so-called ozone mini-holes, which occur over both hemispheres and have the lowest column ozone levels observed outside the polar vortices, sometimes well under 220 DU (Allaart *et al.*, 2000; Hood *et al.*, 2001; Teitelbaum *et al.*, 2001; Canziani *et al.*, 2002). Ozone mini-holes do not primarily entail a destruction of ozone, but rather its re-distribution. Changes in the spatial and temporal occurrence of synoptic-scale processes and Rossby wave breaking (e.g., storm track displacements) that are induced by climate change or natural variability, could lead to changes in the distribution or frequency of the occurrence of mini-hole and low-ozone events, and thus to regional changes in the mean column ozone (Hood *et al.*, 1999; Reid *et al.*, 2000; Orsolini and Limpasuvan, 2001).

Observations have shown that over the NH the altitude of the extra-tropical tropopause has generally increased over recent decades. Radiosonde measurements over both Europe and Canada show an increase in altitude of about 300–600 m over the past 30 years, with the precise amount depending on location (Forster and Tourpali, 2001; Steinbrecht *et al.*, 2001). Consistent regional increases are also seen in meteorological reanalyses over both hemispheres (Hoinka, 1999; Thompson *et al.*, 2000), although reanalysis trend studies should be viewed with care (Bengtsson *et al.*, 2004). Spatial patterns show increases over the NH and SH beginning at mid-latitudes and reaching a maximum towards the poles. The magnitude of the changes can also depend on the longitude.

However, the effects of tropospheric circulation changes on ozone and the relation of both to tropopause height changes remain poorly understood at present. In particular, the relationship between tropopause height and ozone mentioned earlier applies to single stations; there is no reason to expect it to apply in the zonal mean, or on longer time scales (e.g., seasonal or interannual) over which ozone transport is irreversible. Because of our poor understanding of what controls the zonal-mean mid-latitude tropopause height, or whether it is possible to consider such processes in a zonal-mean approach, it is not clear that the ozone-tropopause height correlations (derived from daily or monthly statistics) can be extended to decadal time scales in order to estimate changes in ozone. Some recent model studies suggest that lower stratospheric cooling caused by ozone depletion, acting together with tropospheric warming due to WMGHGs, can be a contributor to tropopause height changes (Santer *et al.*, 2003a,b), in which case the tropopause height changes cannot be entirely considered as a cause of the ozone changes. One source of uncertainty in these model calculations

is that most climate models cannot resolve the observed tropopause height changes, so these must be inferred by interpolation; another is that the observed ozone changes are not well quantified close to the tropopause (WMO, 2003, Chapter 4). Furthermore there remain considerable differences between the various reanalysis products available, as well as between the model results.

1.3.4.3 Stratosphere-troposphere exchange

Stratosphere-troposphere exchange (STE) processes also affect the ozone distribution and have the capability to affect tropospheric chemistry. STE is a two-way process that encompasses transport from the troposphere into the stratosphere (TST) and from the stratosphere into the troposphere (STT) through a variety of processes (see Holton *et al.*, 1995, and references therein). Some aspects of STE are implicit in the preceding discussions. The net mass flux from the troposphere into the stratosphere and back again is driven by PWD through the Brewer-Dobson circulation (Section 1.1.2; Holton *et al.*, 1995). Although the global approach can explain the net global flux, local and regional processes need to be identified and assessed to fully understand the distribution of trace species being exchanged. Such understanding is relevant both for chemical budgets and for climate change and variability studies. Although there is a net TST in the tropics and a net STT in the extratropics, a number of mechanisms that lead to STT in the tropics and TST in the extratropics have been identified (e.g., Appenzeller and Davies, 1992; Poulida *et al.*, 1996; Hintsä *et al.*, 1998; Ray *et al.*, 1999; Lelieveld and Dentener, 2000; Stohl *et al.*, 2003). In the extratropics TST can significantly affect the composition of the lowermost stratosphere, even if the exchange cannot reach higher into the stratosphere, by introducing, during deep TST events, near-surface pollutants, and ozone-poor and humid air. Similarly, deep STT events can transport ozone-rich air into the mid- and lower troposphere. It should be noted, however, that so-called shallow events, with exchanges near the tropopause, remain the main feature in the extratropics. Regions of occurrence of such exchange processes, at least in the NH (Sprenger and Wernli, 2003), appear to be linked to the storm tracks and their variability, that is, in the same region where mini-holes are most frequent.

The past and future variability of STE remains to be assessed. It is clear that changes in planetary wave activity will modify the Brewer-Dobson circulation and hence affect global transport processes (Rind *et al.*, 1990; Butchart and Scaife, 2001). As for regional mechanisms, seasonal and interannual variability, driven, for example, by the North Atlantic Oscillation (NAO) and the El Niño-Southern Oscillation (ENSO), have already been observed (James *et al.*, 2003; Sprenger and Wernli, 2003). Changes in the occurrence of regional and local weather phenomena could also modify STE. Fifteen-year studies with reanalysis products have not yielded any distinct trends (Sprenger and Wernli, 2003). Given the discrepancies between different approaches to evaluate STE and inhomogeneities in meteorological analyses and reanalyses, consistent trend studies are not available as of yet.

1.3.4.4 The tropical tropopause layer

Air enters the stratosphere primarily in the tropics, and hence the physical and chemical characteristics of air near the tropical tropopause behave as boundary conditions for the global stratosphere. The tropical tropopause is relatively high, near 17 km. The tropospheric lapse rate (up to 12–14 km) is determined by radiative-convective equilibrium, whereas the thermal structure above 14 km is primarily in radiative balance, which is characteristic of the stratosphere (Thuburn and Craig, 2002). Overall, the region of the tropical atmosphere between about 12 km and the tropopause has characteristics intermediate to those of the troposphere and stratosphere, and is referred to as the tropical tropopause layer (TTL) (Highwood and Hoskins, 1998). Thin (sometimes subvisible) cirrus clouds are observed over large areas of the TTL (Wang *et al.*, 1996; Winker and Trepte, 1998), although their formation mechanism(s) and effects on large-scale circulation are poorly known. In the tropics, the background clear-sky radiative balance shifts from cooling in the troposphere to heating in the stratosphere, with the transition occurring at around 15 km. The region of heating above about 15 km is linked to mean upward motion into the lower stratosphere, and this region marks the base of the stratospheric Brewer-Dobson circulation.

The TTL is coupled to stratospheric ozone through its control of stratospheric water vapour and by the transport of tropospheric source gases and ODSs into the lower stratosphere, so changes in the TTL could affect the stratospheric ozone layer. If the residence time of air in the TTL before it is transported into the stratosphere is short, then it may be possible that short-lived halogen compounds (natural or anthropogenic replacements for the CFCs) or their degradation products could enter the lower stratosphere and contribute to ozone loss there (WMO, 2003, Chapter 2).

Air entering the stratosphere is dehydrated as it passes through the cold tropical tropopause, and this drying accounts for the extreme aridity of the global stratosphere (Brewer, 1949). Furthermore, the seasonal cycle in tropopause temperature imparts a strong seasonal variation in stratospheric water vapour, which then propagates with the mean stratospheric transport circulation (Mote *et al.*, 1996). Year-to-year variations in tropical tropopause temperatures are also highly correlated with global stratospheric water vapour anomalies (Randel *et al.*, 2004), although there remain some issues concerning the consistency of decadal-scale changes in water vapour (Section 1.2.3). However, while there is strong empirical coupling between tropopause temperatures and stratospheric water vapour, details of the dehydration mechanism(s) within the TTL are still a topic of scientific debate (Holton and Gettelman, 2001; Sherwood and Dessler, 2001). One critical, unanswered question is whether, and how, the TTL will change in response to climate change and what will be the resulting impact on stratospheric ozone.

1.3.5 Stratosphere-troposphere dynamical coupling

Analysis of observational data shows that atmospheric circulation tends to maintain spatially coherent, large-scale patterns for extended periods of time, and then to shift to similar patterns of opposite phase. These patterns represent preferred modes of variability of the coupled atmosphere-ocean-land-sea-ice system. They fluctuate on intra-seasonal, seasonal, interannual and decadal time scales, and are influenced by externally and anthropogenically caused climate variability. Some of the patterns exhibit seesaw-like behaviour and are usually called oscillations. A few circulation modes, listed below, have been implicated in stratosphere-troposphere dynamical coupling, and thus may provide a coupling between stratospheric ozone depletion and tropospheric climate.

- *Northern Annular Mode (NAM)* (Thompson and Wallace, 1998, 2000; Baldwin and Dunkerton, 1999): The NAM, also referred to as the Arctic Oscillation (AO), is a hemisphere-wide annular atmospheric circulation pattern in which atmospheric pressure over the northern polar region varies out of phase with pressure over northern mid-latitudes (around 45°N), on time scales ranging from weeks to decades.
- *Southern Annular Mode (SAM)* (Gong and Wang, 1999; Thompson and Wallace, 2000): The SAM, also referred to as the Antarctic Oscillation, is the SH analogue of the NAM. The SAM exhibits a large-scale alternation of pressure and temperature between the mid-latitudes and the polar region.
- *North Atlantic Oscillation (NAO)* (Walker and Bliss, 1932; Hurrell, 1995): The NAO was originally identified as a seesaw of sea-level pressure between the Icelandic Low and the Azores High, but an associated circulation (and pressure) pattern is also exhibited well above in the troposphere. The NAO is the dominant regional pattern of wintertime atmospheric circulation variability over the extra-tropical North Atlantic, and has exhibited variability and trends over long time periods (Appenzeller *et al.*, 2000). The relationship between the NAO and the NAM remains a matter of debate (Wallace, 2000; Ambaum *et al.*, 2001; Rogers and McHugh, 2002).

The NAM extends through the depth of the troposphere. During the cold season (January to March), when the stratosphere has large-amplitude disturbances, the NAM also has a strong signature in the stratosphere, where it is associated with variations in the strength of the westerly vortex that encircles the Arctic polar stratosphere; this signature suggests a coupling between the stratosphere and the troposphere (Perlwitz and Graf, 1995; Thompson and Wallace, 1998; Baldwin and Dunkerton, 1999). During winters when the stratospheric vortex is stronger than normal, the NAM (and NAO) tends to be in a positive phase.

Circulation modes can affect the ozone distribution directly (in the troposphere and the lowermost stratosphere; see Lamarque and Hess, 2004), and indirectly by influencing propagation of planetary waves from the troposphere into the

middle atmosphere (Ambaum and Hoskins, 2002). Therefore, changes in circulation modes can produce changes in ozone distribution. It has been shown that because the NAO has a large vertical extent during the winter and because it modulates the tropopause height, it can explain much of the spatial pattern in column ozone trends in the North Atlantic over the past 30 years (Appenzeller *et al.*, 2000).

Stratospheric changes may feed back onto changes in circulation modes. Observations suggest that at least in some cases the large amplitude NAM anomalies tend to propagate from the stratosphere to the troposphere on time scales of weeks to a few months (Baldwin and Dunkerton, 1999; Christiansen, 2001). Furthermore, because of the strong coupling between the stratospheric vortex and the NAM, the recent trend in the NAM and NAO has been associated with processes that are known to affect the strength of the stratospheric polar vortex, such as tropical volcanic eruptions (Kodera, 1994; Kelly *et al.*, 1996; Rozanov *et al.*, 2002; Stenchikov *et al.*, 2002), ozone depletion (Graf *et al.*, 1998; Shindell *et al.*, 2001a), and anthropogenic changes in greenhouse gas concentrations (Shindell *et al.*, 2001a; Gillett *et al.*, 2002a). However, some modelling studies have shown that a simulated trend in the tropospheric NAM and SAM does not necessarily depend on stratospheric involvement (Fyfe *et al.*, 1999; Gillett *et al.*, 2002b). Global climate modelling simulations that include interactive stratospheric chemistry suggest that one mechanism by which solar variability may affect tropospheric climate is through solar-forced changes in upper-stratospheric ozone that induce changes in the leading mode of variability of the coupled troposphere-stratosphere circulation (Shindell *et al.*, 2001b).

A number of modelling studies have examined the effect of increased concentrations of greenhouse gases on the annular modes (e.g., Perlwitz *et al.*, 2000; Shindell *et al.*, 2001a; Gillett *et al.*, 2002b; Rauthe *et al.*, 2004). Most coupled atmosphere-ocean climate models agree in finding a positive NAM trend under increasing greenhouse-gas concentrations, a trend which is qualitatively consistent with the observed positive NAM trend. A more positive NAM is consistent with a stronger stratospheric vortex. On the other hand, an intensified polar vortex is related to changes in planetary- and synoptic-scale wave characteristics, and may produce tropospheric circulation anomalies similar to the positive phase of the NAM. These potential feedbacks obscure cause and effect. For example, whereas Rind *et al.* (2002) and Sigmond *et al.* (2004) found that in the middle stratosphere the perturbation to the NAM from a $2 \times \text{CO}_2$ climate depends on modelled changes in sea-surface temperatures (SSTs), Sigmond *et al.* (2004) suggested that perturbations in the zonal wind near the surface (which will affect the response to SSTs) are mainly caused by doubling of stratospheric CO_2 .

The stratosphere-troposphere dynamical coupling through the circulation modes discussed in this section suggests that stratospheric dynamics should be accounted for in the problem of detection and prediction of future tropospheric climate change. Because increased concentrations of greenhouse gases may cause changes in stratospheric dynamics (and in ozone,

which in turn cause changes in stratospheric dynamics), greenhouse-gas changes may induce changes in surface climate through stratosphere-troposphere dynamical coupling, in addition to radiative forcing.

1.3.6 Possible dynamical feedbacks of ozone changes

The effect of ozone loss on polar stratospheric temperatures results in concomitant changes in stratospheric zonal winds and polar vortex structure, and also possible changes in planetary-wave behaviour. The strongest effect is seen in the Antarctic, where a large cooling of the lower stratosphere, which is associated with the ozone hole (Randel and Wu, 1999), has resulted in an intensified and more persistent springtime polar vortex. Waugh *et al.* (1999) show that since the ozone hole developed, the break-up date of the Antarctic vortex occurs two to three weeks later (moving from mid-November to early December) than before. Recent research has shown that trends in surface temperatures over Antarctica (cooling over the interior and part of the warming over the peninsula) may be in part traceable, at least over the period 1980–2000, to trends in the lower stratospheric polar vortex, which are largely caused by the ozone hole (Thompson and Solomon, 2002). It has been suggested that during the early summer the strengthening of the westerly flow extends all the way to the surface (Thompson and Solomon, 2002). The role of this mechanism – which has yet to be elucidated – has been highlighted by the modelling study of Gillett and Thompson (2003), who prescribed ozone depletion in an atmospheric climate model. They found that the seasonality, structure and amplitude of the modelled changes in 500 hPa geopotential height and near-surface air temperature in the Antarctic had similar spatial patterns to observations, which were a cooling over the Antarctic interior and a warming over the peninsula and South America (Figure 1.14). This result suggests that anthropogenic emissions of ozone-depleting gases have had a distinct impact on climate not only in the stratosphere but also at the Earth's surface. These surface changes appear to act in the same direction as changes resulting from increases in greenhouse gases (Shindell and Schmidt, 2004).

An increase in the strength of the Antarctic polar vortex by stratospheric ozone depletion does not affect only surface winds and temperatures. Using a 15,000-year integration of a coupled ocean-atmosphere model, Hall and Visbeck (2002) showed that fluctuations of the mid-latitude westerly winds generate ocean circulation and sea-ice variations on interannual to centennial time scales.

Cause and effect are more difficult to separate in the Arctic stratosphere than in the Antarctic stratosphere because of higher 'natural' meteorological variability, relatively smaller ozone losses and a less clear separation between transport and chemical effects on ozone. Furthermore, temperatures need to be sufficiently low in any given year to initiate polar ozone chemistry. Nonetheless, in several years during the mid-1990s the Arctic experienced low ozone, low temperatures in late spring and enhanced vortex persistence (Randel and Wu, 1999; Waugh *et al.*,

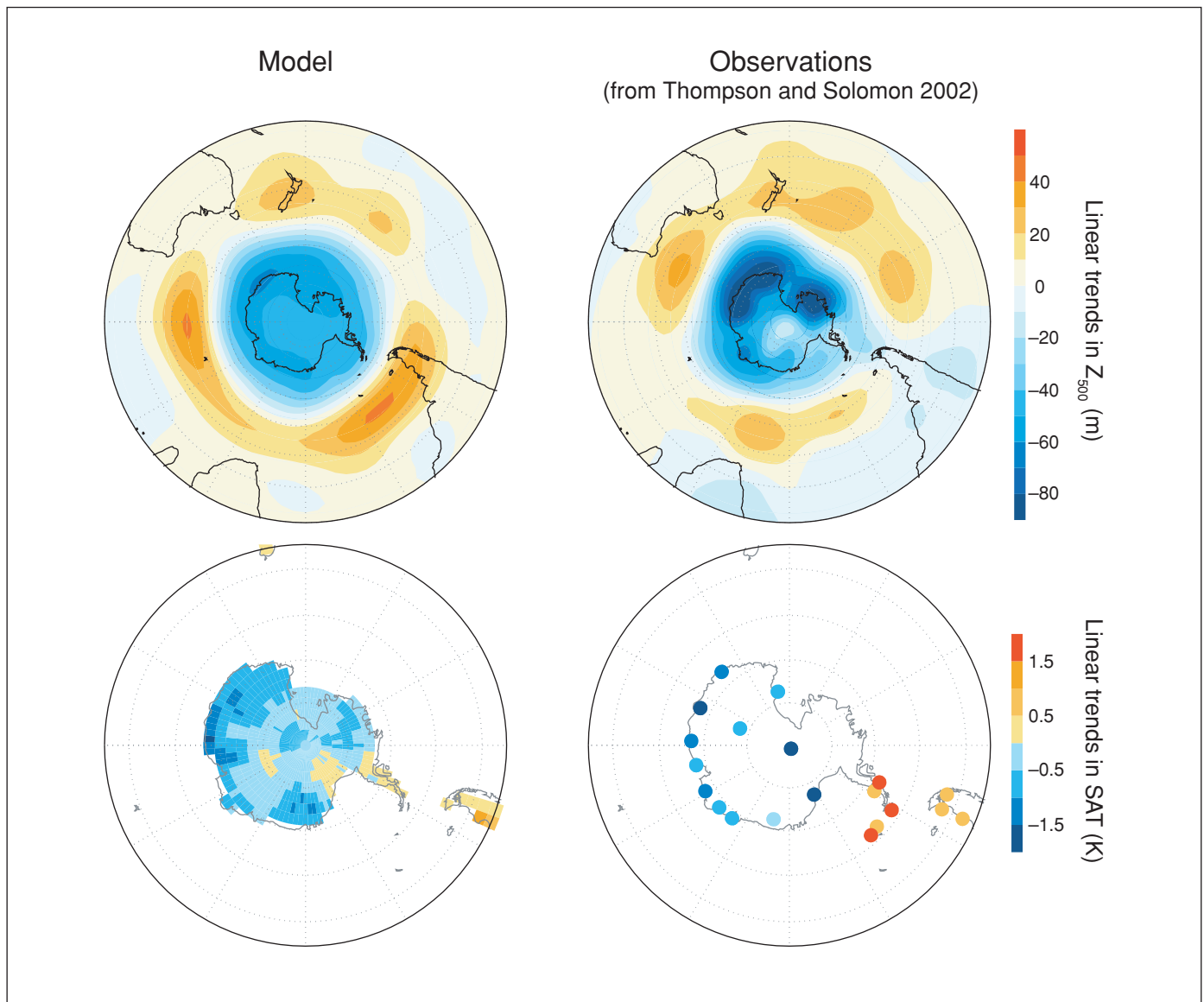


Figure 1.14. Simulated (left column) and observed (right column) changes in the 500 hPa geopotential height (Z_{500} , in m) (upper row) and surface air temperature (SAT, in K) (lower row). Observed changes are linear trends over 22 years (1979–2000) in the 500 hPa geopotential height, and over 32 years (1969–2000) in surface air temperature, averaged over December to May. Simulated changes are differences between the perturbed and control integrations in the 500 hPa geopotential height and the land surface temperature averaged over December to February. Adapted from Gillett and Thompson (2003).

1999), which resembled the coupled changes observed in the Antarctic.

A crucial issue is the potential feedback between changes in stratospheric climate and planetary wave forcing (through both modification of tropospheric planetary wave sources and changes in wave propagation into and within the stratosphere). However, this topic is poorly understood at present. Chen and Robinson (1992) and Limpasuvan and Hartmann (2000) have argued that stronger vertical shear of the zonal wind at high latitudes will reduce the strength of stratospheric PWD, whereas

Hu and Tung (2002) have argued for precisely the opposite effect. Many climate model simulations (e.g., Rind *et al.*, 1990; Butchart and Scaife, 2001) found enhanced PWD in an atmosphere with elevated WMGHG concentrations, which leads to a stronger Brewer-Dobson circulation; however models were not unanimous on this result (Shindell *et al.*, 2001a). Because planetary wave forcing is a primary driver of the stratospheric circulation, improved understanding of this coupling will be necessary to predict future ozone changes.

1.4 Past and future stratospheric ozone changes (attribution and prediction)

1.4.1 Current understanding of past ozone changes

In Section 1.3 a number of processes were described that can influence the distribution of and changes in stratospheric ozone. Here we discuss the current understanding of past ozone changes, based in part on numerical models that attempt to include these processes. A hierarchy of models of increasing sophistication is used (see Box 1.5). Some models include relatively few processes (e.g., box models, which include only chemical processes, but perhaps in great detail), whereas others attempt to include many more (e.g., the chemistry-climate models, CCMs). The models have their different uses, and strengths, some of which are described in the remainder of Section 1.4.

The understanding of polar and mid-latitude ozone decline has been assessed most recently in Chapters 3 and 4 of WMO (2003). The material here relies heavily on that report, which deals with these topics in much greater detail.

1.4.1.1 Mid-latitude ozone depletion

In the upper stratosphere the observed ozone depletion over the last 25 years is statistically robust in the sense that its value is not sensitive to small differences in the choice of the time period analyzed (WMO, 2003, Chapter 4). This behaviour accords with the fact that in this region of the atmosphere, ozone is under photochemical control and thus only weakly affected by dynamical variability. We therefore expect upper-stratospheric ozone abundance to reflect long-term changes in temperature and in the abundance of species (principally halogens) that react chemically with ozone.

Over the past 25 years there have been large changes in the abundance of halogen compounds, and the extent of the observed ozone decrease is consistent with the observed increase in anthropogenic chlorine, as originally predicted by Molina and Rowland (1974) and Crutzen (1974). In particular, the vertical and latitudinal profiles of ozone trends in the upper stratosphere are reproduced by 2-D photochemistry models. In the upper stratosphere the attribution of ozone loss in the last couple of decades to anthropogenic halogens is clear-cut. The 2-D models indicate that changes in halogens make the largest contribution to the observed loss of about 7% per decade (WMO, 2003, Chapter 4). The observed cooling of the upper stratosphere (of perhaps 2 K per decade, see Figure 1.10) will have reduced the rate of ozone destruction in this region. If we take the observed variation of ozone with temperature in the upper stratosphere (e.g., Barnett *et al.*, 1975; Froidevaux *et al.*, 1989), then a cooling of 2 K per decade should have led to an increase in ozone of about 2% per decade, partially compensating the loss caused by halogens. Note, however, that in the upper stratosphere radiative-transfer models suggest roughly equal contributions to the cooling from ozone decreases and carbon dioxide increases (Figure 1.10); the changes in the ozone-temperature system are nonlinear. Changes in CH₄ and N₂O will have also played a

small role here. Note also that although 2-D models have been widely used in many ozone assessments, they have important limitations in terms of, for example, their ability to include the full range of feedbacks between chemistry and dynamics, or their ability to reproduce the polar vortex (which will then influence the treatment of mid-latitudes). They are expected to be most accurate in the upper stratosphere, where dynamical effects on ozone are weakest.

However, the changes in upper-stratospheric ozone represent only a small contribution to the total changes in column ozone observed over the last 25 years, except in the tropics where there is no statistically significant trend in column ozone (WMO, 2003, Chapter 4). Most of the column ozone depletion in the extratropics occurs in the lower stratosphere, where the photochemical time scale for ozone becomes long and the ozone distribution is sensitive to dynamical variability as well as to chemical processes. This complicates the problem of attribution of the observed ozone decline. Strong ozone variability and complex coupled interactions between dynamics and chemistry, which are not separable in a simple manner, make attribution particularly difficult.

A number of 2-D models contributed to Chapter 4 of WMO (2003), and a schematic showing their simulations of column ozone between 60°S and 60°N from 1980 to 2050 is provided in the figure in Box 1.7 (in Section 1.4.2). The symbols in this figure show the observed changes relative to 1980. As there are no significant trends in tropical ozone, the observed and modelled changes are attributable to mid-latitudes. The shaded area shows the results of 2-D photochemistry models forced by observed changes in halocarbons, other source gases and aerosols (and in some cases, temperatures) from 1980 to 2000. Overall, the models broadly reproduce the long-term changes in mid-latitude column ozone for 1980–2000, within the range of uncertainties of the observations and the model range. The spread in the model results comes mainly from their large spread over the SH mid-latitudes, and is at least partly a result of their treatment of the Antarctic ozone hole (which cannot be well represented in a 2-D model). In addition, the agreement between models and observations over 60°S to 60°N hides some important disagreements within each hemisphere. In particular, models suggest that the chemical signal of ozone loss following the major eruption of the Mt. Pinatubo volcano in the early 1990s should have been symmetric between the hemispheres, but observations show a large degree of inter-hemispheric asymmetry in mid-latitudes (see the more detailed discussion in Section 4.6 of WMO, 2003).

As discussed in Section 1.3.4, changes in atmospheric dynamics can also have a significant influence on NH mid-latitude column ozone on decadal time scales. Natural variability, changes in greenhouse gases and changes in column ozone itself are all likely to contribute to these dynamical changes. Furthermore, because chemical and dynamical processes are coupled, their contributions to ozone changes cannot be considered in isolation. This coupling is especially complex and difficult to understand with regard to dynamical changes in the

Box 1.5. Atmospheric models

The chemical composition and the thermal and dynamical structure of the atmosphere are determined by a large number of simultaneously operating and interacting processes. Therefore, numerical mathematical models have become indispensable tools to study these complex atmospheric interactions. Scientific progress is achieved in part by understanding the discrepancies between atmospheric observations and results from the models. Furthermore, numerical models allow us to make *predictions* about the future development of the atmosphere. Today, a hierarchy of atmospheric models of increasing complexity is employed for the investigation of the Earth's atmosphere. Models range from simple (with perhaps one process or one spatial dimension considered) to the most complex 3-D and interactive models. In the following list, a brief summary of the most important types of models is given:

- *Fixed dynamical-heating (FDH) model*: Calculation of stratospheric temperature changes and radiative forcing with a radiation scheme, assuming that the stratosphere is in an equilibrium state and no dynamical changes occur in the atmosphere.
- *Trajectory (Lagrangian) model*: Simulation of air-parcel movement through the atmosphere based on meteorological analyses.
- *Box-trajectory model*: Simulation of chemical processes within a parcel of air that moves through the atmosphere.
- *Mesoscale (regional) model*: Analysis and forecast of medium-scale (a few tens of kilometers) radiative, dynamical and chemical structures in the atmosphere; investigation of transport and exchange processes.
- *Contour-advection model*: Simulation of highly resolved specific two-dimensional (2-D) fluid-dynamical processes, such as processes at transport barriers in the atmosphere.
- *Mechanistic circulation model*: Simplified 3-D atmospheric circulation model that allows for the investigation of specific dynamical processes.
- *Two-dimensional photochemistry model*: Zonally averaged representation of the middle atmosphere, with detailed chemistry but highly simplified transport and mixing.
- *General-circulation climate model (GCM)*: Three-dimensional simulation of large-scale radiative and dynamical processes (spatial resolution of a few hundred kilometers) in the atmosphere over years and decades; investigation of the climate effects of atmospheric trace gases (greenhouse gases); investigations of the interaction of the atmosphere with the biosphere and oceans.
- *Chemistry-transport model (CTM)*: Three-dimensional (or 2-D latitude-longitude) simulation of chemical processes in the atmosphere employing meteorological analyses derived from observations or GCMs; simulation of spatial and temporal development and distribution of chemical species.
- *Chemistry-climate model (CCM)*: Interactively coupled 3-D GCM with chemistry; investigation of the interaction of radiative, dynamical, physical and chemical processes of the atmosphere; assessment of future development of chemical composition and climate.

Several decades ago, when numerical models of the atmosphere were first developed, much less computational power was available than today. Early studies with numerical models focused on the simulation of individual radiative, dynamical or chemical processes of the atmosphere. These early and rather simple models have evolved today into very complex tools, although, for reasons of computational efficiency, simplifying assumptions (parametrizations) must still be made. For example, the atmosphere in a global model requires discretization, which is generally done by decomposing it into boxes of a specific size. Processes acting on smaller scales than the boxes cannot be treated individually and must be parametrized, that is, their effects must be prescribed by functional dependencies of resolved quantities.

tropopause region. There is an observed relationship between column ozone and several tropospheric circulation indices, including tropopause height (Section 1.3.4.2). Over time scales of up to about one month, it is the dynamical changes that cause the ozone changes (Randel and Cobb, 1994), whereas on longer time scales feedbacks occur and the causality in the relationship becomes unclear. Thus, although various tropospheric circulation indices (including tropopause height) have changed over the last 20 years in the NH in such a way as to imply a decrease

in column ozone, this inference is based on an extrapolation of short-time-scale correlations to longer time scales, which may not be valid (Section 4.6 of WMO, 2003).

Above the tropopause, stratospheric PWD drives the seasonal winter-spring ozone build-up in the extratropics, and has essentially no interannual memory (Fioletov and Shepherd, 2003). It follows that the observed decrease in NH PWD in the late winter and spring has likely contributed to the observed decrease in NH column ozone over the last 20 to 25 years (Fusco

and Salby, 1999; Randel *et al.*, 2002). The effect of changes in PWD on the ozone distribution is understood in general terms, but its quantification in observations is relatively crude.

The seasonality of the long-term changes in mid-latitude column ozone differs between hemispheres. In the NH, the maximum decrease is found in spring, and it decays through to late autumn. Fioletov and Shepherd (2003) have shown that in the NH the ozone decreases in summer and early autumn are the photochemically damped signal of winter-spring losses, and thus arise from the winter-spring losses (however they occur) without any need for perturbed chemistry in the summertime. The same seasonality is not enough for explaining the summer and early autumn ozone decreases observed in the SH mid-latitudes (Fioletov and Shepherd, 2003) because they are comparable with the winter-spring losses and therefore point to the influence of transport of ozone-depleted air into mid-latitudes following the break-up of the ozone hole.

In summary, the vertical, latitudinal and seasonal characteristics of past changes in mid-latitude ozone are broadly consistent with the understanding that halogens are the primary cause of these changes. However, to account for decadal variations it is necessary to include consideration of the interplay between dynamical and chemical effects as well as the impact of variations in aerosol loading (WMO, 2003, Chapter 4); our inadequate quantitative understanding of these processes limits our predictive capability.

1.4.1.2 Winter-spring polar depletion

Polar ozone depletion in the winter-spring period is generally considered separately from mid-latitude depletion, because of the extremely severe depletion that can occur in polar regions from heterogeneous chemistry on PSCs (Section 1.3.1). We consider first the Antarctic, and then the Arctic.

The Antarctic ozone hole represents the most striking example of ozone depletion in the atmosphere. It developed through the 1980s as chlorine loading increased, and has recurred every year since then (Figure 1.5). The Antarctic ozone hole has been clearly attributed to anthropogenic chlorine through field campaigns and photochemical modelling (WMO, 1999, Chapter 7). An ozone hole now occurs every year because, in addition to the availability of anthropogenic chlorine, wintertime temperatures in the Antarctic lower stratosphere are always low enough for chlorine activation to occur on PSCs prior to the return of sunlight to the vortex in the spring, and the air is always sufficiently isolated within the vortex for it to become strongly depleted of ozone (see Box 1.1). There is nevertheless dynamically induced variability in the extent and severity of the ozone hole, as seen in Figure 1.5. The most dramatic instance of such variability occurred in 2002, when the Antarctic stratosphere experienced its first observed sudden warming (see Box 1.6). The sudden warming split the vortex in two (figure in Box 1.6) and halted the development of the ozone hole that year. Such events occur commonly in the NH, as a result of the stronger planetary-wave forcing in the NH, but had never before been seen in the SH, although there had been previous instances of disturbed winters

(e.g., 1988). Although unprecedented, this event resulted from dynamical variability and was not indicative of ozone recovery; indeed, the ozone hole in 2003 was back to a severity characteristic of the 1990s (Figure 1.5 and figure in Box 1.6).

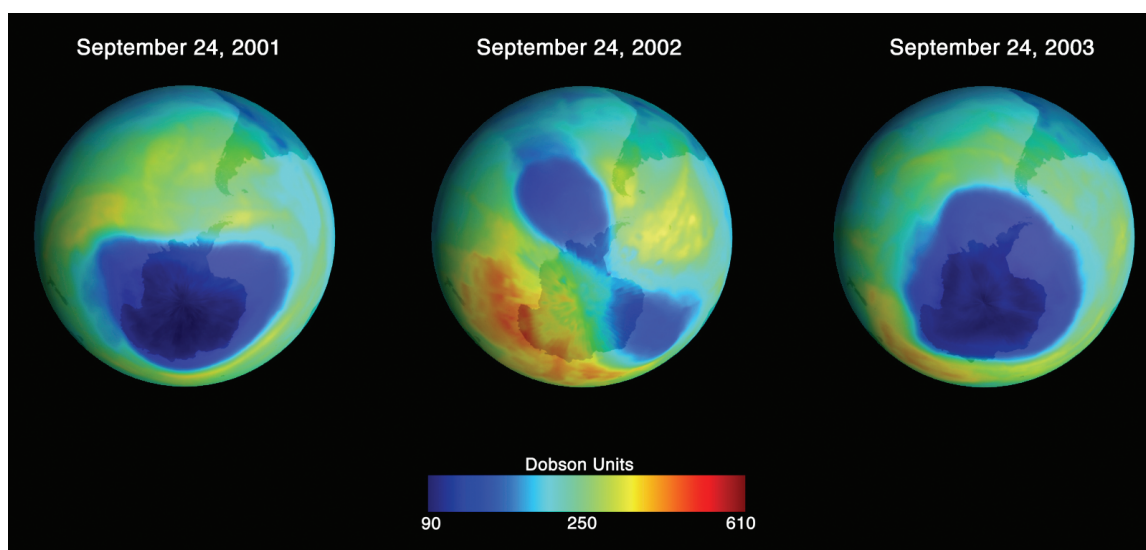
Given the fairly predictable nature of the Antarctic ozone hole, its simulation constitutes a basic test for models. Two-dimensional models are not expected to represent the ozone hole well because they cannot properly represent isolation of polar vortex air (WMO, 2003, Chapter 4), and their estimates of Antarctic ozone loss vary greatly. However, an emerging tool for attribution is the 3-D chemistry-climate model (CCM). These models include an on-line feedback of chemical composition to the dynamical and radiative components of the model. The CCMs currently available have been developed with an emphasis on the troposphere and stratosphere. They consider a wide range of chemical, dynamical and radiative feedback processes and can be used to address the question of why changes in stratospheric dynamics and chemistry may have occurred as a result of anthropogenic forcing. The models specify WMGHGs, source gases, aerosols and often SSTs, but otherwise run freely and exhibit considerable interannual variability (in contrast with the 2-D models). Thus in addition to issues of model accuracy, it is necessary to consider how representative are the model simulations.

In recent years a number of CCMs have been employed to examine the effects of climate change on ozone (Austin *et al.*, 2003). They have been used for long-term simulations to try to reproduce observed past changes, such as ozone and temperature trends. The models have been run either with fixed forcings to investigate the subsequent 'equilibrium climate' (so-called time-slice runs) or with time-varying forcings (so-called transient runs). The current CCMs can reproduce qualitatively the most important atmospheric features (e.g., stratospheric winds and temperatures, and ozone columns and profiles) with respect to the mean conditions and the seasonal and interannual variability; the long-term changes in the dynamical and chemical composition of the upper troposphere and the stratosphere are also in reasonable agreement with observations. But a reasonable reproduction of the timing of the ozone hole and an adequate description of total column ozone do not necessarily mean that all processes in the CCMs are correctly captured. There are obvious discrepancies between the models themselves, and between model results and detailed observations. Some of the differences among the models are caused by the fact that the specific model systems employed differ considerably, not only in complexity (e.g., the number of chemical reactions considered and the parametrization of sub-grid-scale processes), but also in the vertical extent of the model domain and in the horizontal and vertical resolutions.

An important difference between models and observations originates to a large extent from the cold bias (the 'cold-pole problem') that is found in the high latitudes of many CCMs, particularly near the tropopause and in the lower stratosphere. The low-temperature bias of the models is generally largest in winter over the South Pole, where it is of the order of 5–10 K;

Box 1.6. The 2002 Antarctic ozone hole

The unusual behaviour of the Antarctic ozone hole in 2002 highlights the important role that tropospheric climate and dynamics play in ozone depletion processes. Year-to-year changes in ozone hole area (or depth) are more likely to reflect changes in stratospheric dynamics that influence ozone loss over the short term, rather than long-term issues such as changes in stratospheric concentrations of ODSs controlled by the Montreal Protocol. During the early winter of 2002, the Antarctic ozone hole was unusually disturbed (Allen *et al.*, 2003; Stolarski *et al.*, 2005) as a result of a series of wave events (Newman and Nash, 2005). The anomalously high stratospheric wave activity was forced by strong levels of planetary wave 1 (a single wave encircling the globe) in the mid-latitude lower troposphere and a tropopause wave propagation regime that favoured transmission of these waves to the lower stratosphere. The wave events occurred irregularly over the course of the winter and preconditioned the polar vortex for an extremely large wave event on 22 September. This large wave event resulted in the first ever major stratospheric sudden warming to be observed in the SH, which split the Antarctic ozone hole in two (see figure). Such a splitting of the vortex in two is a characteristic signature of wave-2 sudden warmings in the NH and is well understood dynamically.



Box 1.6, Figure. Comparison of the first split ozone hole on record (middle, 2002) and the Antarctic ozone hole at the same time one year earlier (left, 2001) and one year later (right, 2003). The hole is dark blue. In 2001, the area of the ozone layer thinning over Antarctica reached 26.5 million km², larger than the size of the entire North American continent. Because of higher Antarctic winter temperatures, the 2002 ‘hole’ appears to be about 40% smaller than in 2001. In 2003, Antarctic winter temperatures returned to normal and the ozone hole returned to its usual state. Figure provided by Stuart Snodgrass, NASA/Goddard Space Flight Center Scientific Visualization Studio (SVS).

this magnitude of bias could be significant in controlling planetary-wave dynamics and restricting the interannual variability of the models. A low-temperature bias in the lower stratosphere of a model has a significant impact not only on model heterogeneous chemistry (i.e., leading to enhanced ozone destruction via enhanced occurrence of PSCs), but also on the transport of chemical species and its potential change due to changes in circulation. Moreover, changes in stratospheric dynamics alter the conditions for wave forcing and wave propagation (of small-scale gravity waves as well as large-scale planetary waves), which in turn influence the seasonal and interannual variability of the atmosphere. The reasons for the cold bias in the models are still unknown. This bias has been reduced in some models, for example by considering non-orographic gravity-wave drag

schemes (Manzini and McFarlane, 1998), but the problem is not yet solved. Without its resolution, the reliability of these models for attribution and prediction is reduced.

Despite these potential problems, CCMs simulate the development of the Antarctic ozone hole reasonably well (Figure 1.15). The models examined in the intercomparison of Austin *et al.* (2003) agree with observations of minimum Antarctic springtime column ozone over 1980–2000 within the model variability (Figure 1.15a), confirming that the Antarctic ozone hole is indeed a robust response to anthropogenic chlorine. The cold-pole biases of some models seem not to affect minimum column ozone too much, although some modelled minima are significantly lower than observed. None of the models exhibited a sudden warming as seen in 2002, although several exhibit

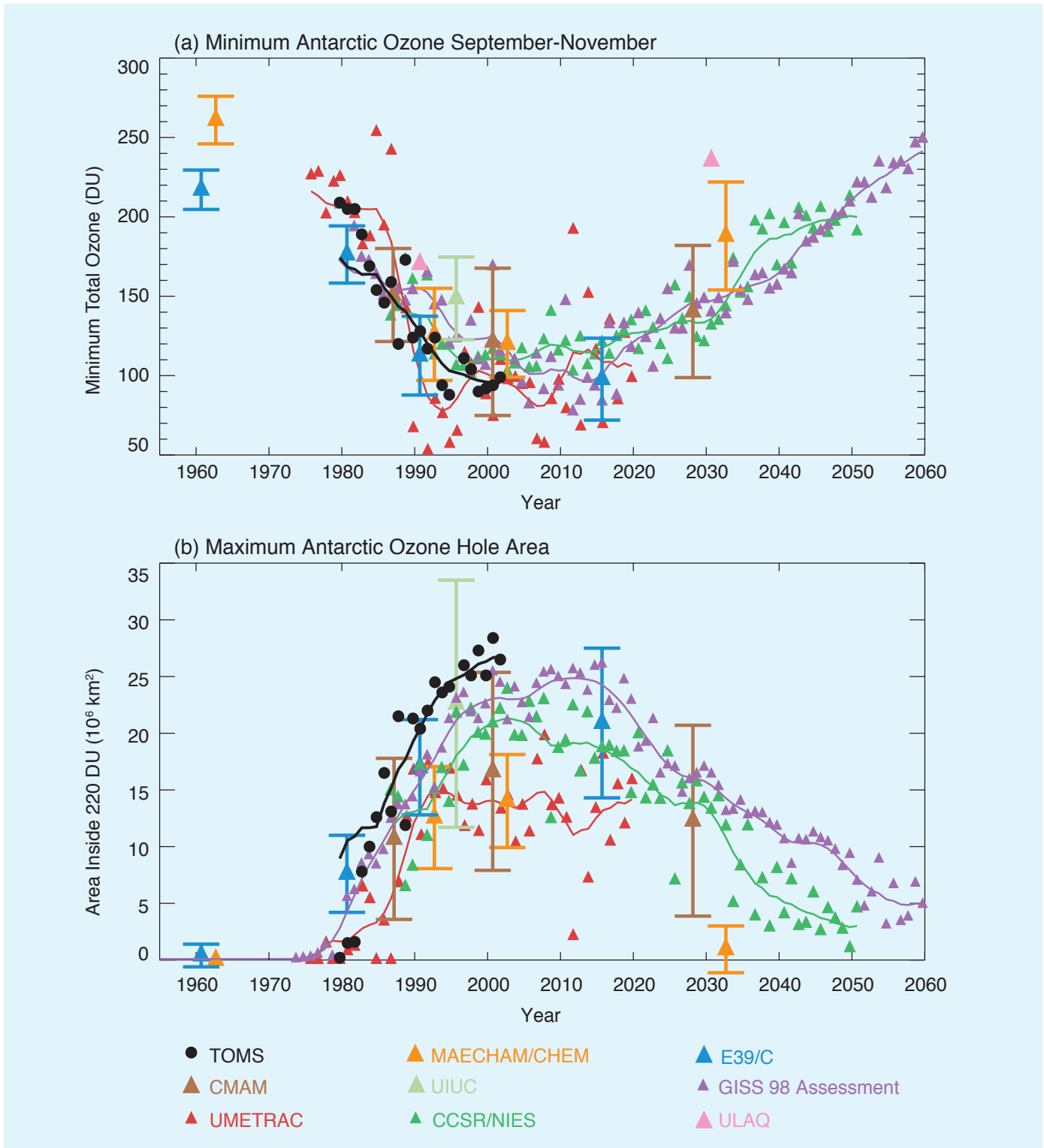


Figure 1.15. (a) Time development of the Antarctic ozone column: measurements (TOMS, black dots) and CCM model calculations (coloured triangles) of minimum total ozone from 60°S to 90°S for September to November. For the transient simulations (small triangles), the solid lines show the results of a Gaussian smoothing applied to the annual results. For the time-slice simulations, the mean and twice the standard deviation of the values within each model sample are indicated by the large coloured triangles and the error bars, respectively. For the MAECHAM/CHEM model only, the values have been plotted two years late for clarity, and a standard tropospheric ozone column of 40 DU has been added to the computed stratospheric columns. (b) As (a), but for the time development of the maximum area of the ozone hole, defined by the 220 DU contour, for September to November. Adapted from WMO (2003) based on Austin *et al.* (2003).

years with a disturbed vortex, as seen in their interannual variability in minimum column ozone. (The models with cold-pole biases appear to underestimate the observed variability of the ozone hole, as would be expected.) However, minimum total ozone is not the only diagnostic of the ozone hole. Figure 1.15b shows the modelled ozone hole area in comparison with observations. Many models significantly underestimate the area of the ozone hole.

In contrast with the Antarctic, winter-spring ozone abundance in the Arctic exhibits significant year-to-year variability, as seen in Figure 1.6. This variability arises from the highly disturbed nature of Arctic stratospheric dynamics, including relatively frequent sudden warmings (every 2 to 4 years). Because dynamical variability affects both transport and temperature, dynamical and chemical effects on ozone are coupled. The dynamical variability is controlled by stratospheric PWD; years with strong PWD, compared with years with weak PWD, have stronger downwelling over the pole, and thus higher temperatures, a weaker vortex and more ozone transport (Newman *et al.*, 2001). Because low temperatures and a stronger vortex tend to favour chemical ozone loss in the presence of elevated halogen levels (Section 1.3.2), it follows that dynamical and chemical effects tend to act in concert. In the warmest years (e.g., 1999) there is essentially no chemical ozone loss and ozone levels are similar to those seen pre-1980. The chemical ozone loss was calculated for cold years using various methods in Section 3.3 of WMO (2003), and the agreement between the methods provided confidence in the estimates. The calculations showed a roughly linear relationship between chemical ozone loss and temperature (see also Figure 1.13, which shows the relationship of ozone loss to V_{PSC} , which itself varies linearly with temperature (Rex *et al.*, 2004)). Furthermore, the *in situ* chemical ozone loss was found to account for roughly one half of the observed ozone decrease between cold years and warm years. Given the high confidence in the estimates of chemical ozone loss, the remaining half can be attributed to reduced ozone transport, as is expected in cold years with weak PWD, a strong vortex, and weak downwelling over the pole. From this it can be concluded that in cold years, chlorine chemistry doubled the ozone decrease that would have occurred from transport alone (WMO, 2003, Chapter 3).

Compared with other recent decades, the 1990s had an unusually high number of cold years, and these led to low values of Arctic ozone (Figure 1.6). In more recent years, Arctic ozone has been generally higher, although still apparently below pre-1980 values. This behaviour does not reflect the time evolution of stratospheric chlorine loading (Figure 1.7d). Rather, it reflects the meteorological variability in the presence of chlorine loading. In this respect the Arctic ozone record needs to be interpreted in the context of the meteorology of a given year, far more than is generally the case in the Antarctic.

This interpretation of Arctic ozone changes is consistent with the fact that the observed decrease in Arctic stratospheric temperature over 1980–2000 cannot be explained from direct radiative forcing due to ozone depletion or changes in green-

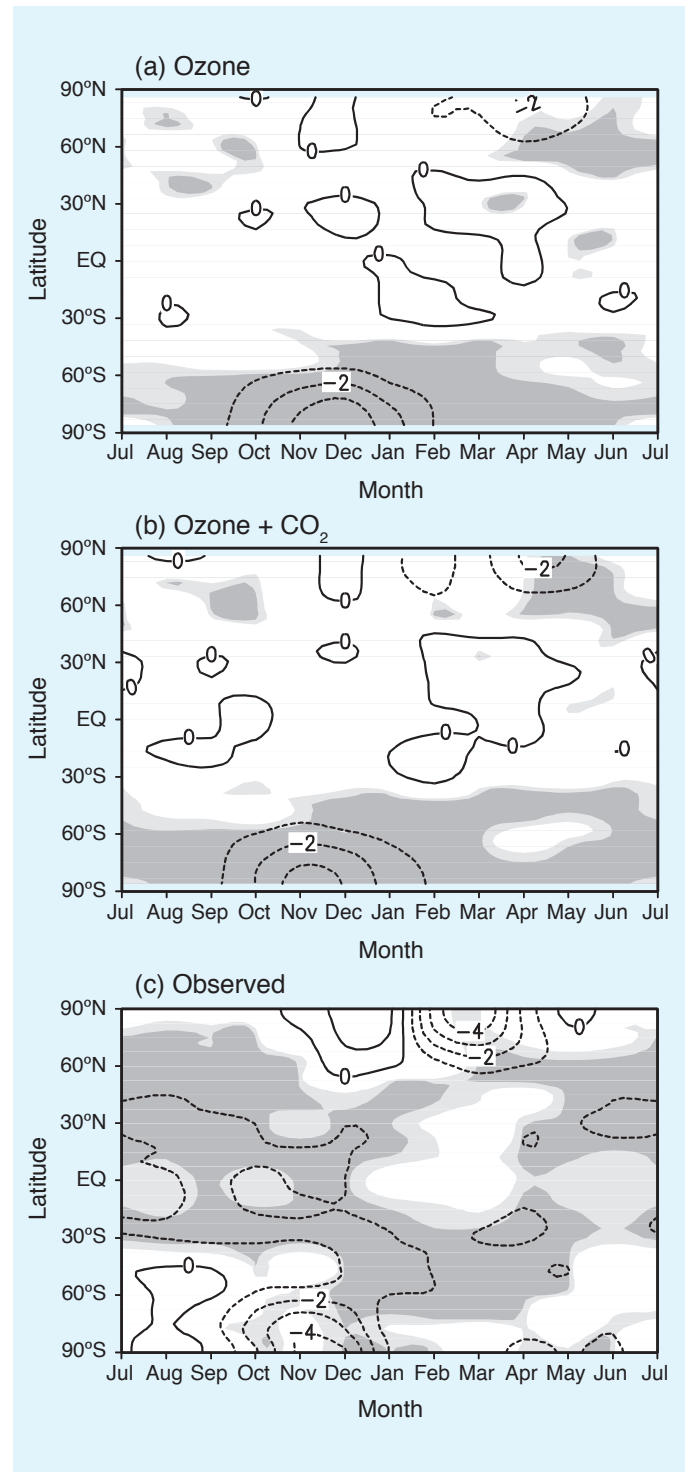


Figure 1.16. Latitude-month distribution of the zonal-mean temperature trend (in K per decade) at 100 hPa over the period 1980–2000: (a) modelled trend obtained by imposing the observed ozone trend over the same period (note that this was not done with a CCM), (b) modelled trend obtained by imposing the observed ozone trend plus the observed CO_2 trend, and (c) observed trend derived from NCEP reanalysis data. The contour interval is 1 K per decade. Dark (light) shaded areas denote regions where the trend is significant at the 99% (95%) confidence level. From Langematz *et al.* (2003).

house gases alone (Shine *et al.*, 2003), although they do make a contribution. The inference is that the observed springtime cooling was mainly the result of decadal meteorological variability in PWD. This is in contrast with the Antarctic, where the observed cooling in November and the prolonged persistence of the vortex have been shown to be the result of the ozone hole (Randel and Wu, 1999; Waugh *et al.*, 1999). These results (for both hemispheres) are illustrated by Figure 1.16. There is seen to be little impact from CO₂ at these altitudes over this time period. In the Arctic, the cooling induced by ozone loss is too small and too late in the season to account for the observed cooling. Rather, as discussed above, the observed cooling is required in order to initiate severe Arctic ozone depletion.

It is not known what has caused the recent decadal variations in Arctic temperature. Rex *et al.* (2004) have argued that the value of V_{PSC} in cold years has systematically increased since the 1960s. However, the Arctic exhibits significant decadal variability (Scaife *et al.*, 2000) and it is not possible to exclude natural variability as the cause of these changes.

These considerations have implications for the attribution of past changes. No matter how good a CCM is and how well its climate-change experiments are characterized, it cannot exactly reproduce the real atmosphere because the real atmosphere is only one possible realization of a chaotic system. The best one can expect, even for a perfect model (that is, a model that correctly considers all relevant processes), is that the observations fall within the range of model-predicted behaviours, according to appropriate statistical criteria. Whether this permits a meaningful prediction depends on the relative magnitudes and time scales of the forced signal and the natural noise. Whereas the evolution of Antarctic ozone is expected to be fairly predictable over decadal time scales (past and future), it is not at all clear whether this is the case in the Arctic. Thus, it is not a priori obvious that even a perfect CCM would reproduce the decreases in Arctic ozone observed over the past 20 years, for example.

Bearing these caveats in mind, the simulations of past Arctic minimum ozone from the CCMs considered in Austin *et al.* (2003) are shown in Figure 1.17. (Because of the large degree of scatter, the results are shown separately for the transient and time-slice simulations.) The models seem generally to have a positive bias with respect to the observations over the same period. None of the CCMs achieve column ozone values as low as those observed, and the modelled ozone trends are generally smaller than the observed trend (Austin *et al.*, 2003). However, the range of variability exhibited by each of the models is considerable, and it is therefore difficult to say that the models are definitely deficient on the basis of the ozone behaviour alone; more detailed diagnostics are required – such as comparison with the observed relationship shown in Figure 1.13 and with observations of other chemical species.

In summary, the development of the Antarctic ozone hole through the 1980s was a direct response to increasing chlorine loading, and the severity of the ozone decrease has not changed since the early 1990s, although there are year-to-year variations (especially in 2002, which was a surprising anomaly). In the

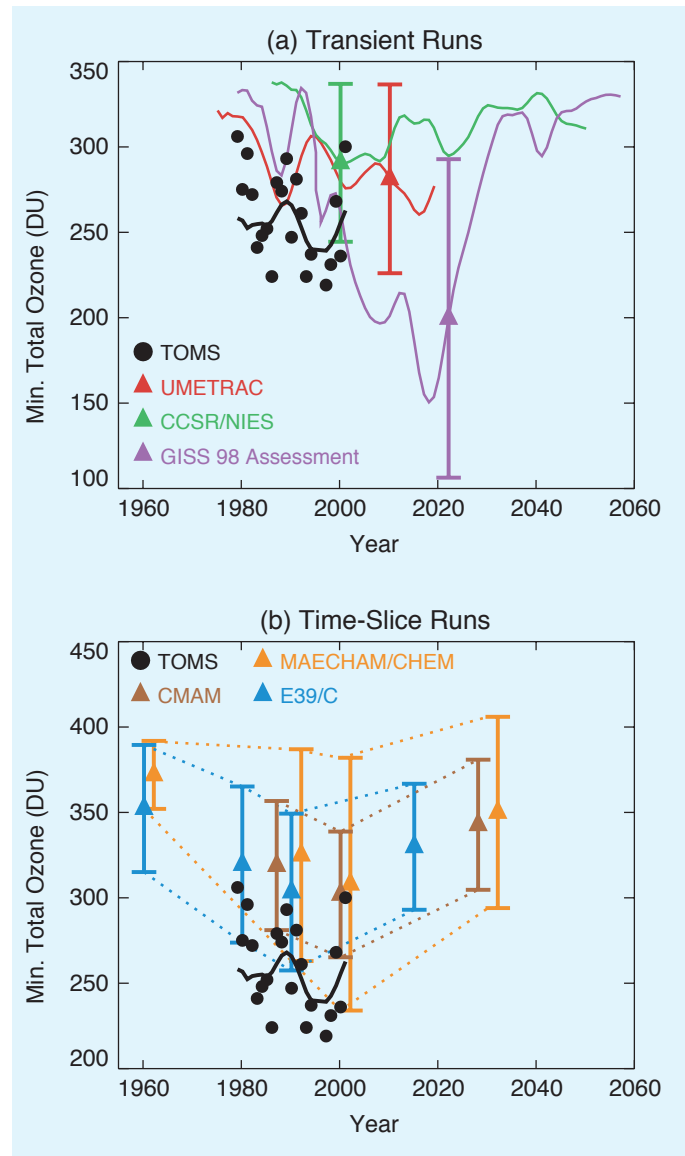


Figure 1.17. Development of the Arctic ozone column: measurements (TOMS, black dots) and model calculations of minimum total ozone from 60°N to 90°N for March and April. For the transient simulations (panel (a)), the solid lines show the results of a Gaussian smoothing applied to the annual results, and the error bars denote the standard deviation of the annual values from the smoothed curve (plotted just once for clarity). For the time-slice simulations (panel (b)), the mean and twice the standard deviation of the values within each model sample are indicated by the coloured triangles and the error bars, respectively. For the MAECHAM/CHEM model only, the values have been plotted two years late for clarity, and a standard tropospheric ozone column of 100 DU has been added to the computed stratospheric columns. Adapted from Austin *et al.* (2003).

Arctic, the extent of chemical ozone loss due to chlorine depends on the meteorology of a given winter. In winters that are cold enough for the existence of PSCs, chemical ozone loss has been identified and acts in concert with reduced transport (the

effects being of a similar magnitude in terms of column ozone loss) to give Arctic ozone depletion. There was particularly severe Arctic ozone depletion in many years of the 1990s (and in 2000), as a result of a series of particularly cold winters. It is not known whether this period of low Arctic winter temperatures is just natural variability or a response to changes in greenhouse gases.

1.4.2 *The Montreal Protocol, future ozone changes and their links to climate*

The halogen loading of the stratosphere increased rapidly in the 1970s and 1980s. As a result of the Montreal Protocol and its Amendments and Adjustments, the stratospheric loading of chlorine and bromine is expected to decrease slowly in the coming decades, reaching pre-1980 levels some time around 2050 (WMO, 2003, Chapter 1). If chlorine and bromine were the only factors affecting stratosphere ozone, we would then expect stratospheric ozone to ‘recover’ at about the same time. Over this long (about 50-year) time scale, the state of the stratosphere may well change because of other anthropogenic effects, in ways that affect ozone abundance. For example, increasing concentrations of CO₂ are expected to further cool the stratosphere, and therefore to influence the rates of ozone destruction. Any changes in stratospheric water vapour, CH₄ and N₂O, all of which are difficult to predict quantitatively, will also affect stratospheric chemistry and radiation. In addition, natural climate variability including, volcanic eruptions, can affect ozone on decadal time scales. For these reasons, ‘recovery’ of stratospheric ozone is a complicated issue (see Box 1.7). A number of model calculations to investigate recovery were reported in Chapters 3 and 4 of WMO (2003), using both 2-D and 3-D models. The main results from that assessment, and new studies reported since then, are summarized here. As with the discussion of past ozone changes, we first discuss mid-latitude (or global) changes and then polar changes.

1.4.2.1 *Mid-latitude ozone*

Predictions of future mid-latitude ozone change in response to expected decreasing halogen levels have been extensively discussed in Chapter 4 of WMO (2003), based primarily on simulations with eight separate 2-D photochemistry models that incorporated predicted future changes in halogen loading. Several scenarios for future changes in trace climate gases (CO₂, N₂O and CH₄) were also incorporated in these simulations (based on IPCC, 2001, Chapter 4), although the ozone results were not particularly sensitive to which scenario was employed. Results of the simulations for the period 1980–2050 are illustrated in the figure in Box 1.7, which shows the range of near-global (60°N to 60°S) mean column-ozone anomalies derived from the set of 2-D models. The models generally predict a minimum in global column ozone in 1992–1993 following the eruption of Mt. Pinatubo, followed by steady increases (although some models have a secondary minimum in about 2000). The latter evolution is primarily determined by changes in atmospheric

chlorine and bromine loading, which reaches a maximum in approximately 1995 and then slowly decreases (Figure 1.7d). There is, however, a large spread in the times the models predict that global ozone will return to 1980 levels, ranging from 2025 to after 2050. The spread of results arises in part from the differences between the models used.

Two of the 2-D models used in the simulations included interactive temperature changes caused by increasing greenhouse gases, which result in a long-term cooling of the stratosphere (one model includes this feedback throughout the entire stratosphere, and the other only above about 30 km). Cooling in the upper stratosphere results in slowing of the gas-phase chemical cycles that destroy ozone there (Section 1.3.2), and consequently these two models show a greater increase with time of total ozone (defining the upper range in the middle 21st century in the figure in Box 1.7) than the other models. An important caveat is that most of the past (1980–2000) column ozone change has occurred in the lower stratosphere, and future temperature feedback effects are more complicated and uncertain in the lower stratosphere. Furthermore, these effects involve changes in transport, heterogeneous chemistry and polar processes, which are not accurately simulated in 2-D models. (Note, however, that at least one CCM (Pitari *et al.*, 2002) also predicts a similar fast recovery.) At present there is considerable uncertainty regarding the details of temperature feedbacks on future mid-latitude column ozone changes.

Because 2-D models can be expected to capture the main chemical processes involved in ozone recovery, reliable predictions of future changes in the coupled ozone-climate system require the use of CCMs, since they consider possible changes in climate feedback mechanisms. Despite some present limitations, these models have been employed in sensitivity studies to assess the global future development of the chemical composition of the stratosphere and climate. The results have been compared with each other to assess the uncertainties of such predictions (Austin *et al.*, 2003), and have been documented in international assessment reports (WMO, 2003, Chapter 3; EC, 2003, Chapter 3). However most of the attention has been focused on polar ozone.

As discussed in Section 1.3.4, two dynamical influences appear to be related to NH mid-latitude ozone decreases over 1980–2000: a decrease in PWD and an increase in tropopause height. These mechanisms likewise have the potential to influence future ozone. If the past dynamical changes represent natural variability, then one cannot extrapolate past dynamical trends, and ozone recovery could be either hastened or delayed by dynamical variability. If, on the other hand, the past dynamical changes represent the dynamical response to WMGHG-induced climate change, then one might expect these changes to increase in magnitude in the future. This would decrease future ozone levels and delay ozone recovery. In the case of tropopause height changes, to the extent that they are themselves caused by ozone depletion, the changes should reverse in the future.

Another potential dynamical influence on ozone arises via

Box 1.7. Stratospheric ozone recovery

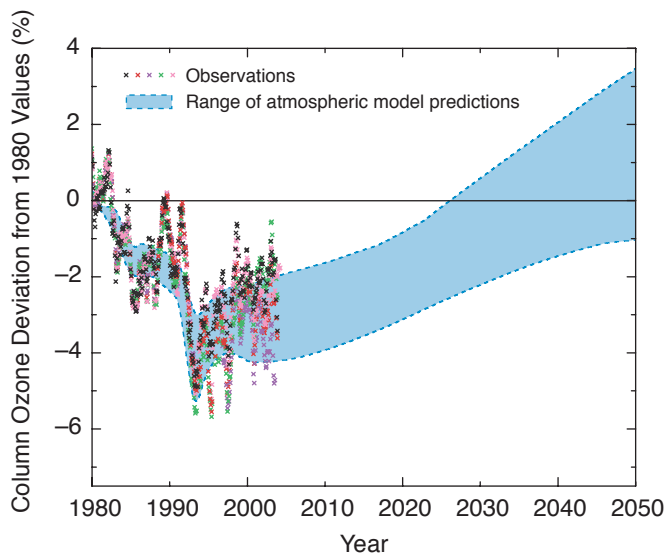
It is well established that the depletion of the ozone layer, both globally and in the polar regions, is attributable to an atmospheric chlorine burden that has been strongly enhanced, compared with natural levels, by anthropogenic emissions of halogen-containing compounds. Today, the production of such compounds has largely stopped following the regulations of the Montreal Protocol. However, owing to the long lifetime of the most important halogen source gases, the removal of these gases from the atmosphere will take many decades. The expectation that they will be ultimately removed is based on the assumption that global compliance with the Montreal Protocol will continue.

As a consequence, it might be expected that in about 50 years ozone depletion as it is observed today will have disappeared or, in other words, that the ozone layer will have ‘recovered’ (see figure). However, because of global climate change the state of the atmosphere has changed in recent decades and is expected to change further over the coming decades, so that a recovery to precisely the pre-1980 (that is, to the pre-‘ozone hole’) conditions will not occur.

Therefore, it is not obvious what should be considered as a detection of the *onset* of a ‘recovery’ of the ozone layer. A true detection of the onset of recovery requires more than the observation of a slow down or even a reversal of a downward ozone trend in a particular region, even if known natural periodic signals, such as the quasi-biennial oscillation or the 11-year solar cycle, have been accounted for. Rather, a detection of the onset of recovery requires that any temporal change in ozone in a particular region of the atmosphere can be *attributed* to the reduction of the atmospheric concentrations of anthropogenic halogen compounds as a result of the Montreal Protocol. Although one recent paper (Newchurch *et al.*, 2003) has reported that the first stage of a recovery of the ozone layer has been detected in observations of upper-stratospheric ozone, there is currently no consensus in the scientific community that the recovery of stratospheric ozone has been unequivocally established.

1. The detection of the onset of the recovery of stratospheric ozone will result from careful comparisons of the latest ozone measurements with past values. It is expected that ozone recovery will be first noticeable as a change in particular features, including: An increase in global column ozone towards values observed before 1980, when halogen source-gas abundances were much lower than they are today.
2. A sustained reduction in the maximum size of the Antarctic ozone hole, and an increase in the minimum value of column ozone in the hole.
3. Less ozone depletion in those Arctic winters in which temperatures fall below the threshold for the existence of polar stratospheric clouds (195 K).

As the ozone layer approaches full recovery, we expect to observe changes in all these features.



Box 1.7, Figure. Observed and modelled changes in low and middle latitude (60°S–60°N) de-seasonalized column ozone relative to 1980. The black symbols indicate ground-based measurements, and the coloured symbols various satellite-based data sets, updated from Fioletov *et al.* (2002). The range of model predictions comes from the use of several different 2-D photochemistry models forced with the same halocarbon scenario (WMO, 2003, Chapter 4); some models also allowed for the effect on stratospheric temperatures of changing CO₂ amounts. The measurements show that 60°S–60°N column ozone values decreased beginning in the early 1980s, and the models capture the timing and extent of this decrease quite well. Modelled halogen source-gas concentrations decrease in the early 21st century in response to the Montreal Protocol (Figure 1.7), so the simulated ozone values increase and recover towards pre-1980 values. Adapted from Figure Q20-1 of WMO (2003).

water vapour. Stratospheric water vapour is controlled by two processes: methane oxidation within the stratosphere and the transport of water vapour into the stratosphere. The latter depends in large part on the temperature of the tropical tropopause, although the precise details of this relationship remain unclear (see Section 1.3.4.4). In the future, changes in tropical tropopause temperature could conceivably affect the water vapour content of the stratosphere.

Unfortunately, our ability to predict future dynamical influences on ozone is very poor, for two reasons. First, dynamical processes affecting ozone exhibit significant temporal variability and are highly sensitive to other aspects of the atmospheric circulation. This means that the WMGHG-induced signal is inherently difficult to isolate or to represent accurately in CCMs, whereas the climate noise is relatively high (especially in the NH). Second, there are still uncertainties in the performance of the CCMs, which are the tools needed to address this question. As discussed in Section 1.4.1, predictions of WMGHG-induced dynamical changes by CCMs do not even agree on the sign of the changes: some models predict a weakened PWD, which would decrease mid-latitude (and polar) ozone by weakening transport, whereas others predict a strengthened PWD. Note that these dynamical changes would also affect the lifetime of stratospheric pollutants, with stronger PWD leading to shorter lifetimes (Rind *et al.*, 1990; Butchart and Scaife, 2001). (The latter effect acts on the several-year time scale associated with the Brewer-Dobson circulation, in contrast with the essentially instantaneous effect of PWD on ozone transport.) Thus, the direct effect of PWD change on ozone transport (no matter what its sign) would be reinforced over decadal time scales by altered chemical ozone loss arising from PWD-induced changes in stratospheric chlorine loading.

To summarize the results from 2-D models, upper-stratospheric ozone in the mid-latitudes will recover to pre-1980 levels well before stratospheric chlorine loading returns to pre-1980 levels, and could even overshoot pre-1980 levels because of CO₂-induced upper-stratospheric cooling (see, for example, WMO, 2003, Chapter 4). However, details of this future evolution are sensitive to many factors (uncertain emission scenarios, future climate change, changes in water vapour, volcanic eruptions, etc.) and there is significant divergence between different models. In terms of mid-latitude column ozone, where changes are expected to be dominated by ozone in the lower stratosphere, 2-D models all predict a steadily increasing ozone abundance as halogen levels decrease. While these models usually include a detailed treatment of polar chemistry, they do not include a detailed treatment of polar dynamics and mixing to mid-latitudes, or of dynamical aspects of climate change. Any future changes in stratospheric circulation and transport, or a large Pinatubo-like volcanic eruption, could have the potential to affect global column ozone, both directly and indirectly via chemical processes. Quantitative prediction is clearly difficult. At this stage, CCM simulations provide sensitivity calculations, which allow for the exploration of some examples of possible future evolution.

1.4.2.2 Polar ozone

As noted earlier, 2-D models do not provide a realistic treatment of polar processes, so predictions of polar ozone rely principally on CCMs. An intensive intercomparison of CCM predictions, the first of its kind, was performed for Chapter 3 of WMO (2003) (see Austin *et al.*, 2003). It is important to recognize that, apart from model deficiencies, CCM predictions are themselves subject to model variability and thus must be viewed in a statistical sense. Because of computer limitations (CPU time and mass storage), a large number of simulations with a single CCM cannot be carried out, so the models cannot yet be generally employed for ensemble runs. The approach taken in Austin *et al.* (2003) was to regard the collection of different CCMs as representing an ensemble. The collection included, moreover, a mixture of transient and time-slice runs (see Section 1.4.1).

For the Antarctic, where the CCMs all reproduce the development of the ozone hole in a reasonably realistic manner, the predicted future evolution is shown in Figure 1.15. Considering all the models, there is an overall consensus that the recovery of the Antarctic ozone hole will essentially follow the stratospheric chlorine loading. There is a hint in Figure 1.15 of a slight delay in the recovery compared with the peak in chlorine loading, presumably because of a cooling arising from the specified increase in WMGHG concentrations. Austin *et al.* (2003) estimated that the recovery of the Antarctic ozone layer can be expected to begin any year within the range 2001 to 2008. This would mean that Antarctic ozone depletion could slightly increase within the next few years despite a decrease in stratospheric chlorine loading, because lower temperatures would increase chlorine activation. However there is considerable natural variability, so it is also quite possible that the most severe Antarctic ozone hole has already occurred.

In the Arctic, where ozone depletion is more sensitive to meteorological conditions, the picture drawn by the CCMs is not consistent (Figure 1.17). Whereas most CCMs also predict a delayed start of Arctic ozone recovery (according to Austin *et al.* (2003), any year within the range 2004 to 2019), others indicate a different development: they simulate an enhanced PWD that produces a more disturbed and warmer NH stratospheric vortex in the future. (Enhanced PWD would also lead to a stronger meridional circulation and faster removal of CFCs.) This ‘dynamical heating’ more than compensates for the radiative cooling due to enhanced greenhouse-gas concentrations. Under these circumstances, and in combination with reduced stratospheric chlorine concentrations, polar ozone in these CCMs recovers within the next decade to values measured before the start of stratospheric ozone depletion. However, none of the current models suggest that an ‘ozone hole’, similar to that observed in the Antarctic, will occur over the Arctic (Figure 1.17). In this respect, the earlier GISS result (Shindell *et al.*, 1998), which is also depicted in Figure 1.17a, has not been supported by the more recent models (Austin *et al.*, 2003; WMO, 2003, Chapter 3). Analyses of model results show that the choice of the prescribed SSTs seems to play a critical role in the planetary-wave forcing (Schnadt and Dameris, 2003). Predicted SSTs (derived

from coupled atmosphere-ocean models) vary in response to the same forcings that are already included in CCMs. Realistic predictions of future SSTs are therefore a necessary prerequisite for stratospheric circulation predictions, at least in the NH extratropics.

The differences between the currently available CCM results clearly indicate the uncertainties in the assessment of the future development of polar ozone. In the NH the differences are more pronounced than in the SH. Part of these differences arises from the highly variable nature of the NH circulation, as is reflected in the past record (Section 1.4.1). Until now, the different transient model predictions have been based on single realizations, not ensembles, so it is not yet possible to determine whether the differences between the models – with the sole exception of the GISS results shown in Figure 1.17, which are significantly different from the other model results – are statistically significant. The time-slice simulations give some indication of the range of natural variability that is possible, and allow for a wide range of future possibilities. Nevertheless there are also significant uncertainties arising from the performance of the underlying dynamical models. Cold biases have been found in the stratosphere of many of the models, with obvious direct consequences for chemistry. In consequence, at the current stage of model development, uncertainties in the details of PSC formation and sedimentation (denitrification) might be less important than model temperature biases for simulating accurate ozone amounts, although it is possible that the models underestimate the sensitivity of chemical ozone loss to temperature changes. However, because it has been shown that denitrification does contribute significantly to Arctic ozone loss and is very sensitive to temperature, both problems have to be solved before a reliable estimate of future Arctic ozone losses is possible. Further investigations and model developments, combined with data analysis, are needed in order to reduce or eliminate these various model deficiencies and quantify the natural variability.

In summary, the Antarctic ozone hole is expected to recover more or less following the decrease in chlorine loading, and return to 1980 levels in the 2045 to 2055 time frame. There may be a slight delay arising from WMGHG-induced cooling, but natural variability in the extent of the ozone hole is sufficiently large that the most severe ozone hole may have already occurred, or may occur in the next five years or so. With regard to the Arctic, the future evolution of ozone is potentially sensitive to climate change and to natural variability, and will not necessarily follow strictly the chlorine loading. There is uncertainty in even the sign of the dynamical feedback to WMGHG changes. Numerical models like CCMs are needed to make sensitivity studies to estimate possible future changes, although they are currently not fully evaluated and their deficiencies are obvious. Therefore, the interpretation of such ‘predictions’ must be performed with care. Progress will result from further development of CCMs and from comparisons of results between models and with observations. This will help to get a better understanding of potential feedbacks in the atmosphere, thereby leading to more reliable estimates of future changes.

1.5 Climate change from ODSs, their substitutes and ozone depletion

Previous sections in this chapter have primarily been concerned with complex interactions between stratospheric ozone loss and the climate of the stratosphere, including past and future behaviour. In this section we discuss and use the concept of radiative forcing to quantify the effect of ODSs and their substitutes on *surface* climate. Radiative forcing is used to quantify the direct role of these compounds, as well as their indirect role through stratospheric ozone depletion. Section 1.5.1 discusses the applicability of radiative forcing, Section 1.5.2 examines the direct radiative forcing from ODSs and their substitutes, and Section 1.5.3 goes on to discuss their indirect radiative forcing. Lastly, Section 1.5.4 presents an example scenario for the net (direct plus indirect) radiative forcing from the ODSs and their substitutes, placing it within our general understanding of climate change.

1.5.1 Radiative forcing and climate sensitivity

Sections 1.5.2 to 1.5.4 compare the radiative forcings from halocarbons and ozone to assess their roles in climate change. To make this comparison we have to assume that (a) radiative forcings can be compared between different mechanisms and (b) radiative forcing is related to the climate change issue of interest. The first assumption is equivalent to saying that the climate sensitivity (λ) is constant between different mechanisms (see Box 1.3), and is implicit whenever direct and indirect radiative forcings are compared (e.g., Section 1.5.4).

However, several climate modelling studies have found that for many climate mechanisms λ varies with the latitude of the imposed forcing, and is higher for changes in the extratropics than for changes in the tropics (IPCC, 2001, Chapter 6; Joshi *et al.*, 2003). Additionally, several climate-modelling studies have compared the climate sensitivity for stratospheric ozone increases (WMO, 2003, Chapter 4; Joshi *et al.*, 2003) and generally found that global stratospheric ozone increases have a 20–80% higher climate sensitivity than carbon dioxide. This finding has been attributed to an additional positive feedback that results from an increase in stratospheric water vapour, which in turn arises from a warmer tropical tropopause (Stuber *et al.*, 2001; Joshi *et al.*, 2003). However, the latter studies all used idealized stratospheric ozone changes, and to date no study has performed similar analyses with realistic ozone changes.

Climate models also typically have different responses to equivalent forcings from carbon dioxide and from other WMGHGs (Wang *et al.*, 1992; Govindasamy *et al.*, 2001); these results indicate possible differences in climate sensitivity for CO₂ and halocarbons. The two studies that have examined this directly reached contradictory conclusions. Hansen *et al.* (1997) found halocarbons to have about a 20% larger climate sensitivity than carbon dioxide, mainly because of a stronger positive cloud feedback in their halocarbon experiments. In contrast, Forster and Joshi (2005) found that, because halocar-

bons preferentially heat the tropical tropopause region rather than the surface (see Box 1.4), climate sensitivity for halocarbon changes was 6% smaller than for carbon dioxide changes.

The trade-off or partial cancellation between direct and indirect radiative forcing discussed in Section 1.5.4 only occurs in the global mean: the latitudinal forcing patterns actually complement each other. Both stratospheric ozone depletion and increases in halocarbons realize more positive forcing in the tropics and more negative forcing at higher latitudes (IPCC, 2001, Chapter 6). Therefore, the variation in climate sensitivity with latitude of any applied forcing would likely mean that, even if the halocarbon and ozone forcing cancelled each other out in the global mean (to give a net forcing of zero), an overall global cooling would result. Further, the patterns of surface temperature response may well be distinct.

Radiative forcing estimates, such as those shown in Figure 1.3, are measured as changes from pre-industrial times and are indicative of the equilibrium surface temperature change one might have expected since then. Radiative forcing is not necessarily indicative of patterns of temperature change, transient temperature changes or other metrics. In reality, only 60–80% of the temperature changes associated with the radiative forcing shown in Figure 1.3 would have already been realized in the observed surface warming of the last 150+ years (IPCC, 2001, Chapter 6). From any time period, such as the present, future temperature changes will come from the combination of temperatures continuing to respond to past radiative forcing and any new changes to the radiative forcing. The rate of change of radiative forcing is potentially more important for evaluating short-term climate change and possibilities for mitigation than the total radiative forcing. It is therefore useful to examine the rate, as well as the total radiative forcing (Solomon and Daniel, 1996).

In summary, adopting radiative forcing and examining its rate of change are among the best methods for comparing the climate roles of carbon dioxide, ozone-depleting gases, their substitutes and ozone. However, radiative forcing gives an estimate only of the equilibrium globally averaged surface temperature response, and could lead to errors of around 50% (given the range in model results discussed above) when comparing the predicted global mean temperature change from ozone and the halocarbons with that from carbon dioxide.

1.5.2 Direct radiative forcing of ODSs and their substitutes

The direct radiative forcing from the ozone-depleting gases and their substitutes are relatively well known, and have been comprehensively assessed in Chapter 1 of WMO (2003) and Chapter 6 of IPCC (2001). The radiative forcing of the substitute gases is re-assessed in Chapter 2 of this report. The radiative forcings of the ODSs have individual uncertainties of about 10%, and together they have contributed about 0.26 W m⁻² (22%) to the total WMGHG radiative forcing since 1970 (Figure 1.3; Table 1.1).

Table 1.1. Positive direct radiative forcing by WMGHGs, including halocarbon gases, since 1750 and since 1970, and negative indirect radiative forcing since 1980 (no indirect forcing occurred prior to 1980). Based on data in Chapter 6 of IPCC (2001) and Chapter 1 of WMO (2003). Totals may not sum up consistently because of rounding.

Species	Radiative Forcing (W m ⁻²)		
	Direct		Indirect
	1750–2000	1970–2000	1980–2000
<i>CFCs</i>			
CFC-11	0.066	0.053	-0.043
CFC-12	0.17	0.14	-0.034
CFC-13	0.001	0.001	n.a.
CFC-113	0.025	0.023	-0.010
CFC-114	0.005	0.003	n.a.
CFC-115	0.002	0.002	n.a.
Total	0.27	0.22	-0.088
<i>HCFCs</i>			
HCFC-22	0.028	0.026	-0.002
HCFC-141b	0.0018	0.0018	0
HCFC-142b	0.0024	0.0024	0
HCFC-124	0.0005	0.0005	n.a.
Total	0.033	0.031	-0.002
<i>Halons and methyl bromide</i>			
Halon-1211	0.0012	0.0012	-0.010
Halon-1301	0.0009	0.0009	-0.004
Halon-2402	0.0001	0.0001	-0.002
CH ₃ Br	0.0001	0.0001	-0.006
Total	0.0022	0.0022	-0.023
<i>Chlorocarbons</i>			
CH ₃ Cl	0.0007	0.0001	~0
CCl ₄	0.0127	0.0029	-0.023
CH ₃ CCl ₃	0.0028	0.0018	-0.015
Total	0.021	0.0048	-0.038
Total ODSs	0.32	0.26	-0.150
<i>HFCs</i>			
HFC-23	0.0029	0.0029	
HFC-134a	0.0024	0.0024	
HFC-125	0.0003	0.0003	
HFC-152a	0.0002	0.0002	
Total	0.0058	0.0058	
<i>PFCs</i>			
CF ₄	0.0029	0.0029	
C ₂ F ₆	0.0006	0.0006	
C ₃ F ₈	0.0001	0.0001	
C ₄ F ₈	0.0003	0.0003	
Total	0.0039	0.0039	
Total halocarbons	0.33	0.26	-0.150
<i>Other WMGHGs</i>			
CO ₂	1.50	0.67	
Methane	0.49	0.13	
Nitrous oxide	0.15	0.068	
SF ₆	0.0024	0.0024	
Total	2.14	0.87	
Total WMGHGs	2.48	1.14	-0.150

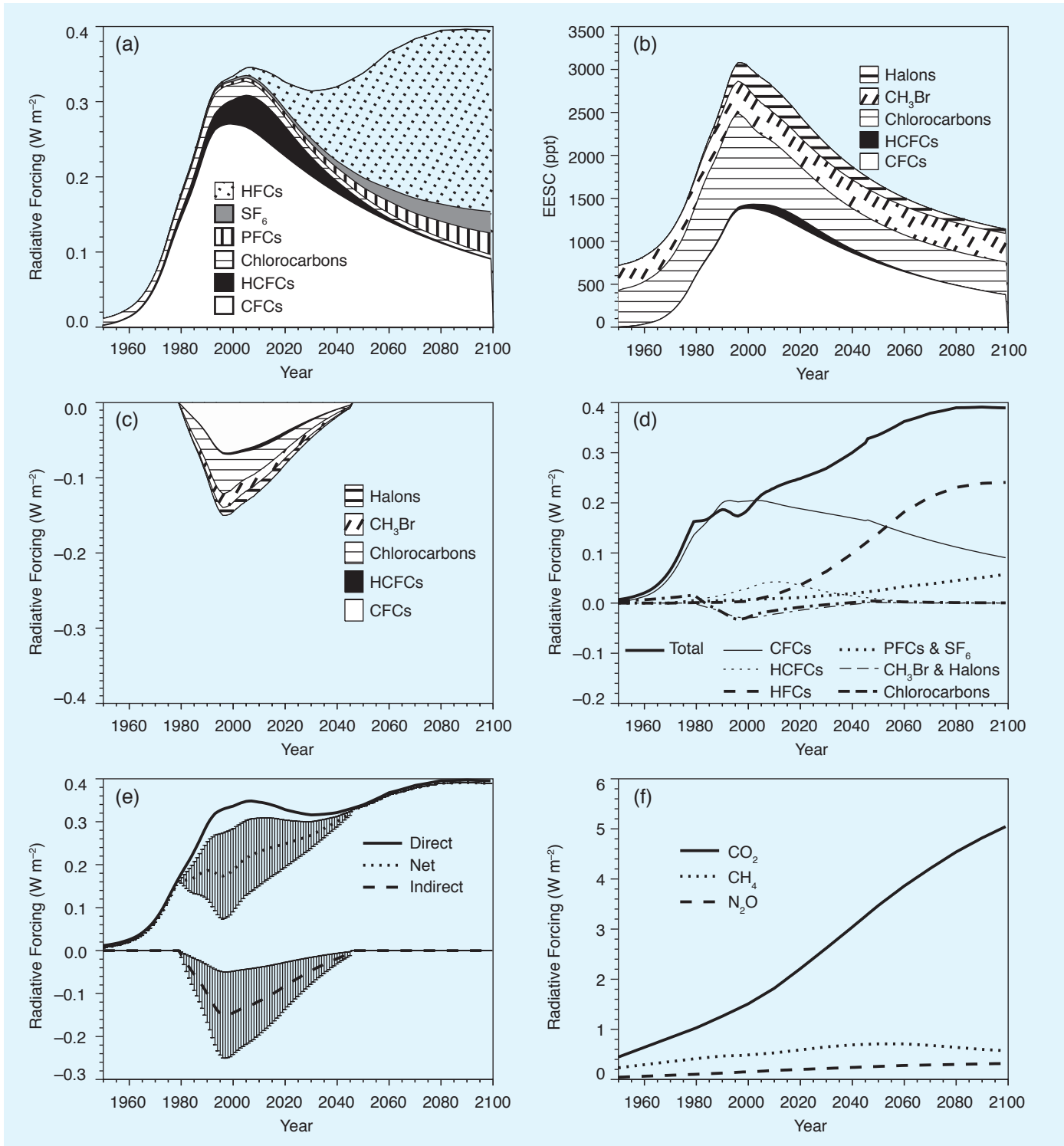


Figure 1.18. The breakdown of (a) the total direct radiative forcing, (b) EESC, (c) the indirect radiative forcing, and (d) the net radiative forcing time-series for individual halocarbon groups. In (e) the total direct, indirect and net radiative forcings are shown, with error bars arising from uncertainties in the stratospheric ozone radiative forcing from Chapter 6 of IPCC (2001). In (f) the radiative forcing for CO₂, N₂O and CH₄ is shown for comparison with the halocarbons. For (a), (b) and (c) the individual forcings have been stacked to show the total forcing. These time-series are derived from data in scenario Ab from Chapter 1 of WMO (2003) for the ozone-depleting halocarbons and scenario SRES A1B from Chapter 6 of IPCC (2001) for the other gases. The EESC has been calculated using data in Chapter 1 of WMO (2003), assuming that bromine is 45 times more effective on a per-atom basis at destroying ozone than chlorine. The change in EESC between 1979 and 1997 is assumed to give an indirect radiative forcing of -0.15 W m^{-2} (IPCC, 2001, Chapter 6). This radiative forcing scales with EESC amounts above the 1979 threshold. From Forster and Joshi (2005).

Section 1.2.2 discussed past changes and a future scenario for the abundances of the ozone-depleting gases. Chapter 2 discusses a range of future scenarios for the substitute gases. In this section we examine scenarios for future radiative forcing of the ODSs themselves. One possible future scenario is the A1B scenario from the Special Report on Emission Scenarios (SRES; IPCC, 2000), which for the ODSs is consistent with the Ab scenario from WMO (2003). Figure 1.18a shows a time-series of radiative forcing for the different groups of gases for this scenario. The figure shows that the current radiative forcing from ODSs is beginning to decline. However, because of their long lifetime in the atmosphere and their continued emission from the ‘ODS bank’ (namely those ODSs that have already been manufactured but have not yet been released into the atmosphere), they could dominate the radiative forcing for the next four to five decades. In this scenario HFCs dominate the radiative forcing by the end of the century, but this is only one example of several possible scenarios (see Chapter 2).

As the production of ODSs has now essentially ceased (WMO, 2003, Chapter 1), the principal issue for the emissions of ODSs concerns the treatment of the ODS bank. The scenario for ODSs in Figure 1.18a includes continued emissions of ODSs from the ODS bank, and if these emissions from the bank could be cut by recovering the ODSs, the radiative forcing time-series could be somewhat altered. Figure 1.19 illustrates the role of post-2004 releases from the ODS bank in continuing the ODS radiative forcing, and compares it with the HFC radiative forcing. If emissions of ODSs from the bank continue at their current rate, ODS radiative forcing will still decrease. However, for at least the next two decades, the continued emission from the ODS bank is expected to have a comparable contribution to the total radiative forcing with that of HFC emissions. This calculation does not take into account the effect that ODSs have on the stratospheric ozone radiative forcing, which is discussed next.

1.5.3 Indirect radiative forcing of ODSs

IPCC (2001) gives the value for the radiative forcing of stratospheric ozone as -0.15 W m^{-2} , with a range of $\pm 0.1 \text{ W m}^{-2}$. This radiative forcing primarily arises from mid- and high-latitude ozone depletion in the lower stratosphere (see Box 1.3). Past calculations of this radiative forcing have extensively employed observed trends in ozone. It is generally assumed that these observed ozone trends have been caused entirely by emissions of ODSs, so the negative radiative forcing of stratospheric ozone can be thought of as ‘indirect’. For the ODSs it is possible to calculate EESC values and use them to scale the ozone radiative forcing (see Box 1.8). EESC values for different ODSs are shown in Figure 1.18b. The indirect radiative forcing of each ODS is shown in Figure 1.18c. These values have been calculated by assuming that EESC values above a 1979 background level give a forcing that scales with the -0.15 W m^{-2} best-estimate forcing from Chapter 6 of IPCC (2001) over 1979–1997. This calculation follows the approaches of Daniel *et al.* (1999)

and Forster and Joshi (2005). It results in a value of the indirect forcing that is purely from stratospheric ozone loss and ignores any possible changes to tropospheric chemistry and climate, which are discussed in Chapter 2. Table 1.1 shows the indirect radiative forcing of stratospheric ozone broken down by species.

Uncertainties in the indirect radiative forcing of stratospheric ozone arise from many different factors:

- The quoted IPCC (2001, Chapter 6) range of $\pm 0.1 \text{ W m}^{-2}$ for the radiative forcing of stratospheric ozone is based on differing model results and arises primarily from the underlying uncertainty in the vertical distribution of the ozone trend relative to the tropopause. The quoted range can be used to scale the indirect radiative forcing in Figure 1.18c, as shown with the error bars in Figure 1.18e.
- The future radiative forcing from ozone is in fact more uncertain than the range quoted in IPCC (2001) because there is a lack of confidence in the details of future ozone changes, particularly near the tropopause, and many different scenarios are possible. These scenarios are discussed further in Section 1.5.4.
- Although most of the ozone changes can be attributed to ODSs, a sizeable fraction of the NH changes could have oth-

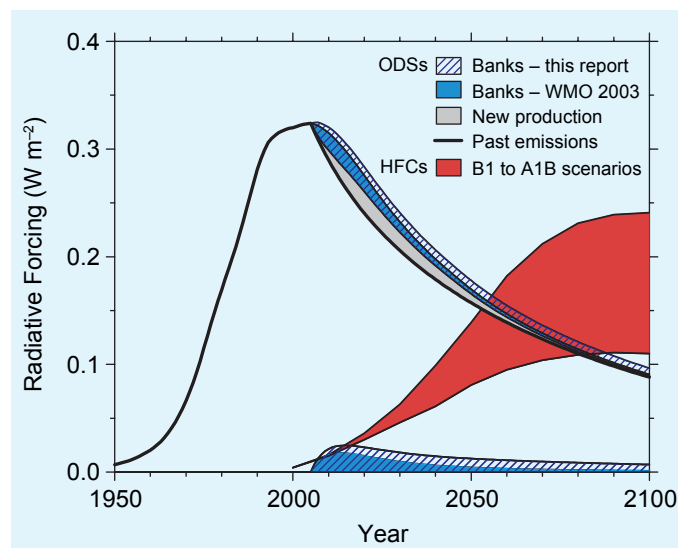


Figure 1.19. Direct radiative forcing of all ODSs compared with that of SRES projections for HFCs. The direct radiative forcing is split up into contributions from the commitment of past emissions (solid black line), release of allowed new production under the Montreal Protocol (grey shaded area), and release from ODS banks existing in 2004. Two estimates are given for these latter emissions, one based on bank estimates from WMO (2003), and one based on estimates in Ashford *et al.* (2004) – see Chapter 11. Radiative forcing due to HFCs is shown for the SRES B1 and A1B scenarios (boundaries of the red shaded area). The contribution due to the delayed release of ODSs in banks is shown separately and is comparable to that projected due to HFCs for the next two decades. ODSs also have other effects on radiative forcing.

Box 1.8. Ozone depletion potentials (ODPs) and equivalent effective stratospheric chlorine (EESC)

Ozone depletion potentials (ODPs) are used as a simple measure for quantifying the effect of various ozone-depleting compounds on the ozone layer, and have proved to be an important quantity for the formulation of the Montreal Protocol and its Amendments. The ODP is defined as the integrated change in total ozone per unit mass emission of a specific ozone-depleting substance relative to the integrated change in total ozone per unit mass emission of CFC-11 (WMO, 1995; WMO, 2003).

For the calculation of the ODP of an ozone-depleting substance, the change in total ozone per unit mass of emission of this substance may be determined with numerical models. As an alternative, Solomon *et al.* (1992) have formulated a semi-empirical approach for determining ODPs based mainly on observations rather than on models.

The quantities required for the semi-empirical approach are the physical properties of the halocarbons, their lifetimes, the so-called fractional release factor Φ – a factor representing the factor of inorganic halogen release in the stratosphere from observations relative to CFC-11 – and in the case of bromine, a quantification of the catalytic efficiency of ozone destruction relative to chlorine. For long-lived gases that are well mixed in the troposphere the definition of the semi-empirical ODP of a particular halogen compound is (Solomon *et al.*, 1992; Chapter 1 of WMO, 2003)

$$\text{ODP} = \Phi \cdot \alpha \cdot \frac{\tau_x}{\tau_{\text{CFC-11}}} \cdot \frac{M_{\text{CFC-11}}}{M_x} \cdot \frac{n_x}{3}$$

Here, τ is the global lifetime of the long-lived gas, M is the molecular weight, n is the number of halogen atoms and α is the relative efficiency of any halogen compound compared with chlorine. For bromine, $\alpha = 45$ (Daniel *et al.*, 1999). The current best estimates of ODPs by both the model and the semi-empirical methods are listed in Table 1.2 together with the ODP values originally adopted for the formulation of the Montreal Protocol.

The equivalent effective stratospheric chlorine (EESC) is an index that is similar to an ODP. It relates the total stratospheric chlorine and bromine levels to the tropospheric release of halocarbons. It was defined as a mixing ratio by Daniel *et al.* (1995):

$$\text{EESC} = \left(\sum_{\text{chlorine-containing compounds}} n_x C I_{\text{trop}}^{t-3} \Phi + \sum_{\text{bromine-containing compounds}} n_x \alpha B r_{\text{trop}}^{t-3} \Phi \right) F_{\text{CFC-11}}$$

where $C I_{\text{trop}}^{t-3}$ represents the stratospheric halocarbon mixing ratio at time t , and accounts for the approximately three years it takes to travel from the source of emission into the lower stratosphere; $F_{\text{CFC-11}}$ is the fractional release of halogens into the stratosphere from CFC-11, which is considered to be proportional to the change in column ozone.

er causes, especially those that occur close to the tropopause (Section 1.4.1). This means that a small but possibly significant part of the radiative forcing of stratospheric ozone may not be attributable to ODSs (Forster and Tourpali, 2001).

- The simple linear scaling between EESC values, above a 1979 background level, and the stratospheric ozone radiative forcing is used for obtaining an approximation to the ozone radiative forcing time-series. It was first proposed by Daniel *et al.* (1999). For EESC values below the 1979 level there is assumed to be no ozone depletion and no indirect radiative forcing. This simplistic approximation does not

take into account the many chemistry and climate feedbacks discussed in this chapter (see also Daniel *et al.*, 1999).

1.5.4 Net radiative forcing

Figures 1.18d–f show the direct, indirect and net radiative forcing time-series for the ODSs and other WMGHGs, based on the data in Figures 1.18a–c. These time-series depend critically on which scenario is used, which in the case of Figure 1.18 is the A1B SRES scenario from IPCC (2000). Nevertheless the figure gives one estimate of the possible global mean trade-offs

involved in assessing the role of halocarbons in climate. Direct radiative forcing from halocarbons has risen sharply since 1980. However, ozone depletion has contributed a negative indirect forcing. Uncertainties in the magnitude of the indirect forcing are sufficiently large that the net radiative forcing since 1980 may have either increased or decreased (Figure 1.18e). The best estimate is that the indirect forcing has largely offset the increase in the direct radiative forcing. This suggests that surface temperatures over the last few decades would have increased even more rapidly if stratospheric ozone depletion had not occurred. However, it is important to note that ozone depletion since 1980 is the result, in part, of ODS increases prior to 1980.

The balance between direct and indirect radiative forcing varies substantially between different classes of ODSs (Table 1.1). For the halons, the negative indirect forcing dominates their very small positive direct effect, causing their net forcing to be negative. In contrast, the CFCs and HCFCs have a net positive radiative forcing, despite their associated ozone loss.

The scenario shown in Figure 1.18 assumes that concentrations of ODS substitutes will increase rapidly in the future while those of the ODSs will decay. In that case, even though the direct radiative forcing of the halocarbons would decrease during the next few decades, the net forcing would actually increase because of ozone recovery. (Note that the future positive forcing from ozone recovery is not included in the SRES scenarios.) However, this increase in net forcing depends on which scenario is used for the ODS substitutes. The detailed quantification of the radiative forcing from the ODS substitutes is discussed in Chapter 2.

Table 1.2. Steady-state ozone depletion potentials (ODPs) for long-lived halocarbons (normalized to unity for CFC-11).

Halocarbon	Steady-State ODPs		
	WMO (1999) Model	WMO (2003) Semi- Empirical	Montreal Protocol
CFC-11		1	1
CFC-12	0.82	1.0	1.0
CFC-113	0.90	1.0	0.8
CFC-114	0.94 ^a		1.0
CFC-115	0.44 ^a		0.6
Halon-1301	12	12	10.0
Halon-1211	5.1	5.3 ^b	3.0
Halon-2402		<8.6	6.0
Halon-1202		1.3	
CCl ₄	1.20	0.73	1.1
CH ₃ CCl ₃	0.11	0.12	0.1
HCFC-22	0.034	0.05	0.055
HCFC-123	0.012	0.02	0.02
HCFC-124	0.026	0.02	0.022
HCFC-141b	0.086	0.12	0.11
HCFC-142b	0.043	0.07	0.065
HCFC-225ca	0.017	0.02	0.025
HCFC-225cb	0.017	0.03	0.033
CH ₃ Cl		0.02	
CH ₃ Br	0.37	0.38	0.6
Upper limits for selected hydrofluorocarbons			
HFC-134a	<1.5 × 10 ⁻⁵		
HFC-23	<4 × 10 ⁻⁴		
HFC-125	<3 × 10 ⁻⁵		

^a Updated in WMO (2003).

^b Value was erroneously reported in Table 1-5 of WMO (2003) as 6.0.

References

- Allaart, M., P. Valks, R. van der A, A. Piters, H. Kelder, and P. F. J. van Velthoven, 2000: Ozone mini-hole observed over Europe, influence of low stratospheric temperature on observations. *Geophysical Research Letters*, **27**, 4089–4092.
- Allen, D. R., R. M. Bevilacqua, G. E. Nedoluha, C. E. Randall, and G. L. Manney, 2003: Unusual stratospheric transport and mixing during the 2002 Antarctic winter. *Geophysical Research Letters*, **30**(12), 1599.
- Ambaum, M. H. P. and B. J. Hoskins, 2002: The NAO troposphere-stratosphere connection. *Journal of Climate*, **15**, 1969–1978.
- Ambaum, M. H. P., B. J. Hoskins, and D. B. Stephenson, 2001: Arctic Oscillation or North Atlantic Oscillation? *Journal of Climate*, **14**(16), 3495–3507.
- Andrews, D. G., J. R. Holton, and C. B. Leovy, 1987: *Middle Atmosphere Dynamics*. Academic Press, Orlando, 489 pp.
- Appenzeller, C. and H. C. Davies, 1992: Structure of stratospheric intrusions into the troposphere. *Nature*, **358**, 570–572.
- Appenzeller, C., A. K. Weiss, and J. Staehelin, 2000: North Atlantic oscillation modulates total ozone winter trends. *Geophysical Research Letters*, **27**(8), 1131–1134.
- Ashford, P., D. Clodic, A. McCulloch, L. Kuijpers, 2004: Emission profiles from the foam and refrigeration sectors compared with atmospheric concentrations, Part 2 – Results and discussion. *International Journal of Refrigeration*, **27**(7), 701–716.
- Austin, J., D. Shindell, S. R. Beagley, C. Brühl, M. Dameris, E. Manzini, T. Nagashima, P. Newman, S. Pawson, G. Pitari, E. Rozanov, C. Schnadt, and T. G. Shepherd, 2003: Uncertainties and assessments of chemistry-climate models of the stratosphere. *Atmospheric Chemistry and Physics*, **3**, 1–27.
- Baldwin, M. P. and T. J. Dunkerton, 1999: Propagation of the Arctic Oscillation from the stratosphere to the troposphere. *Journal of Geophysical Research – Atmospheres*, **104**(D24), 30,937–30,946.
- Barnett, J. J., J. T. Houghton, and J. A. Pyle, 1975: The temperature dependence of the ozone concentration near the stratosphere. *Quarterly Journal of the Royal Meteorological Society*, **101**, 245–257.
- Bengtsson, L., S. Hagemann, and K. I. Hodges, 2004: Can climate trends be calculated from reanalysis data? *Journal of Geophysical Research – Atmospheres*, **109**(D11), doi:10.1029/2004JD004536.
- Bodeker, G. E., J. C. Scott, K. Kreher, and R. L. McKenzie, 2001: Global ozone trends in potential vorticity coordinates using TOMS and GOME intercompared against the Dobson network: 1978–1998. *Journal of Geophysical Research – Atmospheres*, **106**(D19), 23,029–23,042.
- Bojkov, R. D., C. S. Zerefos, D. S. Balis, I. C. Ziomas, and A. F. Bais, 1993: Record low total ozone during northern winters of 1992 and 1993. *Geophysical Research Letters*, **20**(13), 1351–1354.
- Borrmann, S., S. Solomon, J. E. Dye, D. Baumgardner, K. K. Kelly, and K. R. Chan, 1997: Heterogeneous reactions on stratospheric background aerosols, volcanic sulfuric acid droplets, and type I polar stratospheric clouds: Effects of temperature fluctuations and differences in particle phase. *Journal of Geophysical Research – Atmospheres*, **102**(D3), 3639–3648.
- Bösch, H., C. Camy-Peyret, M. P. Chipperfield, R. Fitzenberger, H. Harder, U. Platt, and K. Pfeilsticker, 2003: Upper limits of stratospheric IO and OIO inferred from center-to-limb-darkening-corrected balloon-borne solar occultation visible spectra: Implications for total gaseous iodine and stratospheric ozone. *Journal of Geophysical Research – Atmospheres*, **108**(D15), 4455, doi:10.1029/2002JD003078.
- Bregman, B., P. H. Wang, and J. Lelieveld, 2002: Chemical ozone loss in the tropopause region on subvisible ice clouds, calculated with a chemistry-transport model. *Journal of Geophysical Research – Atmospheres*, **107**(D3), doi:10.1029/2001JD000761.
- Brewer, A.M., 1949: Evidence of a world circulation provided by the measurement of helium and water distribution in the stratosphere. *Quarterly Journal of the Royal Meteorological Society*, **75**, 351–363.
- Butchart, N. and A. A. Scaife, 2001: Removal of chlorofluorocarbons by increased mass exchange between the stratosphere and troposphere in a changing climate. *Nature*, **410**(6830), 799–802.
- Butler, J. H., M. Battle, M. Bender, S. A. Montzka, A. D. Clarke, E. S. Saltzman, C. Sucher, J. Severinghaus, and J. W. Elkins, 1999: A twentieth century record of atmospheric halocarbons in polar firn air. *Nature*, **399**, 749–755.
- Canziani, P. O., R. H. Compagnucci, S. A. Bischoff, and W. E. Legnani, 2002: A study of impacts of tropospheric synoptic processes on the genesis and evolution of extreme total ozone anomalies over southern South America. *Journal of Geophysical Research – Atmospheres*, **107**(D24), 4741, doi:10.1029/2001JD000965.
- Chen, P. and W. A. Robinson, 1992: Propagation of planetary waves between the troposphere and stratosphere. *Journal of the Atmospheric Sciences*, **49**, 2533–2545.
- Chipperfield, M. P., 2003: A three-dimensional model study of long-term mid-high latitude lower stratosphere ozone changes. *Atmospheric Chemistry and Physics*, **3**, 1253–1265.
- Christiansen, B., 2001: Downward propagation of zonal mean zonal wind anomalies from the stratosphere to the troposphere: Model and reanalysis. *Journal of Geophysical Research – Atmospheres*, **106**(D21), 27,307–27,322.
- Considine, D. B., J. E. Rosenfield, and E. L. Fleming, 2001: An interactive model study of the influence of the Mount Pinatubo aerosol on stratospheric methane and water trends. *Journal of Geophysical Research – Atmospheres*, **106**(D21), 27,711–27,727.
- Crutzen, P. J., 1974: Estimates of possible future ozone reductions from continued use of fluorochloro-methanes (CF₂Cl₂, CFC₁₃). *Geophysical Research Letters*, **1**, 205–208.
- Daniel, J. S., S. Solomon, and D. L. Albritton, 1995: On the evaluation of halocarbon radiative forcing and global warming potentials. *Journal of Geophysical Research – Atmospheres*, **100**(D1), 1271–1285.
- Daniel, J. S., S. Solomon, R. W. Portmann, and R. R. Garcia, 1999: Stratospheric ozone destruction: The importance of bromine relative to chlorine. *Journal of Geophysical Research – Atmospheres*, **104**, 23,871–23,880.
- DeMore, W. B., C. J. Howard, S. P. Sander, A. R. Ravishankara, D. M. Golden, C. E. Kolb, R. F. Hampson, M. J. Molina, and M. J. Kurylo, 1997: Chemical Kinetics and Photochemical

- Data for Use in Stratospheric Modeling. Evaluation Number 12. JPL Publication No. 97-4, National Aeronautics and Space Administration, Jet Propulsion Laboratory, California Institute of Technology, Pasadena, California. (Available at http://jpldataeval.jpl.nasa.gov/pdf/Atmos97_Anotated.pdf)
- Dickinson, R. E.**, 1978: Effect of chlorofluoromethane infrared radiation on zonal atmospheric temperatures. *Journal of the Atmospheric Sciences*, **35**(11), 2142–2152.
- Dlugokencky, E. J.**, S. Houweling, L. Bruhwiler, K. A. Masarie, P. M. Lang, J. B. Miller, and P. P. Tans, 2003: Atmospheric methane levels off: Temporary pause or a new steady-state? *Geophysical Research Letters*, **30**(19), 1992, doi:10.1029/2003GL018126.
- Dobson, G. M. B.**, 1963: *Exploring the Atmosphere*. Clarendon Press, London.
- Dvortsov, V. L.** and S. Solomon, 2001: Response of the stratospheric temperatures and ozone to past and future increases in stratospheric humidity. *Journal of Geophysical Research – Atmospheres*, **106**(D7), 7505–7514.
- EC**, 2003: *Ozone-Climate Interactions*. Air Pollution Research Report No. 81, EUR 20623, European Commission, Office for Official Publications of the European Communities, Luxembourg, 143 pp.
- Fioletov, V. E.** and T. G. Shepherd, 2003: Seasonal persistence of midlatitude total ozone anomalies. *Geophysical Research Letters*, **30**(7), 1417, doi:10.1029/2002GL016739.
- Fioletov, V. E.**, G. E. Bodeker, A. J. Miller, R. D. McPeters, and R. Stolarski, 2002: Global and zonal total ozone variations estimated from ground-based and satellite measurements: 1964–2000. *Journal of Geophysical Research – Atmospheres*, **107**(D22), 4647, doi:10.1029/2001JD001350.
- Fish, D. J.**, H. K. Roscoe, and P. V. Johnston, 2000: Possible causes of stratospheric NO₂ trends observed at Lauder, New Zealand. *Geophysical Research Letters*, **27**(20), 3313–3316.
- Fleming, E. L.**, S. Chandra, J. J. Barnett, and M. Corney, 1990: Zonal mean temperature, pressure, zonal wind and geopotential height as functions of latitude. *Advances in Space Research*, **12**, 1211–1259.
- Forster, P. M. d. F.** and M. Joshi, 2005: The role of halocarbons in the climate change of the troposphere and stratosphere. *Climatic Change* (in press).
- Forster, P. M. d. F.** and K. Tourpali, 2001: Effect of tropopause height changes on the calculation of ozone trends and their radiative forcing. *Journal of Geophysical Research – Atmospheres*, **106**(D11), 12,241–12,251.
- Fortuin, J. P. F.** and H. Kelder, 1998: An ozone climatology based on ozonesonde and satellite measurements. *Journal of Geophysical Research – Atmospheres*, **103**(D24), 31,709–31,734.
- Fortuin, J. P. F.** and U. Langematz, 1994: An update on the global ozone climatology and on concurrent ozone and temperature trends. *SPIE, Atmospheric Sensing and Modeling*, **2311**, 207–216.
- Fraser, P. J.**, D. E. Oram, C. E. Reeves, S. A. Penkett, and A. McCulloch, 1999: Southern Hemispheric halon trends (1978–1998) and global halon emissions. *Journal of Geophysical Research – Atmospheres*, **104**, 15,985–15,999.
- Froidevaux, L.**, M. Allen, S. Berman, and A. Daughton, 1989: The mean ozone profile and its temperature sensitivity in the upper stratosphere and lower mesosphere. *Journal of Geophysical Research*, **94**, 6389–6417.
- Froidevaux, L.**, J. W. Waters, W. G. Read, P. S. Connell, D. E. Kinnison, and J. M. Russell, 2000: Variations in the free chlorine content of the stratosphere (1991–1997): Anthropogenic, volcanic, and methane influences. *Journal of Geophysical Research – Atmospheres*, **105**(D4), 4471–4481.
- Fusco, A. C.** and M. L. Salby, 1999: Interannual variations of total ozone and their relationship to variations of planetary wave activity. *Journal of Climate*, **12**(6), 1619–1629.
- Fyfe, J. C.**, G. J. Boer, and G. M. Flato, 1999: The Arctic and Antarctic oscillations and their projected changes under global warming. *Geophysical Research Letters*, **26**(11), 1601–1604.
- Gillett, N. P.** and D. W. J. Thompson, 2003: Simulation of recent Southern Hemisphere climate change. *Science*, **302**(5643), 273–275.
- Gillett, N. P.**, M. R. Allen, R. E. McDonald, C. A. Senior, D. T. Shindell, and G. A. Schmidt, 2002a: How linear is the Arctic Oscillation response to greenhouse gases? *Journal of Geophysical Research*, **107**(D3), 10.1029/2001JD000589.
- Gillett, N. P.**, M. R. Allen, and K. D. Williams, 2002b: The role of stratospheric resolution in simulating the Arctic Oscillation response to greenhouse gases. *Geophysical Research Letters*, **29**(10), doi:10.1029/2001GL014444.
- Gong, D. Y.** and S. W. Wang, 1999: Definition of Antarctic Oscillation Index. *Geophysical Research Letters*, **26**(4), 459–462.
- Govindasamy, B.**, K. E. Taylor, P. B. Duffy, B. D. Santer, A. S. Grossman, and K. E. Grant, 2001: Limitations of the equivalent CO₂ approximation in climate change simulations. *Journal of Geophysical Research – Atmospheres*, **106**, 22,593–22,603.
- Graf, H. F.**, J. Perlwitz, I. Kirchner, and I. Schult, 1995: Recent Northern Hemisphere climate trends, ozone changes, and increased greenhouse gas forcing. *Beiträge zur Physik der Atmosphäre*, **68**, 233–248.
- Graf, H. F.**, I. Kirchner, and J. Perlwitz, 1998: Changing lower stratospheric circulation: The role of ozone and greenhouse gases. *Journal of Geophysical Research – Atmospheres*, **103**(D10), 11,251–11,261.
- Groß, J. U.**, R. Müller, G. Becker, D. S. McKenna, and P. J. Crutzen, 1999: The upper stratospheric ozone budget: An update of calculations based on HALOE data. *Journal of Atmospheric Chemistry*, **34**(2), 171–183.
- Hall, A.** and M. Visbeck, 2002: Synchronous variability in the Southern Hemisphere atmosphere, sea ice, and ocean resulting from the annular mode. *Journal of Climate*, **15**(21), 3043–3057.
- Hansen, J.**, M. Sato, and R. Ruedy, 1997: Radiative forcing and climate response. *Journal of Geophysical Research – Atmospheres*, **102**(D6), 6831–6864.
- Highwood, E. J.** and B. J. Hoskins, 1998: The tropical tropopause. *Quarterly Journal of the Royal Meteorological Society*, **124**, 1579–1604.
- Hints, E. J.**, K. A. Boering, E. M. Weinstock, J. G. Anderson, B. L. Gary, L. Pfister, B. C. Daube, S. C. Wofsy, M. Loewenstein, J.

- R. Podolske, J. J. Margitan, and T. P. Bui, 1998: Troposphere-to-stratosphere transport in the lowermost stratosphere from measurements of H₂O, CO₂, N₂O and O₃. *Geophysical Research Letters*, **25**, 2655–2658.
- Hoinka**, K. P., 1999: Temperature, humidity, and wind at the global tropopause. *Monthly Weather Review*, **127**, 2248–2265.
- Holton**, J. R. and A. Gettelman, 2001: Horizontal transport and the dehydration of the stratosphere. *Geophysical Research Letters*, **28**(14), 2799–2802.
- Holton**, J. R., P. H. Haynes, M. E. McIntyre, A. R. Douglass, R. B. Rood, and L. Pfister, 1995: Stratosphere-troposphere exchange. *Reviews of Geophysics*, **33**(4), 403–439.
- Hood**, L., S. Rossi, and M. Beulen, 1999: Trends in lower stratospheric zonal winds, Rossby wave breaking behavior, and column ozone at northern midlatitudes. *Journal of Geophysical Research – Atmospheres*, **104**(D20), 24,321–24,339.
- Hood**, L. L., B. E. Soukharev, M. Fromm, and J. P. McCormack, 2001: Origin of extreme ozone minima at middle to high northern latitudes. *Journal of Geophysical Research – Atmospheres*, **106**(D18), 20,925–20,940.
- Hu**, Y. and K.-K. Tung, 2002: Interannual and decadal variations of planetary wave activity, stratospheric cooling, and Northern Hemisphere annular mode. *Journal of Climate*, **15**, 1659–1673.
- Hurrell**, J. W., 1995: Decadal trends in the North Atlantic Oscillation – Regional temperatures and precipitation. *Science*, **269**(5224), 676–679.
- IPCC**, 2000: *Emissions Scenarios*. Special Report of the Intergovernmental Panel on Climate Change [Nakicenovic, N. and R. Swart (eds.)]. Cambridge University Press, Cambridge, United Kingdom, and New York, NY, USA, 570 pp.
- IPCC**, 2001: *Climate Change 2001: The Scientific Basis. Contribution of Working Group I to the Third Assessment Report of the Intergovernmental Panel on Climate Change* [Houghton, J. T., Y. Ding, D. J. Griggs, M. Noguer, P. J. van der Linden, X. Dai, K. Maskell, and C. A. Johnson (eds.)]. Cambridge University Press, Cambridge, United Kingdom, and New York, NY, USA, 944 pp.
- James**, P. M., 1998: A climatology of ozone mini-holes over the Northern Hemisphere. *International Journal of Climatology*, **18**(12), 1287–1303.
- James**, P., A. Stohl, C. Forster, S. Eckhardt, P. Seibert, and A. Frank, 2003: A 15-year climatology of stratosphere-troposphere exchange with a Lagrangian particle dispersion model – 2. Mean climate and seasonal variability. *Journal of Geophysical Research – Atmospheres*, **108**(D12), 8522, doi:10.1029/2002JD002639.
- Joshi**, M., K. Shine, M. Ponater, N. Stuber, R. Sausen, and L. Li, 2003: A comparison of climate response to different radiative forcings in three general circulation models: Towards an improved metric of climate change. *Climate Dynamics*, **20**(7–8), 843–854.
- Jucks**, K. W. and R. J. Salawitch, 2000: Future changes in upper stratospheric ozone. In: *Atmospheric Science Across the Stratopause* [Siskind, D. E., S. D. Eckermann, and M. E. Summers (eds.)] Geophysical Monograph Series No. 123, American Geophysical Union, pp. 241–255.
- Keim**, E. R., D. W. Fahey, L. A. Del Negro, E. L. Woodbridge, R. S. Gao, P. O. Wennberg, R. C. Cohen, R. M. Stimpfle, K. K. Kelly, E. J. Hints, J. C. Wilson, H. H. Jonsson, J. E. Dye, D. Baumgardner, S. R. Kawa, R. J. Salawitch, M. H. Proffitt, M. Loewenstein, J. R. Podolske, and K. R. Chan, 1996: Observations of large reductions in the NO/NO_y ratio near the mid-latitude tropopause and the role of heterogeneous chemistry. *Geophysical Research Letters*, **23**(22), 3223–3226.
- Kelly**, P. M., P. D. Jones, and P. Q. Jia, 1996: The spatial response of the climate system to explosive volcanic eruptions. *International Journal of Climatology*, **16**(5), 537–550.
- Khalil**, M. A. K., R. A. Rasmussen, and R. Gunawardena, 1993: Atmospheric methyl bromide: Trends and global mass balance. *Journal of Geophysical Research – Atmospheres*, **98**, 2887–2896.
- Kirk-Davidoff**, D. B., E. J. Hints, J. G. Anderson, and D. W. Keith, 1999: The effect of climate change on ozone depletion through changes in stratospheric water vapour. *Nature*, **402**(6760), 399–401.
- Kodera**, K., 1994: Influence of volcanic eruptions on the troposphere through stratospheric dynamical processes in the Northern Hemisphere winter. *Journal of Geophysical Research – Atmospheres*, **99**(D1), 1273–1282.
- Lamarque**, J.-F. and P. G. Hess, 2004: Arctic Oscillation modulation of the Northern Hemisphere spring tropospheric ozone. *Geophysical Research Letters*, **31**, L06127, doi:10.1029/2003GL019116.
- Langematz**, U., M. Kunze, K. Krüger, K. Labitzke, and G. L. Roff, 2003: Thermal and dynamical changes of the stratosphere since 1979 and their link to ozone and CO₂ changes. *Journal of Geophysical Research – Atmospheres*, **108**(D1), 4027, doi:10.1029/2002JD002069.
- Lee**, A. M., H. K. Roscoe, and S. Oltmans, 2000: Model and measurements show Antarctic ozone loss follows edge of polar night. *Geophysical Research Letters*, **27**(23), 3845–3848.
- Lelieveld**, J. and F. J. Dentener, 2000: What controls tropospheric ozone? *Journal of Geophysical Research – Atmospheres*, **105**, 3531–3551.
- Li**, J. L., D. M. Cunnold, H. J. Wang, E. S. Yang, and M. J. Newchurch, 2002: A discussion of upper stratospheric ozone asymmetries and SAGE trends. *Journal of Geophysical Research – Atmospheres*, **107**(D23), 4705, doi:10.1029/2001JD001398.
- Liley**, J. B., P. V. Johnston, R. L. McKenzie, A. J. Thomas, and I. S. Boyd, 2000: Stratospheric NO₂ variations from a long time series at Lauder, New Zealand. *Journal of Geophysical Research – Atmospheres*, **105**(D9), 11,633–11,640.
- Limpasuvan**, V. and D. L. Hartmann, 2000: Wave-maintained annular modes of climate variability. *Journal of Climate*, **13**, 4414–4429.
- Manzini**, E. and N. A. McFarlane, 1998: The effect of varying the source spectrum of a gravity wave parameterization in a middle atmosphere general circulation model. *Journal of Geophysical Research – Atmospheres*, **103**(D24), 31,523–31,539.
- McCormick**, M. P., L. W. Thomason, and C. R. Trepte, 1995: Atmospheric effects of the Mount Pinatubo eruption. *Nature*, **373**, 399–404.
- McElroy**, M. B., R. J. Salawitch, and K. Minschwaner, 1992: The changing stratosphere. *Planetary and Space Science*, **40**, 373–401.

- McLinden**, C. A., S. C. Olsen, M. J. Prather, and J. B. Liley, 2001: Understanding trends in stratospheric NO_y and NO_2 . *Journal of Geophysical Research – Atmospheres*, **106**(D21), 27,787–27,793.
- Millard**, G. A., A. M. Lee, and J. A. Pyle, 2002: A model study of the connection between polar and midlatitude ozone loss in the Northern Hemisphere lower stratosphere. *Journal of Geophysical Research – Atmospheres*, **107**(D5), 8323, doi:10.1029/2001JD000899.
- Molina**, M. J. and F. S. Rowland, 1974: Stratospheric sink for chlorofluoromethanes: Chlorine atom catalysed destruction of ozone. *Nature*, **249**, 810–812.
- Montzka**, S. A., J. H. Butler, J. W. Elkins, T. M. Thompson, A. D. Clarke, and L. T. Lock, 1999: Present and future trends in the atmospheric burden of ozone-depleting halogens. *Nature*, **398**, 690–694.
- Montzka**, S. A., J. H. Butler, B. D. Hall, D. J. Mondeel, and J. W. Elkins, 2003: A decline in tropospheric organic bromine. *Geophysical Research Letters*, **30**(15), 1826, doi:10.1029/2003GL017745.
- Mote**, P. W., K. H. Rosenlof, M. E. McIntyre, E. S. Carr, J. C. Gille, J. R. Holton, J. S. Kinnerson, H. C. Pumphrey, J. M. Russell III, and J. C. Waters, 1996: An atmospheric tape recorder: The imprint of tropical tropopause temperatures on stratospheric water vapor. *Journal of Geophysical Research – Atmospheres*, **101**, 3989–4006.
- Nedoluha**, G. E., D. E. Siskind, J. T. Bacmeister, R. M. Bevilacqua, and J. M. Russell, 1998: Changes in upper stratospheric CH_4 and NO_2 as measured by HALOE and implications for changes in transport. *Geophysical Research Letters*, **25**(7), 987–990.
- Newchurch**, M. J., E. S. Yang, D. M. Cunnold, G. C. Reinsel, J. M. Zawodny, and J. M. Russell, 2003: Evidence for slowdown in stratospheric ozone loss: First stage of ozone recovery. *Journal of Geophysical Research – Atmospheres*, **108**(D16), 4507, doi:10.1029/2003JD003471.
- Newman**, P. A. and E. R. Nash, 2000: Quantifying the wave driving of the stratosphere. *Journal of Geophysical Research – Atmospheres*, **105**(D10), 12,485–12,497.
- Newman**, P. A. and E. R. Nash, 2005: The unusual Southern Hemisphere stratosphere winter of 2002. *Journal of the Atmospheric Sciences*, **62**(3), 614–628.
- Newman**, P. A., J. F. Gleason, R. D. McPeters, and R. S. Stolarski, 1997: Anomalous low ozone over the Arctic. *Geophysical Research Letters*, **24**(22), 2689–2692.
- Newman**, P. A., E. R. Nash, and J. E. Rosenfield, 2001: What controls the temperature of the Arctic stratosphere during the spring? *Journal of Geophysical Research – Atmospheres*, **106**(D17), 19,999–20,010.
- Norton**, W. A. and M. P. Chipperfield, 1995: Quantification of the transport of chemically activated air from the Northern Hemisphere polar vortex. *Journal of Geophysical Research – Atmospheres*, **100**(D12), 25,817–25,840.
- O'Doherty**, S., D. M. Cunnold, A. Manning, B. R. Miller, R. H. J. Wang, P. B. Krummel, P. J. Fraser, P. G. Simmonds, A. McCulloch, R. F. Weiss, P. Salameh, L. W. Porter, R. G. Prinn, J. Huang, G. Sturrock, D. Ryall, R. G. Derwent, and S. A. Montzka, 2004: Rapid growth of hydrofluorocarbon 134a, and hydrochlorofluorocarbons 141b, 142b and 22 from Advanced Global Atmospheric Gases Experiment (AGAGE) observations at Cape Grim, Tasmania and Mace Head, Ireland. *Journal of Geophysical Research – Atmospheres*, **109**, D06310, doi:10.1029/2003JD004277.
- Oltmans**, S. J., H. Vömel, D. J. Hofmann, K. H. Rosenlof, and D. Kley, 2000: The increase in stratospheric water vapour from balloonborne, frostpoint hygrometer measurements at Washington, D.C. and Boulder, Colorado. *Geophysical Research Letters*, **27**, 3453–3456.
- Orsolini**, Y. J. and V. Limpasuvan, 2001: The North Atlantic Oscillation and the occurrences of ozone miniholes. *Geophysical Research Letters*, **28**(21), 4099–4102.
- Pawson**, S. and B. Naujokat, 1999: The cold winters of the middle 1990s in the northern lower stratosphere. *Journal of Geophysical Research – Atmospheres*, **104**(D12), 14,209–14,222.
- Perlwitz**, J. and H. F. Graf, 1995: The statistical connection between tropospheric and stratospheric circulation of the Northern Hemisphere in winter. *Journal of Climate*, **8**(10), 2281–2295.
- Perlwitz**, J., H. F. Graf, and R. Voss, 2000: The leading variability mode of the coupled troposphere-stratosphere winter circulation in different climate regimes. *Journal of Geophysical Research – Atmospheres*, **105**(D5), 6915–6926.
- Pitari**, G., E. Mancini, V. Rizi, and D. T. Shindell, 2002: Impact of future climate and emission changes on stratospheric aerosols and ozone. *Journal of the Atmospheric Sciences*, **59**(3), 414–440.
- Potter**, B. E. and J. R. Holton, 1995: The role of monsoon convection in the dehydration of the lower tropical stratosphere. *Journal of the Atmospheric Sciences*, **52**, 1034–1050.
- Poulida**, O., R. R. Dickerson, and A. Heymsfield, 1996: Stratosphere-troposphere exchange in a midlatitude mesoscale convective complex: 1. Observations. *Journal of Geophysical Research – Atmospheres*, **101**, 6823–6836.
- Prather**, M. and A. H. Jaffe, 1990: Global impact of the Antarctic ozone hole: Chemical propagation. *Journal of Geophysical Research – Atmospheres*, **95**(D4), 3473–3492.
- Prather**, M., M. M. Garcia, R. Suozzo, and D. Rind, 1990: Global impact of the Antarctic ozone hole: Dynamic dilution with a three-dimensional chemical transport model. *Journal of Geophysical Research – Atmospheres*, **95**(D4), 3449–3471.
- Prinn**, R. G., R. F. Weiss, P. J. Fraser, P. G. Simmonds, D. M. Cunnold, F. N. Alyea, S. O'Doherty, P. Salameh, B. R. Miller, J. Huang, R. H. J. Wang, D. E. Hartley, C. Harth, L. P. Steele, G. Sturrock, P. M. Midgley, and A. McCulloch, 2000: A history of chemically and radiatively important gases in air deduced from ALE/GAGE/AGAGE. *Journal of Geophysical Research – Atmospheres*, **105**, 17,751–17,792.
- Ramaswamy**, V., M. D. Schwarzkopf, and W. J. Randel, 1996: Fingerprint of ozone depletion in the spatial and temporal pattern of recent lower-stratospheric cooling. *Nature*, **382**(6592), 616–618.
- Randel**, W. J. and J. B. Cobb, 1994: Coherent variations of monthly mean total ozone and lower stratospheric temperature. *Journal of Geophysical Research*, **99**, 5433–5447.
- Randel**, W. J. and F. Wu, 1999: Cooling of the Arctic and Antarctic polar stratospheres due to ozone depletion. *Journal of Climate*, **12**(5), 1467–1479.

- Randel, W. J., F. Wu, J. M. Russell, and J. Waters, 1999:** Space-time patterns of trends in stratospheric constituents derived from UARS measurements. *Journal of Geophysical Research – Atmospheres*, **104**(D3), 3711–3727.
- Randel, W. J., F. Wu, and R. Stolarski, 2002:** Changes in column ozone correlated with the stratospheric EP flux. *Journal of the Meteorological Society of Japan*, **80**(4B), 849–862.
- Randel, W. J., F. Wu, S. J. Oltmans, K. Rosenlof, and G. E. Nedoluha, 2004:** Interannual changes of stratospheric water vapor and correlations with tropical tropopause temperatures. *Journal of the Atmospheric Sciences*, **61**, 2133–2148.
- Rauthe, M., A. Hense, and H. Paeth, 2004:** A model intercomparison study of climate change signals in extratropical circulation. *International Journal of Climatology*, **24**, 643–662.
- Ray, E. A., F. L. Moore, J. W. Elkins, G. S. Dutton, D. W. Fahey, H. Vömel, S. J. Oltmans, and K. H. Rosenlof, 1999:** Transport into the Northern Hemisphere lowermost stratosphere revealed by in situ tracer measurements. *Journal of Geophysical Research – Atmospheres*, **104**(D21), 26,565–26,580.
- Reid, S. J., A. F. Tuck, and G. Kiladis, 2000:** On the changing abundance of ozone minima at northern midlatitudes. *Journal of Geophysical Research – Atmospheres*, **105**(D10), 12,169–12,180.
- Rex, M., R. J. Salawitch, P. von der Gathen, N. Harris, M. P. Chipperfield, and B. Naujokat, 2004:** Arctic ozone loss and climate change. *Geophysical Research Letters*, **31**(4), L04116, doi:10.1029/2003GL018844.
- Rind, D., R. Suozzo, N. K. Balachandran, and M. J. Prather, 1990:** Climate change and the middle atmosphere. 1. The doubled CO₂ climate. *Journal of the Atmospheric Sciences*, **47**(4), 475–494.
- Rind, D., J. Lerner, J. Perlwitz, C. McLinden, and M. Prather, 2002:** Sensitivity of tracer transports and stratospheric ozone to sea surface temperature patterns in the doubled CO₂ climate. *Journal of Geophysical Research – Atmospheres*, **107**(D24), 4800, doi:10.1029/2002JD002483.
- Rinsland, C. P., E. Mahieu, R. Zander, N. B. Jones, M. P. Chipperfield, A. Goldman, J. Anderson, J. M. Russell III, P. Demoulin, J. Notholt, G. C. Toon, J.-F. Blavier, B. Sen, R. Sussmann, S. W. Wood, A. Meier, D. W. T. Griffith, L. S. Chiou, F. J. Murcray, T. M. Stephen, F. Hase, S. Mikuteit, A. Schulz, and T. Blumenstock, 2003:** Long-term trends of inorganic chlorine from ground-based infrared solar spectra: Past increases and evidence for stabilization. *Journal of Geophysical Research – Atmospheres*, **108**(D8), 4252, doi:10.1029/2002JD003001.
- Röckmann, T., J.-U. Groöß, and R. Müller, 2004:** The impact of anthropogenic chlorine emissions, stratospheric ozone change and chemical feedbacks on stratospheric water. *Atmospheric Chemistry and Physics*, **4**, 693–699.
- Rogers, J. C. and M. J. McHugh, 2002:** On the separability of the North Atlantic Oscillation and Arctic Oscillation. *Climate Dynamics*, **19**, 599–608.
- Roscoe, H. K., A. E. Jones, and A. M. Lee, 1997:** Midwinter start to Antarctic ozone depletion: Evidence from observations and models. *Science*, **278**(5335), 93–96.
- Rosenlof, K. H., S. J. Oltmans, D. Kley, J. M. Russell, E. W. Chiou, W. P. Chu, D. G. Johnson, K. K. Kelly, H. A. Michelsen, G. E. Nedoluha, E. E. Remsberg, G. C. Toon, and M. P. McCormick, 2001:** Stratospheric water vapor increases over the past half-century. *Geophysical Research Letters*, **28**(7), 1195–1198.
- Rozañov, E. V., M. E. Schlesinger, N. G. Andronova, F. Yang, S. L. Malyshev, V. A. Zubov, T. A. Egorova, and B. Li, 2002:** Climate/chemistry effects of the Pinatubo volcanic eruption simulated by the UIUC stratosphere/troposphere GCM with interactive photochemistry. *Journal of Geophysical Research – Atmospheres*, **107**(D21), 4594, doi:10.1029/2001JD000974.
- Salby, M. and P. F. Callaghan, 1993:** Fluctuations of total ozone and their relationship to stratospheric air motions. *Journal of Geophysical Research – Atmospheres*, **98**, 2715–2727.
- Sander, S. P., R. R. Friedl, A. R. Ravishankara, D. M. Golden, C. E. Kolb, M. J. Kurylo, R. E. Huie, V. L. Orkin, M. J. Molina, G. K. Moortgat, and B. J. Finlayson-Pitts, 2003:** Chemical Kinetics and Photochemical Data for Use in Atmospheric Studies. Evaluation Number 14. JPL Publication No. 02-25, National Aeronautics and Space Administration, Jet Propulsion Laboratory, California Institute of Technology, Pasadena, CA, USA. (Available at http://jpldataeval.jpl.nasa.gov/pdf/JPL_02-25_rev02.pdf)
- Santer, B. D., M. F. Wehner, T. M. L. Wigley, R. Sausen, G. A. Meehl, K. E. Taylor, C. Ammann, J. Arblaster, W. M. Washington, J. S. Boyle, and W. Bruggemann, 2003a:** Contributions of anthropogenic and natural forcing to recent tropopause height changes. *Science*, **301**(5632), 479–483.
- Santer, B. D., R. Sausen, T. M. L. Wigley, J. S. Boyle, K. Achuta-Rao, C. Doutriaux, J. E. Hansen, G. A. Meehl, E. Roeckner, R. Ruedy, G. Schmidt, and K. E. Taylor, 2003b:** Behavior of tropopause height and atmospheric temperature in models, reanalyses, and observations: Decadal changes. *Journal of Geophysical Research – Atmospheres*, **108**(D1), 4002, doi:10.1029/2002JD002258.
- Scaife, A. A., J. Austin, N. Butchart, S. Pawson, M. Keil, J. Nash, and I. N. James, 2000:** Seasonal and interannual variability of the stratosphere diagnosed from UKMO TOVS analyses. *Quarterly Journal of the Royal Meteorological Society*, **126**(568), 2585–2604.
- Schnadt, C. and M. Dameris, 2003:** Relationship between North Atlantic Oscillation changes and stratospheric ozone recovery in the Northern Hemisphere in a chemistry-climate model. *Geophysical Research Letters*, **30**(9), 1487, doi:10.1029/2003GL017006.
- Seidel, D. J., R. J. Ross, J. K. Angell and G. C. Reid, 2001:** Climatological characteristics of the tropical tropopause as revealed by radiosondes. *Journal of Geophysical Research – Atmospheres*, **106**, 7857–7878.
- Seidel, D. J., J. K. Angell, M. Free, J. Christy, R. Spencer, S. A. Klein, J. R. Lanzante, C. Mears, M. Schabel, F. Wentz, D. Parker, P. Thorne, and A. Sterin, 2004:** Uncertainties in signals of large-scale climate variations in radiosonde and satellite upper-air temperature data sets. *Journal of Climate*, **17**(11), 2225–2240.
- Sexton, D. M. H., H. Grubb, K. P. Shine, and C. K. Folland, 2003:** Design and analysis of climate model experiments for the efficient estimation of anthropogenic signals. *Journal of Climate*, **16**(9), 1320–1336.
- Sherwood, S. C., and A. E. Dessler, 2001:** A model for transport across the tropical tropopause. *Journal of the Atmospheric Sciences*, **58**, 765–779.

- Shindell, D. T.**, 2001: Climate and ozone response to increased stratospheric water vapor. *Geophysical Research Letters*, **28**(8), 1551–1554.
- Shindell, D. T.** and G. A. Schmidt, 2004: Southern Hemisphere climate response to ozone changes and greenhouse gas increases. *Geophysical Research Letters*, **31**, L18209, doi:10.1029/2004GL020724.
- Shindell, D. T.**, D. Rind, and P. Lonergan, 1998: Increased polar stratospheric ozone losses and delayed eventual recovery owing to increasing greenhouse-gas concentrations. *Nature*, **392**(6676), 589–592.
- Shindell, D. T.**, G. A. Schmidt, R. L. Miller, and D. Rind, 2001a: Northern Hemisphere winter climate response to greenhouse gas, ozone, solar, and volcanic forcing. *Journal of Geophysical Research – Atmospheres*, **106**(D7), 7193–7210.
- Shindell, D. T.**, G. A. Schmidt, M. E. Mann, D. Rind, and A. Waple, 2001b: Solar forcing of regional climate during the Maunder Minimum. *Science*, **294**, 2149–2152.
- Shine, K. P.**, M. S. Bourqui, P. M. D. Forster, S. H. E. Hare, U. Langematz, P. Braesicke, V. Grewe, M. Ponater, C. Schnadt, C. A. Smith, J. D. Haigh, J. Austin, N. Butchart, D. T. Shindell, W. J. Randel, T. Nagashima, R. W. Portmann, S. Solomon, D. J. Seidel, J. Lanzante, S. Klein, V. Ramaswamy, and M. D. Schwarzkopf, 2003: A comparison of model-simulated trends in stratospheric temperatures. *Quarterly Journal of the Royal Meteorological Society*, **129**(590), 1565–1588.
- Sigmond, M.**, P. C. Siegmund, E. Manzini, and H. Kelder, 2004: A simulation of the separate climate effects of middle atmospheric and tropospheric CO₂ doubling. *Journal of Climate*, **17**(12), 2352–2367.
- Simmonds, P. G.**, R. G. Derwent, A. J. Manning, P. J. Fraser, P. B. Krummel, S. O’Doherty, R. G. Prinn, D. M. Cunnold, B. R. Miller, H. J. Wang, D. B. Ryall, L. W. Porter, R. F. Weiss, and P. K. Salameh, 2004: AGAGE observations of methyl bromide and methyl chloride at Mace Head, Ireland, and Cape Grim, Tasmania, 1998–2001. *Journal of Atmospheric Chemistry*, **47**, 243–269.
- Siskind, D. E.**, L. Froidevaux, J. M. Russell, and J. Lean, 1998: Implications of upper stratospheric trace constituent changes observed by HALOE for O₃ and ClO from 1992 to 1995. *Geophysical Research Letters*, **25**(18), 3513–3516.
- Siskind, D. E.**, G. E. Nedoluha, M. E. Summers, and J. M. Russell, 2002: A search for an anticorrelation between H₂O and O₃ in the lower mesosphere. *Journal of Geophysical Research – Atmospheres*, **107**(D20), 4435, doi:10.1029/2001JD001276.
- Solomon, S.** and J. S. Daniel, 1996: Impact of the Montreal Protocol and its amendments on the rate of change of global radiative forcing. *Climatic Change*, **32**(1), 7–17.
- Solomon, S.**, M. Mills, L. E. Height, W. H. Pollock, and A. F. Tuck, 1992: On the evaluation of ozone depletion potentials. *Journal of Geophysical Research – Atmospheres*, **97**, 825–842.
- Solomon, S.**, J. P. Smith, R. W. Sanders, L. Perliski, H. L. Miller, G. H. Mount, J. G. Keys, and A. L. Schmeltekopf, 1993: Visible and near-ultraviolet spectroscopy at McMurdo Station, Antarctica. 8. Observations of nighttime NO₂ and NO₃ from April to October 1991. *Journal of Geophysical Research – Atmospheres*, **98**(D1), 993–1000.
- SPARC**, 2000: *SPARC Assessment of Upper Tropospheric and Stratospheric Water Vapour* [Kley, D., J. M. Russell III, and C. Phillips (eds.)]. WMO-TD No. 1043, WCRP Series Report No. 113, SPARC Report No. 2, Stratospheric Processes and Their Role in Climate (SPARC). (Available at <http://www.atmosp.physics.utoronto.ca/SPARC/index.html>)
- Sprenger, M.** and H. Wernli, 2003: A northern hemispheric climatology of cross-tropopause exchange for the ERA15 time period (1979–1993). *Journal of Geophysical Research – Atmospheres*, **108**(D12), 8521, doi:10.1029/2002JD002636.
- Steinbrecht, W.**, H. Claude, U. Kohler, and P. Winkler, 2001: Interannual changes of total ozone and Northern Hemisphere circulation patterns. *Geophysical Research Letters*, **26**, 1191–1194.
- Stenchikov, G.**, A. Robock, V. Ramaswamy, M. D. Schwarzkopf, K. Hamilton, and S. Ramachandran, 2002: Arctic Oscillation response to the 1991 Mount Pinatubo eruption: Effects of volcanic aerosols and ozone depletion. *Journal of Geophysical Research – Atmospheres*, **107**(D24), 4803, doi:10.1029/2002JD002090.
- Stohl, A.**, P. Bonasoni, P. Cristofanelli, W. Collins, J. Feichter, A. Frank, C. Forster, E. Gerasopoulos, H. Gaggeler, P. James, T. Kentarchos, H. Kromp-Kolb, B. Kruger, C. Land, J. Meloan, A. Papayannis, A. Priller, P. Seibert, M. Sprenger, G. J. Roelofs, H. E. Scheel, C. Schnabel, P. Siegmund, L. Tobler, T. Trickl, H. Wernli, V. Wirth, P. Zanis, and C. Zerefos, 2003: Stratosphere-troposphere exchange: A review, and what we have learned from STACCATO. *Journal of Geophysical Research – Atmospheres*, **108**(D12), 8516, doi:10.1029/2002JD002490.
- Stolarski, R. J.**, R. D. McPeters, and P. A. Newman, 2005: The ozone hole of 2002 as measured by TOMS. *Journal of the Atmospheric Sciences*, **62**(3), 716–720.
- Stuber, N.**, M. Ponater, and R. Sausen, 2001: Is the climate sensitivity to ozone perturbations enhanced by stratospheric water vapor feedback? *Geophysical Research Letters*, **28**(15), 2887–2890.
- Sturrock, G. A.**, D. M. Etheridge, C. M. Trudinger, P. J. Fraser, and A. M. Smith, 2002: Atmospheric histories of halocarbons from analysis of Antarctic firn air: Major Montreal Protocol species. *Journal of Geophysical Research – Atmospheres*, **107**(D24), 4765, doi:10.1029/2002JD002548.
- Tabazadeh, A.**, M. L. Santee, M. Y. Danilin, H. C. Pumphrey, P. A. Newman, P. J. Hamill, and J. L. Mergenthaler, 2000: Quantifying denitrification and its effect on ozone recovery. *Science*, **288**(5470), 1407–1411.
- Teitelbaum, H.**, M. Moustououi, and M. Fromm, 2001: Exploring polar stratospheric cloud and ozone minihole formation: The primary importance of synoptic-scale flow perturbations. *Journal of Geophysical Research – Atmospheres*, **106**(D22), 28,173–28,188.
- Thompson, D. W. J.** and S. Solomon, 2002: Interpretation of recent Southern Hemisphere climate change. *Science*, **296**(5569), 895–899.
- Thompson, D. W. J.** and J. M. Wallace, 1998: The Arctic Oscillation signature in the wintertime geopotential height and temperature fields. *Geophysical Research Letters*, **25**(9), 1297–1300.
- Thompson, D. W. J.** and J. M. Wallace, 2000: Annular modes in the extratropical circulation, part I: Month-to-month variability. *Journal of Climate*, **13**, 1000–1016.

- Thompson**, D. W. J., J. M. Wallace, and G. C. Hegerl, 2000: Annular modes in the extratropical circulation. Part II: Trends. *Journal of Climate*, **13**(5), 1018–1036.
- Thuburn**, J. and G. C. Craig, 2002: On the temperature structure of the tropical stratosphere. *Journal of Geophysical Research – Atmospheres*, **107**(D1–D2), 4017.
- Waibel**, A. E., T. Peter, K. S. Carslaw, H. Oelhaf, G. Wetzel, P. J. Crutzen, U. Poschl, A. Tsias, E. Reimer, and H. Fischer, 1999: Arctic ozone loss due to denitrification. *Science*, **283**(5410), 2064–2069.
- Walker**, G. T. and E. W. Bliss, 1932: World weather V. *Memoirs of the Royal Meteorological Society*, **4**, 53–84.
- Walker**, S. J., R. F. Weiss, and P. K. Salameh, 2000: Reconstructed histories of the annual mean atmospheric mole fractions for the halocarbons CFC-11, CFC-12, CFC-113, and carbon tetrachloride. *Journal of Geophysical Research – Oceans*, **105**(C6), 14,285–14,296.
- Wallace**, J. M., 2000: North Atlantic Oscillation/annular mode: Two paradigms – one phenomenon. *Quarterly Journal of the Royal Meteorological Society*, **126**(564), 791–805.
- Wang**, P.-H., P. Minnis, M. P. McCormick, G. S. Kent, and K. M. Skeens, 1996: A 6-year climatology of cloud occurrence frequency from Stratospheric Aerosol and Gas Experiment II observations (1985–1990). *Journal of Geophysical Research – Atmospheres*, **101**(D23), 29,407–29,429.
- Wang**, W.-C., M. P. Dudek, X.-Z. Liang, and J. T. Kiehl, 1991: Inadequacy of effective CO₂ as a proxy in simulating the greenhouse effect of the other radiatively active gases. *Nature*, **350**, 573–577.
- Wang**, W.-C., M. P. Dudek, and X.-Z. Liang, 1992: Inadequacy of effective CO₂ as a proxy in assessing the regional climate change due to other radiatively active gases. *Geophysical Research Letters*, **19**, 1375–1378.
- Waugh**, D. W., W. J. Randel, S. Pawson, P. A. Newman, and E. R. Nash, 1999: Persistence of the lower stratospheric polar vortices. *Journal of Geophysical Research – Atmospheres*, **104**(D22), 27,191–27,201.
- Weber**, M., S. Dhomse, F. Wittrock, A. Richter, B. M. Sinnhuber, and J. P. Burrows, 2003: Dynamical control of NH and SH winter/spring total ozone from GOME observations in 1995–2002. *Geophysical Research Letters*, **30**(11), 1583.
- Winker**, D. M. and C. R. Trepte, 1998: Laminar cirrus observed near the tropical tropopause by LITE. *Geophysical Research Letters*, **25**(17), 3351–3354.
- WMO**, 1986: *Atmospheric Ozone: 1985*. Global Ozone Research and Monitoring Project – Report No. 16, World Meteorological Organization (WMO), Geneva.
- WMO**, 1995: *Scientific Assessment of Ozone Depletion: 1994*. Global Ozone Research and Monitoring Project – Report No. 37, World Meteorological Organization (WMO), Geneva.
- WMO**, 1999: *Scientific Assessment of Ozone Depletion: 1998*. Global Ozone Research and Monitoring Project – Report No. 44, World Meteorological Organization (WMO), Geneva.
- WMO**, 2003: *Scientific Assessment of Ozone Depletion: 2002*. Global Ozone Research and Monitoring Project – Report No. 47, World Meteorological Organization, Geneva, 498 pp.
- Yokouchi**, Y., D. Toom-Saunty, K. Yazawa, T. Inagaki, and T. Tamaru, 2002: Recent decline of methyl bromide in the troposphere. *Atmospheric Environment*, **36**(32), 4985–4989.
- Zeng**, G. and J. A. Pyle, 2003: Changes in tropospheric ozone between 2000 and 2100 modelled in a chemistry-climate model. *Geophysical Research Letters*, **30**(7), 1392, doi:10.1029/2002GL016708.
- Zhou**, X. L., M. A. Geller, and M. H. Zhang, 2001: Cooling trend of the tropical cold point tropopause temperatures and its implications. *Journal of Geophysical Research – Atmospheres*, **106**(D2), 1511–1522.